

THE EFFECT OF LONG-TERM MERCURY CONTAMINATION ON THE COMPOSITION
AND DIVERSITY OF SOIL BACTERIAL COMMUNITIES IN RIVERINE ECOSYSTEMS

by

ASPASSIA D. CHATZIEFTHIMIOU

A dissertation submitted to the
Graduate School-New Brunswick
Rutgers, The State University of New Jersey

In partial fulfillment of the requirements

For the degree of

Doctor of Philosophy

Graduate Program in Ecology and Evolution

Written under the direction of

Tamar Barkay

And approved by

New Brunswick, New Jersey

January, 2012

ABSTRACT OF THE DISSERTATION

The Effect of Long-Term Mercury Contamination on the Composition and Diversity of Soil Bacterial Communities in Riverine Ecosystems

by ASPASSIA D. CHATZIEFTHIMIOU

Dissertation Director:

Dr. Tamar Barkay

Hg contamination in riverine ecosystems is a persistent problem and clean-up efforts are a priority for EPA and local federal governments as potential methylation of Hg increases its toxicity due to its bioaccumulation and biomagnification in aquatic food chains. Understanding the microbial contribution to Hg contamination is of particular importance as microbial communities occupy the base of the food chain and the way they transform Hg has bottom-up effects to all trophic levels. The broad objective of this dissertation was to investigate the role of abiotic factors in shaping the composition, diversity and distribution of bacterial communities inhabiting floodplain soils of the East Fork Poplar Creek (EFPC), TN, and South River (SR), VA, chronically contaminated with Hg as a result of industrial processes. Analysis of soil samples from the EFPC by direct cultivation and isolation, revealed a metabolic-dependent effect of Hg-stress on bacterial populations, with copiotrophs exhibiting higher mercury reduction potentials, as well as phylogenetic and functional diversity, than oligotrophs. As the great majority of the strains contained a *merA* gene in their genome, Hg-resistance in these isolates may have been conferred by the functions of the mercury resistance (*mer*) system. A total of 27 phylogenetic incongruencies were observed between this and the 16S rRNA genes of the isolates, suggesting that

horizontal gene transfer may play a role in Hg adaptation. The culture-independent method of 16S rRNA-fingerprinting was used to assess spatial distribution and diversity of bacterial communities along the Hg-contamination gradient in SR. Higher levels of diversity were obtained in communities that experience low as compared to high soil Hg levels. The best predictors of community diversity were pH, moisture and soil texture, whereas THg and geography were poor predictors. In this study a new *merA*-based t-RFLP method was designed to assess distribution and diversity of *merA* genes. Results show high levels of diversity for this gene and clustering based on geographical proximity. These findings highlight the impact of long-term Hg-stress on microbial communities in riverine ecosystems and provide a micro-ecological framework for future remedial actions in Hg contaminated sites.

Acknowledgements

In my academic career in Rutgers, I have been honored to work with brilliant, passionate and kind scientists, administrators and students. I acknowledge that who I have come to be as a scientist and a person reflects directly on them and for that I am eternally indebted. First and foremost, I want to thank Tamar Barkay for being such an infallibly excellent mentor guiding me through my scientific quest. For the past 10 years, Tamar has encouraged me to follow my curiosity, and has been generous with her time, support and advice. She has been the keystone species of my graduate studies, and has enriched my intellect, culture and writing skills.

I want to show my appreciation to all the professors that have served as members in my qualifying, preliminary and defense committees: Elisabetta Bini, John Dighton, Max Hagbloom, Costa Vetriani, and Peter Morin. Their participation and advice have enhanced greatly my research projects. Thanks are due also to Julie Lockwood, the graduate program director in Ecology and Evolution, for her tireless efforts on the behalf of all the graduate students and particularly myself.

In memoriam of Ted Stiles who introduced me to the natural beauty of New Jersey through the field trips taken during the month of September 2005, as part of the course: concepts in evolution. Through his teachings I learned to think in ecological terms, but most importantly I learned that it is through our mistakes that we progress our science. Peter Morin, a truly gifted teacher, who untirely answered all my questions, furthered my knowledge in community ecology. Through Peter I also had the opportunity to give microbial ecology tours in the Hutchinson memorial forest, and be featured in the Rutgers web site. I am very grateful for collaborating with Diane Davis in teaching General and Applied Microbiology labs. Our discourses and interactions allowed me to evolve a more efficient teaching style.

I thank George Southworth and J. R. Flanders for providing me with the soil samples from the East Fork Poplar Creek in Oak Ridge Tennessee and South River in Virginia, respectively. I acknowledge Jonna Coombs and Erica Gehr for their help on plasmid extractions, and Lee Kerkhof, Mei Fang-Chien and Lora McGuiness, who collaborated with me to create the new *merA*-t-RFLP method. Lora McGuiness did a wonderful job in helping me with every part of the process from experimentation to analysis and I strongly believe that without her help I wouldn't have achieved the same results. I am indebted to Yanping Wang for designing the *merA* primers that I have used extensively in both of my studies presented here and of course all her help with troubleshooting. I thank John Dighton for his help with the CCA analysis and for always welcoming me at the Pinelands Field Station.

The Barkay-Lab has always been a home for me and my fellows a family, with the added advantage that they understand me when I "talk science". Sharron Crane or *Sharonella* sp., Melitza Crespo-Medina, Zachary Freedman or *Zacharymonas socioinformaticus*, Kritee or *Kritee kritee*^T, and Kim Cruz or *Kimothrix jenesaisquaticus*, brainstormed with me on ecological, mercurial and endless other matters, and together we advanced our philosophical quests in friendly harmony. Riqing Yu has always been an exemplary hard worker and encouraged all of us to do the same. Annette Møller and Gunnar Øregaard, visiting scholars from Denmark, and Lucelia Cabral and Juliana Gandelman, visiting scholars from Brazil, with whom I shared office space, allowed me to get a glimpse on their overseas way of performing research. Last, but most definitely not least, Chu-Ching Lin, my former office mate whose appreciation of my capabilities as a researcher and a teacher encouraged me to proceed with the synthesis of this dissertation.

I also want to show my appreciation to the hundreds of students that I have taught through the years in General and Applied Microbiology and Microbial Ecology courses and to the 4 students whom I mentored in their research projects. Jackie

Deitz, my first-born academic child, tested with me the methods to be used in my Riverine Systems. Alison Isola or LIA, Joe Jang and Keya Thakar, all helped me with molecular work in both my studies. My teaching philosophy has evolved through my interaction with all of them.

Gavin Swiatek is a supreme human being and a fantastic teacher. His Socratic method allowed me to overcome road-blocks in my scientific thought processes. I thank my fellow microbial ecologist Aabir Banerji, for with him I had innumerable discussions about how we can align macro-ecological theories to microbes, in the gardens of Rutgers, in the spirit of the Aristotelian peripatetic school. Isabel Gray, Nora Lopez-Chiaffarelli, Ileana Perez-Rodriguez, Molly Mcleod, Natalie Howe and Talia Young, I thank you for furthering my knowledge in microbiological and ecological subjects and for your loving support.

I am also indebted to Molly Nelson for hosting me in Merrifield Farm, Maine for a writing retreat. Angelique Mouyis and Niko Tsakalako both have helped me with the creative process of writing and through their eyes I have seen the wonders of science illuminated by art. Shea Paris took me back to the basics when my logic became paradoxical, during the dissertation writing process, and always found funny and kind words of encouragement to keep me going.

I am grateful for the help with administrative and technical issues provided by Peter Anderson, Eileen Glick, Kathy Maguire, Jessie Maguire, and Arleen Nabel. My most sincere and warmest thanks are reserved for Marsha Morin, the mother to all the graduate students in the Ecology and Evolution program, who always makes sure that we have everything that we need from funding to personal peace.

I want to acknowledge the funding sources that made this research possible: U.S. Department of Energy grant DE-FG02-99ER62864, Graduate and Teaching Assistantships from Department of Biochemistry and Microbiology, NSF Minority

Grant for the 2006 Plasmid Biology Meeting, and Rutgers University, Graduate School Travel Award for American Society for the 2009 Microbiology meeting.

Dedication

I dedicate my dissertation to my family whose love and support has encouraged and enabled me to successfully reach all my Ithakas; to my demanding muse, Claudia, in whose eyes exists the Aleph, and to my Starr, the single member of her species who has worked so hard for a PhD dissertation.

Table of Contents

	Page
Abstract.....	ii
Acknowledgements.....	iv
Dedication.....	viii
List of Figures.....	x
List of Tables.....	xiii
Chapter 1 – Dissertation Introduction.....	1
Chapter 2 – Effect of Nutrient Disturbance and Mercury Stress on Diversity of Floodplain Bacterial Community in East Fork Poplar Creek, Oak Ridge, Tennessee	19
Chapter 3 – Biogeographical Patterns of Bacterial Communities Along the Mercury Contaminated Floodplains of South River, Virginia.....	75
Chapter 4 – Dissertation Conclusion.....	115
Appendix – Supplementary Information on Phylogenetic and Functional Analyses in Chapter 2.....	120
Bibliography.....	128
Curriculum Vitae.....	141

List of Figures

Page

- Figure 2.1.** Map of the Oak Ridge Reservation (ORR) in Oak Ridge, Tennessee. East Fork Poplar Creek (EFPC) originates at the Y-12 National Security Complex (Y-12 NSC) and spans for 24 Km from East to Northwest flowing into the Poplar Creek, a tributary of that Clinch River (Taken from Brooks and Southworth, 2011)..... 48
- Figure 2.2.** Bar graph of LS (black bars) and FS (grey bars) isolates indicating the original Hg concentration on which the isolates were obtained. Percentile distribution of isolates that were obtained at each Hg concentration, are displayed on top of each bar..... 52
- Figure 2.3.** Pie chart of taxonomic associations of LS isolates based on 16S rRNA gene sequence BLASTN searches. The Actinobacteria are shown with solid perimetric lines. The Proteobacteria have dotted lines for the *alpha*, dash lines for the *beta*, and double lines for the *gamma*. Sequences that were similar to uncultured clones are marked as unknown and have a solid black fill..... 53
- Figure 2.4.** Pie chart of taxonomic associations of FS isolates based on 16S rRNA gene sequence BLASTN searches. The Actinobacteria are shown with solid perimetric lines. The Proteobacteria have dotted lines for the *alpha*, dash lines for the *beta*, and double lines for the *gamma*..... 54
- Figure 2.5.** Class and phylum level taxonomic distribution of LS (black bars) and FS (grey bars) isolates based on 97% 16S rRNA gene sequence similarity (species level). *Alpha*, *beta* and *gamma*, refer to classes of the Gram negative Proteobacteria. Actinobacteria are High G+C, Gram positive organisms..... 55
- Figure 2.6.** Phylogenetic tree of LS isolates and their closest relatives (accession numbers) based on 16S rRNA gene sequences. The Neighbor-Joining tree was constructed using Phylo_Win and the Bootstrap values higher than 50 are shown. Bar indicates 5% estimated nucleotide substitution per site. Color of bracket indicates taxonomic affiliation. Red: Actinobacteria, Green: *gammaproteobacteria*, Purple: *betaproteobacteria*, Orange: *alphaproteobacteria*. Numbers in parentheses indicate clonal sequences. *Sulfolobus solfataricus* was used as an outgroup..... 56
- Figure 2.7.** Phylogenetic tree of FS isolates and their closest relatives based on 16S rRNA gene sequences. The Neighbor-Joining tree was constructed using Phylo_Win and the Bootstrap values higher than 50 are shown. Bar indicates 4% estimated substitution. Color of bracket indicates taxonomic affiliation. Red: Actinobacteria, Green: *gammaproteobacteria*, Purple: *betaproteobacteria*, Orange: *alphaproteobacteria*. Numbers in parentheses indicate clonal sequences. *Sulfolobus solfataricus* was used as an outgroup..... 57
- Figure 2.8.** Rarefaction curves calculated for the LS isolates, using different grouping criteria. (■) 100%, (▲) 97%, (◆) 96-95% percent 16S rRNA gene sequence similarity..... 58

Figure 2.9. Rarefaction curves calculated for the FS isolates, using different grouping criteria. (■) 100%, (▲) 97%, (●) 95% percent 16S rRNA gene sequence similarity..... 59

Figure 2.10. Taxonomic distribution of LS (black bars) and FS (grey bars) isolates based on the *merA* gene sequence similarity. *Alpha*, *beta* and *gamma*, refer to classes of the Gram negative Proteobacteria. Actinobacteria and Firmicutes are High and Low G+C Gram positive organisms, respectively..... 62

Figure 2.11. Pie chart of taxonomic associations of LS isolates based on MerA amino acid sequence BLASTP searches. The Actinobacteria are shown with solid perimetric lines. The Proteobacteria have dotted lines for the *alpha*, dash lines for the *beta*, and double lines for the *gamma*. Sequences that were similar to uncultured clones are marked as unknown and have a solid black fill..... 63

Figure 2.12. Pie chart of taxonomic associations of FS isolates based on MerA amino acid sequence BLASTP searches. The Actinobacteria are shown with solid perimetric lines. The Proteobacteria have dotted lines for the *alpha*, dash lines for the *beta*, and double lines for the *gamma*. Firmicutes are shown in solid black..... 64

Figure 2.13. Rarefaction curves calculated for the LS isolates, using different grouping criteria. (■) 100%, (▲) 99% and (◆) 95% percent *merA* gene sequence similarity..... 66

Figure 2.14. Rarefaction curves calculated for the FS isolates, using different grouping criteria. (■) 100%, (▲) 98% percent *merA* gene sequence similarity.....67

Figure 2.15. Neighbor-joining analysis of 16S rRNA gene and MerA protein sequences of selected LS isolates that show incongruencies and of reference strains. The names of the isolates in both trees correspond to organism's phylogenetic group (16S rRNA gene). Bootstrap values higher than 50 are shown. Bar indicates 5% and 7% estimated substitution. Color indicates taxonomic affiliation. Orange: *alphaproteobacteria*, Purple: *betaproteobacteria*, Green: *gammaproteobacteria*, Red: Actinobacteria. *Sulfolobus solfataricus* was used as an outgroup for the 16S rRNA tree and *Thermus thermophilus* for the MerA tree..... 68

Figure 3.1. Map of the South River, which originates south of Staunton, Virginia and flows northward through the town of Waynesboro where the DuPont site sits, to the confluence with North River at Port Republic. These rivers are tributaries to the South Fork Shenandoah River (Reproduced from Flanders et al, 2010)..... 99

Figure 3.2. THg Concentrations in floodplain surface soil samples of 2-year (●), 5-year (●) and 62-year (●) flooding frequency (FP) along the South River as compared with the EPA Residential Soil Screening Value (–) (23 mg/Kg). At the point source the THg levels are the highest in all FP and the 2-year (●) (FP) exhibits the highest THg across the 26-Km of the gradient (Jordan et al, 2008)..... 100

Figure 3.3. Number of Hg^R colony forming units per g⁻¹ soil that appeared on day 3 (white bar), day 10 (grey bar) and day 17 (black bar) on 0.2X TSA amended with 100 μM HgCl₂ and inoculated with 100 μL of serially diluted soil suspensions of South River floodplain samples across the gradient.....102

Figure 3.4. Comparison of Hg^R CFU per gram of soil⁻¹ between non-spiked and spiked samples from sites RRM 9.1 and 19.7, that appeared on day 3 (white bar), day 10 (grey bar) and day 17 (black bar) on 0.2X TSA amended with 100 μM HgCl₂ and inoculated with 100 μL of serially diluted soil suspensions. Spiked samples were exposed to 10 μg/g HgCl₂ for 24 hrs prior to plating..... 103

Figure 3.5. Percentile contribution of the most abundant OTUs to the total relative abundance observed in all sites. Only peaks contributing >1% of the total relative abundance in all sites based on 16S rRNA gene-t-RFLP fingerprints are included. The black circles (●) indicate the number of sites that contained this OTU in their fingerprints. Colors indicate the environmental variable, which influences their distribution. Brown bar: clay content, yellow bar: pH, and blue bar: moisture content..... 105

Figure 3.6. Percentile distribution of the most abundant OTUs per site (colors in each bar) along the mile gradient based on 16S rRNA-t-RFLP fingerprints. Only OTUs that represent >1% of the total relative abundance in all sites are included..... 106

Figure 3.7. The percentile contribution of the most abundant OTUs. Only peaks contributing >1% of the total relative abundance in all sites based on *merA*-t-RFLP fingerprints are included. The black circles (●) indicate the number of sites that contained this OTU in their fingerprints..... 107

Figure 3.8. Rooted dendrogram of similarity values for South River samples. Similarity levels are indicated on each node. The Sorensen Similarity index was used to calculate similarity values based on peak presence/absence on the 16S rRNA gene-t-RFLP fingerprints. Clustering was done using the Un-weighted Pair Group Mean Average (UPGMA). The type of gradient refers to the variable that best explains the variation observed in these sites, based on the CCA..... 108

Figure 3.9. Rooted dendrogram of similarity values for South River samples. Similarity levels are indicated on each node. The Bray-Curtis index was used to calculate similarity values based on the normalized relative abundance of each peak on the 16S rRNA-t-RFLP fingerprints. Clustering was done using the Un-weighted Pair Group Mean Average (UPGMA). The type of gradient refers to the variable that best explains the variation observed in these sites, based on the CCA. Shannon Diversity Index (H') was calculated based on total abundance of peaks per site..... 109

Figure 3.10. Rooted dendrogram of similarity values for South River samples. Similarity levels are indicated on each node. The Bray-Curtis index was used to calculate similarity values based on the normalized relative abundance of each peak on the *merA*-t-RFLP fingerprints. Clustering was done using the Un-weighted Pair Group Mean Average (UPGMA)..... 110

Figure 3.11. Cluster diagram of similarity values for South River samples. Similarity values were calculated based on Shannon diversity index values and THg concentration in each sample. Clustering was performed using the Nearest Neighbor method. THg concentrations present in each site are also listed as well as calculated Shannon index (H') based on total abundance of peaks per site..... 112

List of Tables

	Page
Table 2.1. Summary of analyses of the physical/chemical properties of the Oak Ridge soil sample.....	49
Table 2.2. Bacterial counts from dilution series plated on 0.01X TSA medium supplemented with a range of mercury concentrations.....	50
Table 2.3. Bacterial counts from dilution series plated on 0.2X TSA medium supplemented with a range of mercury concentrations.....	51
Table 2.4. Diversity of LS and FS isolates' groups based on 16S rRNA gene sequences.....	60
Table 2.5. Primer sets used to amplify the <i>merA</i> gene from LS and FS isolates...	61
Table 2.6. Diversity LS and FS isolates' groups based on <i>merA</i> gene sequences	65
Table 2.7. Comparison of G+C mole% content between recipient strains' genomes and donor <i>merA</i> genes among LS Isolates.....	69
Table 2.8.1. Comparison of G+C mole% content between recipient strains' genomes and donor <i>merA</i> genes among Proteobacterial FS Isolates.....	70
Table 2.8.2. Comparison of G+C mole% content between recipient strains' genomes and donor <i>merA</i> genes among Actinobacterial FS Isolates.....	71
Table 2.9. Indications of HGT of <i>merA</i> among LS Isolates.....	72
Table 2.10.1. Indications of HGT of <i>merA</i> among Proteobacterial FS Isolates.....	73
Table 2.10.2. Indications of HGT of <i>merA</i> among Actinobacterial FS Isolates.....	74
Table 3.1. Physical and chemical characteristics of South River, VA, floodplain surface soils collected in February and March 2008. Samples were collected in forested areas of the floodplain with an average flooding frequency (FP) of 2-years.....	101
Table 3.2. Measures of heterogeneity for 16S rRNA gene- and <i>merA</i> gene-t-RFLP fingerprints and direct plating methods.....	104
Table 3.3. Univariate analysis predicting diversity as a function of site and soil characteristics.....	111
Table 3.4. Summary of results of Canonical Correspondence Analysis of the most abundant peaks ($\geq 1\%$ of the total area cutoff) in 16S rRNA-t-RFLP fingerprints of each site in relation to the environmental variables ^a at that site.....	113
Table 3.5. Weighted correlations among tested environmental variables representing the SR contamination gradient. Variables were extracted from Canonical Correspondence Analysis.....	114

Table A.1. LS isolates' phylogenetic associations based on 16S rRNA gene sequences.....	120
Table A.2. FS isolates' phylogenetic associations based on 16S rRNA gene sequences.....	122
Table A.3. LS isolates' phylogenetic associations based on MerA amino acid sequences.....	124
Table A.4. FS isolates' phylogenetic associations based on MerA amino acid sequence.....	126

Chapter 1 – Dissertation Introduction

1. Historical Perspective – Mercury (Hg)

-a. Global Distribution of Hg

Hg has a global distribution, as a result of natural weathering of its primary deposit, the earth's crust, and/or anthropogenic use in industries that release its vapor form to the atmosphere and its solid and soluble forms to the hydrosphere and pedosphere (Barkay, 2003).

Hg is a heavy metal, which has a unique character in that it can exist as a metallic liquid and vapor and in different ionic salts at standard temperatures and pressures (Summers, 1986). Natural deposits of Hg result from the weathering of cinnabar and every class of igneous rock, which all contain trace concentrations of Hg, as well as from volcanic and geothermal emissions (Baldi, 1997, Osborn et al, 1997). The abundance of Hg in the Earth's crust, ranges from 21 to 56 ppb in the lower and upper crust respectively, as an element or a binary mineral in cinnabar (Barkay et al, 2003). Anthropogenic activity, estimated to account for approximately 75% of the global input of Hg to the environment, has contributed to the widespread release of bioavailable Hg through processes such as burning of fossil fuels, the production of chloroalkali, electrodes and batteries, and dental restorations (Barkay et al, 2003, Osborn et al, 1997).

-b. Hg in Antiquity

Hg has been recognized as an element by scholars and philosophers since ancient times. In Greece, during the 4th century BC, the comic dramatist Phillipos mentioned Hg as a way to explain the movement of a wooden statue of Aphrodite, saying that the sculptor Dedalos had poured quicksilver (another name for Hg) into it.

As early as the 6th century BC in Greece and much earlier in Asia Minor, it was recognized that Hg is associated with cinnabar, a glossy red mineral that occurs naturally in areas of volcanic activity. And in the 3rd century BC, Theophrastus, who succeeded Aristotle in presiding over the Peripatetic school in Plato's Academy, described the isolation of Hg from cinnabar, which is the first mention of isolating any metal from its ore (Theophrastus, 3 BC). The process involves using cinnabar mixed with vinegar and ground in a copper vessel with a copper pestle. The Hg is released by volatilization from cinnabar and the sulfur combines with copper to form copper sulfide, which was used as a treatment for leg ulcers and open wounds by Hippocrates. This is the first account of Hg having practical uses, until the first century BC, when Vitruvius, a Roman architect, described the extraction of gold from its ore, using an old cloth and quicksilver (Takacs, 2000).

-c. Hg in the Post-Industrial Era

Although Hg was recognized as an element having practical uses since antiquity, its toxicity was discovered about 60 years ago. By then Hg was being used widely as a disinfectant (thimerosal and mercurochrome) and in many industrial processes as a catalyst (FDA). In the early 1950's inhabitants of Minamata Bay, Japan, exhibited neurological disorders such as cerebellar ataxia, dysarthria and loss of hearing. Scientists linked the increase in neurological disorders to the fish caught in the bay and consumed by the human population. Fish were found to contain high level of methyl Hg, a neurotoxic substance. The contamination was finally attributed to Nihon Chisso Hyrio Corporation, which discharged their waste effluent from the production of acetaldehydes, using Hg(II) as a catalyst, to the bay (Clarkson, 2002).

These neurological disorders, distinctly named Hg poisoning, were also observed in the early 1970s in Iraq. This time the poisoning was attributed to the

consumption of rice originating from Mexico. The seed grains had been treated with short-chain alkyl Hg against fungal infection (Bakir, 1973).

Soon thereafter, microbial Hg transformations in the environment were discovered. The bacterium *Staphylococcus aureus* detoxified its cellular surroundings from both methyl and elemental Hg in nosocomial settings (Novik and Roth, 1968, Richmond and Madeleine, 1964, Moore, 1960), and other bacteria methylated Hg(II) in aquatic sediments (Baldi, 1997, Swedish Expert Group, 1971). This was a landmark discovery because bacteria are at the base of the aquatic food chain. Thus methyl Hg produced by bacteria, bioaccumulates and biomagnifies in "higher" organisms from plankton to herbivores to top fish predators, such as tuna and sharks, and finally to humans, causing degeneration of the central nervous system leading to Hg poisoning as was the case in Minamata Bay and Iraq.

Since then, Hg resistant bacteria have been isolated from various habitats such as water, sediment, soil, and clinical samples (Osborn et al, 1997). Hg resistance genes of Gram negative bacteria have been isolated from immense geographical distances and are virtually identical to those of the two prototype *mer* operons pKLH2 or Tn5041 representing a well defined subdivision of *mer* operons carried by Gram negative bacteria which diverged almost a billion years ago from *mer* operons of Gram positive bacteria, which also have a worldwide distribution (Bogdonova, 1998, Nakamura and Silver, 1994, Yurieva et al, 1997).

2. The Mercury Detoxification Mechanism: *mer* operon

The most efficient Hg detoxification mechanism among microorganisms is conferred by the mercury resistance (*mer*) operon, which is comprised of genes that encode proteins of regulatory, transport and enzymatic functions (Osborn et al, 1997). In a typical Gram negative *mer* operon there are 4-5 structural genes, *merTPCA(B)*, downstream from the *mer* operator/promoter region. In addition, two

regulatory proteins are encoded by *merR* and *merD*. The protein MerP is a small periplasmic protein that binds Hg(II) by displacing any ligand attached to it with its two cysteines. It then exchanges Hg(II) to the two cysteine residues found in the inner membrane spanning protein MerT. MerT transports Hg(II) in the cytosol where it interacts with MerA, the mercuric reductase enzyme, and gets reduced to Hg⁰, a volatile, lipid soluble form, that diffuses through the membrane without the assistance of efflux pumps (Barkay et al, 2003, Summers, 1992). Some *mer* operons have an additional gene, *merB*, which encodes the organomercurial lyase (MerB), enabling resistance and reduction of organomercury compounds.

Mercuric reductase (MerA) is a flavin-dependent disulfide oxidoreductase that shares great structural similarities, with other proteins of this family, among them, glutathione reductase, and thioredoxin reductase. They also share functional similarities, as they all protect cells from oxidative stress (Clarkson, 2002, Bogdonova et al, 1989, Summers, 1986). These similarities have set the foundation for the widely accepted hypothesis that all these proteins share a common ancestor. Furthermore, while structural similarities between Gram positive and Gram negative MerA proteins, suggest a shared common ancestor, they also exhibit certain distinct structural traits to infer divergence in their evolution (Bogdonova et al, 1989).

3. The Soil Ecosystem and Hg^R Bacterial Communities

Soil is a three-dimensional natural body comprised of 4 abiotic components: air, water, inorganic and organic matter. The different proportions of these 4 components play a fundamental role in the formation of gradients in the soil, rendering it a highly heterogeneous environment, which supports microbial communities of highly diverse taxonomy and functionality. For example, the prokaryotic diversity is the lowest in cultivated forest soils, with 1.4×10^7 cell/g and 35 genome equivalents, calculated by comparison to the *E. coli*'s 4.1×10^6 bps

genome, while pasture soils show the highest abundance of 1.8×10^{10} cell/g and 3500-8800 genome equivalents (Torsvik, et al, 2002)

Microbial cells inhabit soil micro-particles of a few micrometers diameter, which are sometimes thought of as islands, and respond acutely to changes in biotic/abiotic factors. Their fitness depends on two kinds of adaptation strategies. Physiological strategies, which allow microbes to properly interact with the immediate biotic/abiotic environment, and metabolic strategies, that enable microbes to sense the concentration of compounds along a gradient and "fine-tune" their metabolism to these locally-determined conditions (vanElsas, et al, 2007).

Environmental stress such as climate change and heavy metal pollution influence the community composition as well. Short-term Hg stress, at the soil aggregate dimensions, caused no significant change in the abundance of the total heterotrophic bacterial community, while the Hg^R populations' abundance increased. The outer fractions of soil aggregates had the most pronounced increase in the abundance of Hg^R bacteria, which were found to be taxonomically related to Gram negative bacteria (Ranjard et al, 1997).

Freshly added Hg to soil microcosms on the other hand caused a significant change in abundance of both total heterotrophic and Hg^R populations. Hg-stress led to a 10-fold increase in the heterotrophic populations (10^8 CFU/g), while Hg^R communities increased by 5 orders of magnitude replacing all other heterotrophic populations after 18 days of incubation. The total phylogenetic diversity of the heterotrophic community decreased and was replaced by fast-growing Hg^R populations. In contrast, the functional diversity based on sole carbon source utilization by Ecoplates[®], remained the same throughout the incubation and is indicative of Hg adaptation and selection of a few abundant Hg^R species capable of utilizing a broad variety of carbon sources (Rasmussen et al, 2001).

Finally, long-term Hg stress along a gradient, showed that the highest Hg^R heterotrophic community abundance is at the point source, while the highest total heterotrophic abundance is observed away from the point source. The phylogenetic diversity followed the same pattern, while the functional diversity, determined by sole carbon source utilization by Ecoplates[®], remained undisturbed across the gradient (Muller et al, 2001).

In all these studies irrespective of the duration of Hg contamination, one can observe the same patterns in the phylogenetic and functional diversity of the heterotrophic microbial communities. Namely, in the presence of Hg stress, total heterotrophic populations are slightly affected, Hg^R-populations become more abundant, and the functional diversity remains the same as if not influenced by the stress.

4. Effect of Disturbance and Stress on Diversity and Ecosystem Functions

Little is known about the effect of Hg contamination on bacterial communities of floodplain ecosystems such as the East Fork Poplar Creek (EFPC), TN, and the South River, VA. In general, increased stress, in the form of metal contamination, increased competition for limited resources or a sudden change in the local environment of bacterial communities, leads to a decrease in diversity. This manifests in the loss of ecosystem functions and a decrease in species evenness, a measure of redundancy of ecosystem functions in a community. A selection of species with specialized functions, such as Hg detoxification, ensues (Kis-Papo, 2003).

This “purifying effect” is more pronounced at the highest end of the disturbance/stress gradient, similar to the 2 extremes of the r & K continuum, and/or in cases where the chemical conditions in the environment don’t alleviate the stress by reduction of its bioavailability (ie. HgS). The resistant and/or resilient populations,

work to detoxify their immediate environment and given enough time, the local environment returns to pre-disturbance conditions, where ecosystem functions and evenness are restored and equilibrium is reached again (Allison et al, 2008, Kis-Papo, 2003).

The time it takes to return to equilibrium depends on the specialization and redundancy of functions in a given community. These 2 factors also determine how stable an environment is in response to outbreak (Elton, 1958), drought (Tillman, 1996) or any stress for that matter. The tropics exemplify a stable environment where diversity is high due to specialization and redundancy of functions occurring simultaneously (Dobzhansky, 1950).

-a. Oligotrophs and Copiotrophs

Oligotrophs preferentially inhabit niches of low substrate concentration and energy flow although they tend to remain at constant levels in soil, irrespective of local environmental conditions (Semenov, 1991). They metabolize and reproduce under conditions of limited resources at relatively low growth rates (Van Elsas, 2007), as they have effective systems for uptake of both organic and inorganic nutrients at low concentrations, a low energy source:biomass ratio and the O₂ uptake rate is low (Koch, 2001, Semenov 1991).

The term oligotroph was coined by Weber in 1907, and to complement it, in 1981, Pointdexter, invented the term copiotroph (Koch, 2001, Pointdexter, 1981). These heterotrophic organisms metabolize and reproduce at high growth rates, if and only if resources are abundant in the easily oxidizable organic form (Palijan, 2008, Van Elsas, 2007).

-b. r & K Strategists

Life history traits are used by theorists to shed light on the evolutionary forces that shape the fitness of organisms (Pianka, 1970). In microbial ecology body size cannot be used as a distinguishing factor as they all share the same size, yet microbes like “higher organisms” have evolved strategies based on other life history traits such as growth, metabolism and fecundity, that enable them to survive and successfully maintain themselves within communities. One such theory is that of r & K strategists, a term coined by MacArthur and Wilson (1967) as part of island biogeography (MacArthur and Wilson, 1967). In terms of theory, r strategists are ecologically equated to copiotrophs, on the grounds that they both are better fitted in unstable and transient environments, of no crowding, where organic nutrients are of the easily degradable form and metabolites are invested in biosynthesis and reproduction (Semenov 1991). Thus, evolution here is thought to favor productivity (MacArthur and Wilson, 1967).

On the other side of the spectrum, K strategists resemble oligotrophs, as they share physiological responses to life in stable environments of low resources and high crowding conditions. In response to the increased competition for territory at carrying capacity, K-strategists have evolved anticompetitor adaptations in the form of antibiotic and toxin production (De Leij, 1993, Pianka, 1970). Interestingly enough, r-strategists have been shown to be sensitive to antibiotics such as streptomycin and cyclohexamine (Stenstrom, 2001). In K-selection evolution favors efficiency of conversion of food into reproduction, since resources are so limited that wasting them would be detrimental to fitness and survival (MacArthur and Wilson, 1967, Dobzhansky, 1950).

r and K strategists are always present in the environment, in a continuum, determined by substrate bioavailability at any given time. Under conditions of high substrate availability, r can reach up to 100%, while under low substrate availability,

r ranges anywhere from 5-20% of the total community, a shift that takes only a few days in a controlled lab setting (Stenstrom, 2001). The heterogeneity of the soil environment whose spatial structure is patchy, consisting of diverse niches, allows for the co-existence of r & K strategists. Which further substantiates the fact that soil microbiologists find consistently bacteria representing all strategies (Ettema, 2002).

Although, historically r & K selection has been described in terms of species adopting these strategies, it is thought that an environment is in a K-state when it is pristine, undisturbed and where resource availability is limited. It follows that a disturbed and/or in early succession transient environment is at r-state (Deleij, 1993). In general oligotrophic environments have higher evenness and spp. richness than copiotrophic environments (Torsvik et al, 2002, McCaig et al, 2001, Finkel and Kolter, 1998)

-c. N₂ fixation & Organic Matter Decomposition

Organic matter decomposers, belonging to families of the Phylum Actinobacteria, breakdown complex organic compounds, such as cellulose, lignin and chitin releasing readily bioavailable substrates like glucose from high molecular weight plant and fungal polymers (Ventura et al, 2007). Other ecosystem services carried out by Actinobacteria include, but are not limited to, symbiotic N₂ fixation, antibiotic and extra-cellular polysaccharide production, spore formation and production of probiotic secondary metabolites (Conn and Franco, 2004, Graph et al, 1995).

Strains of N₂ fixers are found in 38 bacterial genera, mainly among divergent groups within the alpha Proteobacteria and the Purple Sulfur, and secondarily among the Green Sulfur and Green Non Sulfur groups (Dixon and Wheeler, 1986). They are also found among Actinomycetes, Cyanobacteria and the Archaea. They are metabolically diverse, partaking in autotrophy/heterotrophy/photosynthesis, and

they can be symbiotic or free-living, respiring oxygen or just nitrate. In nature they exist as filaments or single cells (Patriarca et al, 2002). In the nitrogen cycle, denitrifiers lead to the loss of nitrogen, and N_2 fixing organisms turn it back. N_2 -fixation is a highly important ecosystem service as it turns nitrogen into the bioavailable form, to be used for amino acid synthesis and also because the plant-symbiont becomes autotrophic for nitrogen after colonization by the N_2 -fixing bacteria. When in symbioses with plants, N_2 -fixers are supplied with ample amounts of glucose by the host (Patriarca et al, 2002). In free-living conditions, N_2 -fixers depend on the organic matter decomposers for the supply of easily degradable glucose. N_2 -fixers of the *alphaproteobacterial* genus *Rhizobia* are able to lead a free-living existence, but are unable to fix nitrogen in the absence of a host plant (Gadkill, 1959).

N_2 fixers and organic matter decomposers, exemplify K strategists. Usually, Actinobacterial and *alphaproteobacterial* communities in soil remain constant in both species richness and composition across treatment gradients. *Alphaproteobacteria* constitute 18% on average of the total microbiota in the soil system depending on the soil type, while Actinobacteria constitute 13% on average of the total community (Spain et al, 2009, Nemergut, 2008, Jansenn, 2006).

In environments where these two guilds co-exist, N_2 fixers provide Ammonium (NH_4^+) and decomposers provide glucose. This is an essential exchange as short supply of either resource limits the rate of both functions. In C-poor environments, the very elaborate nitrogenase complexes, essential for N_2 -fixation, cannot be produced as they are metabolically expensive, thus N_2 -fixers suffer losses. In turn, the N-limitation, affects decomposers, who make a substantial investment in the decay of lignin for its high N-content and in the process readily bioavailable compounds rich in C-content are released and used to carry out ecosystem services such as N_2 -fixation (Nemergut, 2008, Ventura et al, 2007, Craine et al, 2007).

-d. Hg Detoxification

As there is no-known biological function to Hg and because of its ubiquitous presence in all spheres, bacterial communities have evolved a variety of resistance mechanisms to detoxify their cells and the surrounding environment from the toxic metal (Summers, 1986). It has been reported that 1-10% of all heterotrophic aerobic cultured bacteria in a given community are Hg^R, by the enzymatic activity of proteins encoded by the genes of the mercury resistance (*mer*) operon (Barkay, 1987). This is the most efficient of all microbial Hg detoxification mechanisms thus it qualifies as an evolutionary stable strategy (ESS; Maynard Smith, 1974).

Rasmussen et al, (2001) and Muller et al (2001), independently reported that in controlled lab experiments, addition of Hg to soil microcosms results in a $\geq 5x$ increase of the Hg^R populations. They explain the phenomenon in terms of r & K-selection. Hg^R populations are deemed r-strategists, which replace the Hg sensitive (Hg^S) K-strategists. This explanation is contrary to observations that *alphaproteobacteria* and Actinobacteria (N₂-fixers and organic matter decomposers), classic K-strategists, become more abundant in metal contaminated environments (Sandaa, 1999). It is true and well documented, that Hg addition to soil causes oxidative stress to cells, leading to lysis and death (Casucci et al, 2003, Barkay, 1987, Komura and Izaki, 1971). Thus fast growing r-strategists are selected as the first responders to deal with disturbance caused by the nutrient rich cell exudates and K-strategists, a minority of the community, rip off the benefits of the service that r-strategists provide. Thus on the oligotrophic/copiotrophic gradient the majority of bacteria are indeed r-strategists (Pianka, 1970).

In contrast, on the Hg gradient, resistant organisms, that detoxify their immediate environment are selected, and Hg^S die off or rip the benefits of the detoxification provided by the Hg^R. Lenski and Hattingh (1986) found that resistant and sensitive populations do co-exist in the presence of metal or antibiotic

contamination in model systems (Lenski and Hattingh, 1986), and Slater et al (2010) found that Hg stress felt in sub-millimeter scale gradients in soils selected for Hg^R populations in distances 180-350 μm away from the source, Hg^S populations further than the 350 μm mark, and no cell growth was detected closer than the 180 μm mark (Slater et al, 2010).

The co-occurrence of the oligotrophic/copiotrophic and Hg-stress gradients may be better explained by the 3 response strategies of plants described by Grime (1977), as opposed to the animal-based r & K strategies (Grime, 1977). In the plant model, there is a ruderal (R), a competitive (K) and a stress tolerant (S) strategy, and in situations where the intensity of both disturbance and stress are low, the competitive strategy is selected. In high disturbance and low stress levels, the ruderal strategy outcompetes the rest. And, in low disturbance and high stress levels the stress-tolerant strategists dominate in the community. Finally, no viable strategy exists when the intensities of both disturbance and stress are high, while the 3 coexist in intermediate levels of competition (carrying capacity), disturbance and stress (Grime, 1977). Indeed, Kim et al (2008), showed that spatial structure in the form of patchy habitats, stabilized synthetic multispecies bacterial communities of N₂-fixers, organic matter decomposers, and antibiotic resisters in a lab setting, under oligotrophic conditions, and the separation distance that allowed for the stable co-existence of the 3 species is 0.6 mm (Kim et al, 2008).

5. Horizontal Gene Transfer (HGT)

In Macro-ecology, environmental stress or perturbation, affect the community differentially, depending on the initial biodiversity exhibited by the community. In general, communities with high levels of phylogenetic biodiversity and redundancy in their ecosystem functioning (evenness), are more resilient and resistant to stress and they tend to return to pre-stress equilibrium fast (Wittebolle et al, 2009,

MCGrady-Steed & Morin, 2000, Tilman 1996, Tilman & Downing, 1994).

In Micro-ecology, on the other hand, the positive association between biodiversity and resistance to stress is not as straight-forward. The primary reason for this disconnect is the overwhelming diversity of microorganisms that makes it impossible to identify individual taxa and relate them to ecosystem processes (Allison and Martiny, 2008). Another process that complicates the picture even more, is horizontal transfer of environmentally beneficial traits conferring antibiotic and metal resistance, xenobiotic degradation, and even photosynthesis and N₂-fixation (DeLong et al, 2006, Tyson et al, 2004, Top and Springael, 2003). These traits are selected for and magnified when bacterial communities are under stress or disturbance. HGT results in smudging taxon barriers among members of the community since readily available "anti-stress" gene libraries can be shuffled around irrespective of the members' phylogeny. Thus HGT improves the community's resistance to stress at levels that would have been impossible had that community relied solely on its own "chromosomal" diversity (Gelder et al, 2008, Slater et al, 2008, Gogarten and Townsend, 2005).

HGT is the exchange of genetic material among populations of donor and recipient prokaryotic cells that have no parent-offspring association (van Elsas and Bailey, 2002). HGT can be thought of as the equivalent of sexual reproduction in higher organisms, as both processes lead to genetic variation (Levin and Bergstrom, 2000). The three essential mechanisms that facilitate HGT are transformation, transduction, and conjugation (Davison, 1999) and the newly discovered membrane vesicles that ferry plasmids in the nosocomial pathogen *Acinetobacter baumannii* (Rumbo et al, 2011).

The abiotic factors that determine the effectiveness of HGT are: nutrient availability, presence of surfaces, clay content, water holding capacity and temperature (Hill and Top, 1998, Ashelford, 1997, van Elsas and Trevors, 1990).

HGT is accelerated, when members of the community share genome size, G+C content, and carbon utilization, and is independent of physical proximity of exchanging communities (Jain et al, 2003). The mobile genetic elements (MGE) that carry out these transfer processes are prophages, plasmids, integrons and transposons (van Elsas and Bailey, 2002). Housekeeping genes are not usually carried by MGE, yet there are cases such as the *Rhizobium* sp. NGR234 536 Kb megaplasmid, which carries a wide array of functional genes essential for symbiotic N₂-fixation (Perret, et al, 1999).

Through HGT, *mer* determinants get disseminated globally. *mer* operons isolated from immense geographical distances are virtually identical to those of the two prototypes carried on transposon (Tn5041) and in plasmid (pKLH2) (Bogdonova, 1998, Yurieva, 1997, Nakamura & Silver, 1994). *merA* genes isolated from organisms affiliated to a wide range of Taxonomic groups, show phylogenetic incongruencies, when compared to the 16S rRNA genes, further supporting that HGT influences the evolution of this gene (Lal and Lal, 2010, Osborn et al, 1997).

Also, analysis of proteins specific to Actinobacterial species, were also encoded by the genome of the *alphaproteobacterial Magnetospirillum magnetotacticum*, leading to the hypothesis that these genes were transferred by HGT (Gao et al, 2006). Finally, in members of the N₂-fixing Rhizobia, genes essential for symbiosis with leguminous-plants are carried in both chromosomes and plasmids and show a mosaic structure, suggesting evolution through HGT as is the case for the two *mer* operon prototypes (Gonzalez et al, 2006, Gonzalez et al, 2003, Bogdonova, 1998, Yurieva, 1997).

The specific conditions under which these elements can be maintained and get established in bacterial populations are still elusive (Bergstrom et al, 2000). It is thought that plasmids can be infectious transmitted and maintained as a result of selection sweeps. Selection sweeps occur when mutation or immigration of a favored

gene carried in a plasmid appears in populations and through selection reaches high frequencies leading to reduction of populations' genetic diversity ("purifying effect") (Kis-Papo, 2003). Besides selective sweeps, it is thought that plasmids are maintained, as they provide beneficial or "exotic" genes that bacteria could not otherwise afford to carry since their genomes are under selective pressure to be small and flexible (van Elsas and Bailey, 2002, Lilley et al, 2000)

6. Biogeography

Biogeography is the study of the distribution of taxonomic groups that is influenced by climate. Macroscopic plant and animal species show limited distributions across geographical gradients of habitat area, isolation and latitude (Horner-Devine et al, 2004, MacArthur and Wilson, 1967). The spatial structure of microbes is thus predictable and dependent on climate, dispersal barriers, speciation, extinction and historical contingencies over geological and evolutionary times (Martiny et al, 2006, Green et al, 2004).

The spatial distribution of microbial taxonomic groups is not as clear, nor as predictable. Bacteria have a cosmopolitan distribution rather than a local one, because they are not affected by climatological and geological phenomena the same way microbes do. Bacterial distribution is not influenced by barriers in dispersal, that would lead to speciation, as an estimated 10^{18} viable cells are transported through the atmosphere across continents (Escobar-Paramo et al, 2005). Bacteria also exhibit low negative interactions and enormous population sizes thus extinction events are rare, and species richness is high, based on the equilibrium theory of island biogeography (Falkowski et al, 2008, MacArthur and Wilson, 1967). Taken together, high dispersal ability and low local extinctions, attest to the observed cosmopolitan microbial distribution, which doesn't always abide to the species/area relationship that explains so consistently all ecological patterns of

macrobial species (Reche et al, 2005, Horner-Devine et al, 2004, MacArthur and Wilson, 1967).

Baas Becking and Beijerinck, first formulated this distinctive feature of bacterial species, in the famous statement "everything is everywhere, but the environment selects" (de Wit and Bouvier, 2006, Baas Becking, 1934, Beijerinck, 1913). They observed that specific types of enrichments would always select for particular functions irrespective of active or dormant metabolic activity in their natural habitat, thus they concluded that bacterial distribution can be understood solely in terms of habitat properties and requires no historical explanation.

Indeed, Fierer and Jackson (2006) showed, that distribution of soil bacteria along a continental-wide latitudinal gradient, was not random, but showed different patterns than those observed in macrobes. Bacterial composition and diversity in soils based on t-RFLP fingerprints was highly correlated with pH and not with mean annual temperature and potential evapo-transpiration as is the case for plant and animal communities at this scale.

Examination of genetic divergence among taxonomic groups based on the 16S rRNA gene found in the "island-like" hot spring environments, also agrees with "the environment selects" statement (Papke et al, 2003, Whittaker et al, 2003). Yet when greater phylogenetic resolution is employed, by examination of protein-coding loci, genetic distances do increase proportionally with geographic distance (DeBruyn et al, 2011, Whittaker et al, 2003). This finding is in accordance with the theory, that for bacteria, geographical patterns should be based on the core metabolic machineries, and not on taxonomic groups, as these machineries are maintained and unperturbed over evolutionary times (Falkowski et al, 2008). This type of examination is very attractive, as it bypasses the need for a distinct species concept for microbes, which do not fit the biological (Mayr, 1942), ecological (Van Valen, 1976) and morphological (Cronquist, 1988) species concepts.

Finally, another factor that contributes to the delinquent behavior of bacteria to geographic distribution patterns, is the horizontal transfer of genes. These events are independent of both taxonomic groupings and of physical proximity of exchanging populations, allowing bacteria to overcome constraints to genetic diversification and isolation mechanisms that would otherwise limit their distribution (Jain et al, 2003, van Elsas and Bailey, 2002, Davison, 1999).

7. Study Scope and Objectives

The central scope of this study is to determine the effects of long-term Hg contamination on the phylogenetic, functional, and metabolic diversity of Hg^R bacterial communities in riverine floodplain ecosystems. The floodplains of the East Fork Poplar Creek in Tennessee, and of the South River in Virginia are ideal sites for this study as they were contaminated with Hg, by industrial processes for about 10 years, 60 years ago.

Specific Objectives:

1. Determine the effect of nutrient availability and Hg stress on the diversity and abundance of Hg^R and Hg^S bacteria in the floodplain samples.
2. Isolate Hg^R bacteria and assess their phylogenetic distribution by comparing isolates' 16S rRNA gene sequences to those of known organisms.
3. Assess prevalence of *mer* determinants among the isolates to determine the specific mechanism of Hg detoxification employed by the Hg^R community.
4. Determine incidences of Horizontal Gene Transfer (HGT) among the Hg^R isolates based on
 - a. phylogenetic incongruencies between 16S rRNA gene sequences and MerA amino acid sequences
 - b. G+C content anomalies between 16S rRNA and *merA* gene sequences

-c. presence of plasmids in Hg^R bacterial genomes

5. Determine diversity and coverage of the sampling effort based on 16S rRNA and *merA* gene sequences.
6. Determine ecosystem services provided by Hg^R bacterial isolates in the Carbon and Nitrogen cycles.
7. Design and test a culture-independent method, targeting *merA* genes directly from environmental samples, to overcome limitations of culturing, and assess their diversity.
8. Study biogeography patterns along a gradient of Hg contamination to assess the influence of climate on the distribution of taxonomic groups in the floodplain ecosystem.

Chapter 2 - Effect of Nutrient Disturbance and Mercury Stress on Diversity of Floodplain Bacterial Community (EFPC Floodplain)

Introduction

The Oak Ridge Reservation (ORR) in Tennessee (TN) was built in 1942, as one of the many sites of the Manhattan Project, whose main purpose was to manufacture nuclear weapons. The ORR contained 4 industrial plants in total, among which, the Y-12 National Security Complex (Y-12 NSC) plant was used initially for the enrichment of Uranium-235 (^{235}U) from the heavier ^{238}U by electromagnetic separation processes (Figure 2.1). In the late 40s, the Uranium operations ceased in the Y-12 plant and were replaced by the production of Lithium isotopes ^6Li and ^7Li (Brooks and Southworth, 2011).

Lithium-7 isotope was in increasing demand, for its potential use in molten salt reactors for the aircraft nuclear propulsion program, and ^6Li isotope was used for the production of thermonuclear weapons. Lithium isotope separation, was achieved by the Column Exchange Process (COLEX) in the Y-12 plant, using liquid elemental mercury (Hg) to dissolve ^6Li . It has been estimated that in the 13 years of ^6Li production, 11 million Kilograms of Hg were used, and about 3% were released into the air, soil and waters of the East Fork Poplar Creek (EFPC), which originates on the Y-12 plant and spans 24 kilometers from East to Northwest, flowing into the Poplar Creek, a tributary of the Clinch river (Brooks and Southworth, 2011, Barnett and Turner, 2001, Campbell et al, 1998).

Although the operations for the Lithium isotope separation in the Y-12 plant have ceased for 60 years now, Hg levels in the air, soil, water environments of the EFPC and its associated biota are considerably high (the State of TN's Hg limit in water is 51 ng/L and EFPC level is ~ 200 ng/L). It is thought that groundwater in the headwaters of EFPC, heavily contaminated with dissolved Hg, enters the surface flow

under wet conditions, thus keeping the Hg in the EFPC at high levels (Campbel, 1998). Inorganic Hg is subsequently used as a substrate in the formation of Methyl Hg (MeHg), the neurotoxic substance that poses serious health risks (Gu et al, 2011, Barnett and Turner, 2001).

Mercury in EFPC soils is found primarily in the mercuric sulfide (HgS) form, which dissolves poorly at neutral pH (Pant and Allen, 2007). Thus, its bioavailability is much lower than that of the HgCl₂ form. Since Hg is present in such high levels in EFPC neutral soils, it seems that most of it is not readily bioavailable (Gu et al, 2011). However, recent studies showed that bioavailability of Hg from the HgS compound considerably increases under conditions of 1. high concentrations of the readily decomposable light fraction Organic Carbon (OC), 2. increased forest cover and 3. acidic pH, (Han, et al, 2008, Pant and Allen, 2007). It is thought that Hg binds to the reduced sulfur sites of humic substances in the soil, and since detrital organic carbon of the lighter fraction is higher and more bioavailable under the leaf litter of plant-covered land, Hg dissolution and bioavailability increase (Han et al, 2006).

The percent bioavailability of Hg across the soils of EFPC was determined by an *in vitro* leaching procedure by SW-846 Methods 7470 and 7471 whereby distilled, deionized water is used to obtain the leachate (Ruby et al, 1993). The dissolved fraction of metals in the leaching procedure is termed bioavailable. The reported mean bioavailability was ~ 5%. The HgS form was 1% bioavailable, yet DOC and humic acids increased its solubility. The HgCl₂ form was 100% bioavailable (Barnett and Turner, 2001).

A search of the existing literature on the effect of Hg on the soil bacterial communities of the EFPC site revealed a difference in findings based on the methods used to study these communities. Vishnivetskaya et al (2011) used pyrosequencing, a culture independent method, to amplify the V4 hypervariable region of the 16S rRNA gene, which ranges in size from 200 to 220 bps. It was shown that 11 phyla

were present in 6 sites (5 contaminated and 1 control), and that all the classes of Proteobacteria were the most abundant (23 - 59%) and present in all sites. Actinobacteria (0.01 to 0.8%) and Firmicutes (0.03 to 5.26%) were minorities in the sequence inventories and were not found in the most contaminated site (Point source site EFK 23.4), contrary to the *alphaproteobacteria*, which were positively correlated with contamination levels (Vishnivetskaya et al, 2011).

A direct cultivation method was used by Rasmussen et al (2008) to isolate heterotrophic aerobic soil bacteria on 0.1X Tryptic Soy Agar (TSA) amended with 4 μM of HgCl_2 . It was determined that only 3% of the total Colony Forming Units (CFU) were resistant to Hg at this concentration. Phylogenetic analyses indicated that 93% of the community, were Actinobacteria, 2% *alpha*- and 5% were *betaproteobacteria* (based on 16S rRNA sequences). A pre-incubation that mimicked natural conditions selected for the above plus Firmicutes and Bacteroidetes but in different proportions. Under these conditions *betaproteobacteria* were the majority (73%), Actinobacteria dropped to 11% and *alphaproteobacteria* were just 0.5%.

In soil microbiology, oligotrophs are separated from copiotrophs on the basis of their inability to grow on high-nutrient media such as TSA or Nutrient Broth (NB) (Hashimoto et al, 2006). To select oligotrophs, the media are diluted 100-fold (Whang and Hitori, 1988). Even though the diluted form of NB (DNB) is widely accepted as the "oligotrophic" selection level, in some studies a 10-fold dilution of the media has been used to follow the progression of a community in the r & K continuum (Palijan, 2008, De Leij, 1994). Neither dilution level strictly adheres to Pointdexter's oligotrophic range of organic carbon content (1-15 mg/L), yet the 100-fold dilution is closer (88 mg/L) than the 10-fold dilution (~900 mg/L) (Pointdexter, 1981 Difco™ & BBL™ Manual (2nd Edition)).

Study Scope

Here I report the use of a direct cultivation method to isolate 87 bacteria, under both oligotrophic and copiotrophic conditions in the presence of Hg, from soil samples originating from the long-term Hg contaminated EFPC, and the characterization of the community as reflected by the properties of the selected bacterial strains at the phylogenetic, functional and metabolic levels.

Materials & Methods

Sampling Site and Historical Reference

Soil samples were acquired from the EFPC site in Oak Ridge, Tennessee. EFPC is located north of the Y-12 Plant, one of the main facilities of the U. S. Department of Energy on the Oak Ridge Reservation (ORR). During the mid 1950s and early 1960s, EFPC received effluent discharges from the Y-12 Plant where Hg was used in a lithium isotope separation process for the production of thermonuclear fusion weapons (Campbell et al, 1998).

Soil samples were collected on 8/13/07 from the top 20-30 cm layer of an exposed stream bank (site EFK 24.0). The soil was dry sieved to less than 1 mm. The Hg concentration at the time of collection was about 1000 ppm (George Southworth, Personal Communication). Upon receipt in the lab, the soil samples were stored both at 4 and -20 °C in the dark, for microbiological and chemical and molecular analyses, respectively.

Soil Analyses

The sequential loss on ignition (LOI) is a method commonly used to estimate the organic and inorganic content of soils and sediments (Santisteban et al, 2004). The organic carbon (OC) content has been empirically calculated as half of the

LOI₅₅₀, while the inorganic carbon (IC) content is $0.273 \times \text{LOI}_{950}$. This calculation is based on the assumption that ignition follows a stoichiometric relationship and that the amount of carbonate is $1.73 \times \text{LOI}_{950}$ (Dean, 1974).

The experimental design was based on that of Santisteban et al (2004) and was done in triplicate. Initially, samples were placed in crucibles and incubated at 105 °C for 24 h, to remove water. Dried samples were placed in the furnace oven for 4 h at 550 °C to burn the organic carbon, and at 950 °C for 2 h to burn the inorganic carbon. Crucibles were weighed out empty, filled with soil, and before and after each of the incubations.

To assess the ability of the soil to retain water, nutrients and other minerals, the water holding capacity (WHC) experiment was performed. In general, soils rich in organic matter have greater water holding capacities than those low in organic matter. Weights were taken before every step. Single dry membranes (Whatman Grade 2 Filter paper, Whatman Inc., Piscataway, NJ) were fitted in 3 Hilgard cups and they were moistened with water. Soil was added to the cups and the apparatus was placed in a container with the water level lower than the soil surface. When a wet gleam covered the whole surface of the soil, the cups were transferred and stored for 1 h in a dry container and incubated at 105 °C overnight (Wilke, 2005).

To determine the pH, 20 g of soil was mixed with 20 ml of 2 mM pyrophosphate buffer and stirred for 30 min. The slurry was allowed to sit for 2 h to let the particles settle before a reading was taken using a pH meter (Hartman et al, 2008). The texture of the soil sample was determined by the sedimentation method in the Rutgers Soil Testing Laboratory (Kemper and Rosenau, 1986).

Abundance, isolation, identification and characterization of total and Hg resistant (Hg^R) bacteria from soil samples.

Isolation of Hg^R bacteria from soil samples

Based on reports documenting that 1-10% of all bacteria are Hg^R (Barkay, 1987), a plating efficiency protocol was designed to determine the appropriate Hg concentration that would select for 10% of the total culturable counts (i.e. the Hg^R bacteria) in the soil sample from Oak Ridge. The determination of Hg^R on the specific media used, is an essential step to our future analyses since Hg bioavailability and thus toxicity, varies depending on medium constituents (Ramamoorthy and Kushner, 1975). In general, Hg²⁺ ions bind to sulfhydryl, imino nitrogens and/or carboxyl groups of rich full strength media constituents, such as tryptone and peptone, to form complexes, which decrease the Hg concentration in solution by 30-40% (Chang et al, 1993). To avoid the loss in Hg bioavailability observed with full strength media, we used BBL™ Tryptic Soy Broth (TSB) medium (Becton, Dickson & Comp., Sparks, MD) diluted 5 and 100 times from the original 1X recipe, to get 0.2X [(Full Strength (FS))] and 0.01X [Low Strength (LS)] strengths. The 0.01X TSA medium mimics oligotrophic conditions (total organic carbon content = 88 mg/L) and 0.2X TSA, copiotrophic conditions (total organic carbon content = 1763 mg/L).

Specifically, the soil sample was incubated at 28 °C overnight to resuscitate bacterial activity. Five grams of soil were added to 45 ml of a 20 mM pyrophosphate buffer (10¹ dilution), stirred for 30 min and allowed to settle for 30 min. The aqueous phase formed was used to prepare a series of 1:10 dilutions, by adding 1 ml of the lower dilution into 9 ml of pyrophosphate buffer of the higher dilution until the 10⁶ dilution was reached. One hundred microliters of each dilution were plated on 0.01X and 0.2X TSA containing the fungal inhibitor Nystatin (SIGMA, Inc., Saint Louis, Miss.) at a final concentration of 50 µg/ml, different HgCl₂ concentrations ranging from 0.2 – 10 µM for the 0.01X TSA and 2 – 100 µM for the 0.2X TSA, and 15 g/L agar. The plates were incubated in the dark at 28 °C and colonies were counted after six days of incubation (deLipthey et al, 2008).

The concentration that had about 10% of the colony forming units (CFU) as compared to the 0 μM HgCl_2 plate was deemed the concentration that selected for Hg^{R} bacteria. In the case of the 0.2X TSA this concentration was 100 μM HgCl_2 and for the 0.01X TSA it was 10 μM HgCl_2 .

Colonies were picked based on morphological uniqueness from all the plates regardless of Hg concentrations of the 2 different media and plated on media containing mercury at the concentrations that were determined to select for Hg^{R} bacteria irrespective of the original Hg concentration on which the colonies were obtained. Pure cultures resistant to 10 μM Hg (0.01X TSA) and 100 μM (0.2X TSA) were obtained after 3 consecutive transfers of isolated colonies on the appropriate medium.

Genomic and plasmid DNA extractions from Hg^{R} isolates.

Genomic DNA was extracted from the Hg^{R} isolates, using the UltraClean™ Microbial DNA isolation kit, according to the manufacturer's instructions (MoBio Laboratories, Solana Beach, CA, USA). The FASTBAC plasmid preparation protocol was used to extract plasmid DNA from the isolates (Gehr, E., Personal Communication). In detail, 1.5 ml of overnight cultures were harvested to obtain cell pellets. One hundred microliters of resuspension buffer were added to dissolve the pellet. Alkaline lysis followed by adding 200 μl of SDS/NaOH. After a 5 min incubation at room temperature, 150 μl of ammonium acetate and 150 μl of chloroform were added to the tubes, which were then placed in ice for 10 min and centrifuged for 10 min. Ammonium acetate is used to neutralize NaOH and precipitate DNA along with proteins that have been denatured by the addition of the organic solvent. The supernatant was then transferred in a clean tube that contained 200 μl of a PEG/NaCl in order to precipitate the circular DNA. The tubes were again

chilled in ice for 10 min and centrifuged for 10 min. The supernatant was then removed, and the pellet was dissolved in 100 μ l of TE buffer and stored at -20 $^{\circ}$ C.

Plasmid frequency

To determine the presence of plasmids in the LS and FS isolates, the plasmid preps were loaded onto 0.7 % agarose gels. The loading sample varied between 5-50 μ l depending on the ensuing analysis. The running buffer used here is called Bionic buffer (SIGMA, Inc., Saint Louis, Miss) and it allows for higher voltage applications to the gel without altering the conformational state of the plasmids. Gels were stained with 5 μ g/ml ethidium bromide (Bio-Rad Laboratories, Hercules, CA) and de-stained with dH₂O at the end because this method proved to be the most efficient as it allowed the development of brighter plasmid bands.

Each band on a gel lane, was considered to be a different plasmid. The only exception is the chromosomal band, appearing at the same level as the top band of the λ Hind-III marker (linear 23 Kb piece of DNA) and the bright band near the bottom of the gel, which is the RNA in the plasmid prep.

Identification and phylogenetic analyses of Hg^R bacteria based on the 16S rRNA gene

To determine the phylogeny of the LS and FS isolates, the 16S rRNA gene was PCR amplified using the universal bacterial primer set p27F/p910R (Amann, et al, 1992). The PCR mastermix consisted, per reaction, of 5 μ l of 10X PCR buffer, 1 μ l of 10 mM dNTPs stock, 1.5 μ l of 50 mM MgCl₂, 0.5 μ l of Taq Polymerase (Denville Scientific Inc., Metuchen, NJ, USA), 1 μ l of each primer at 25 pmol/ μ l (IDT, Coralville, IA, USA), 2 μ l of template DNA and 38 μ l of dH₂O for a final volume of 50 μ l. Amplifications were carried at 94 $^{\circ}$ C for 5 min, 35 cycles of 94 $^{\circ}$ C for 30 sec, 62

°C for 30 sec, 72 °C for 1 min, and a final extension cycle for 10 min at 72 °C using Applied Biosystems Gene-Amp PCR System 2700 (PE Applied Biosystems, Foster City, CA, USA).

The PCR products were gel purified with the QIAquick Gel Extraction kit (QIAGEN, Valencia, CA, USA) and the 16S rRNA gene sequencing reactions for both strands were analyzed by an ABI Prism® 3100 Avant Genetic Analyzer (Applied BioSystems, Foster City, CA) as described by the manufacturer.

Gene sequences were used as queries in BlastN searches (www.ncbi.nlm.nih.gov/blast.cgi) to determine the taxonomic affiliation of the OR Hg^R isolates. The 16S rRNA gene sequences of the isolates along with reference 16S rRNA gene sequences were aligned using ClustalX (Version 1.83) (Thompson et al, 1997). The alignment was uploaded onto the Gblocks program which eliminates poorly aligned and divergent regions of the alignment, and creates blocks of highly conserved regions taking out gaps and segments of non-conserved positions (Talavera, et al, 2007, Castresana, J. 2000). The Gblocks file was re-aligned using ClustalX and the alignment was uploaded in Phylo_Win (Version 2.0) in order to construct a bootstrapped (500 replicates) neighbor-joining tree (Galtier et al, 1996). The phylogenetic distances were calculated using the Jukes and Cantor matrix.

Rarefaction and diversity analyses based on 16S rRNA gene sequence similarity

A rarefaction analysis was performed to estimate the efficiency and completeness of the sampling effort for the LS and FS collections of isolates using their 16S rRNA gene sequences (Hughes et al, 2001). In the rarefaction analysis, the cumulative number of types or operational taxonomic units (OTU) observed is plotted against the sampling effort. The relationship between these two factors sheds light on the total diversity of a given sample. In this study, an OTU was defined as a 16S

rRNA gene sequence group in which distance values of 0.03 (>97% gene sequence identity) differentiate at the species level, and distance values of 0.05 (>95% gene sequence identity) differentiate at the Genus level (Konstantinidis and Tiedje, 2004, Schloss and Handelsman, 2004). Specifically, an alignment of the sequences was created using ClustalX, and the DNADIST program of the Phylogeny Inference Package (PHYLIP, version 3.69, Joseph Felsenstein, <http://www.evolution.genetics.washington.edu/phylip.html>) was used to create a distance matrix. This file was used in the MOTHUR program to create rarefaction curve using cutoffs of 0.03 and 0.05 and richness estimates (Schloss et al, 2009). The nonparametric richness estimates, ACE (Chao and Lee, 1992), Chao1 (Chao, 1984), Shannon (H') diversity index (Shannon, 1948) were calculated as a function of the sampling effort from the rarefaction curves. An evenness measure was also calculated based on observed and maximum H' values.

Abundance, isolation, identification and characterization of *merA* genes in LS and FS isolates

Isolation of *merA* genes

In an effort to determine the specific Hg detoxification mechanism employed by these soil isolates, PCR amplifications of the *merA* gene were set up, using both genomic and plasmid DNA of the isolates. A total of 4 primer sets were used so as to capture the expected wide phylogenetic range of the *merA* genes (Table 2.5) as suggested by the taxonomic affiliation of the isolates (Wang et al, 2011). Primer sets 1 & 2 target Gram negative organisms from the phylum Proteobacteria and Gram positive, Low G+C organisms from the phylum Firmicutes. The expected amplicon size is 309 bps and 1249 bps for primer set 1 and 2, respectively. Primer set 3

targets all the above organisms as well as Gram positive, High G+C organisms from the Phyla Actinobacteria and Deinococcus-Thermus. The expected amplicon size for primer set 3 is 1246 bps. Finally, primer set 4 targets Gram-negative organisms that belong to the *alpha* class of the Proteobacteria and the expected product is 800 bps (Øregaard and Sørensen, 2007). Only primer set 3 was used to PCR amplify *merA* genes from plasmid DNA. The PCR mastermixes and program cycles were followed as described in Wang et al (2011) for both genomic and plasmid DNA templates.

Identification, phylogenetic analyses, *merA* diversity and rarefaction analysis of *merA* of OR Hg^R bacteria

merA gene sequences were translated into amino acid sequences using the Expert Protein Analysis System (ExPASy) proteomics server of the Swiss Institute of Bioinformatics (SIB) (<http://ca.expasy.org/tools/dna.html>) and phylogenetic trees were constructed as described above for the 16S rRNA gene. *merA* diversity and rarefaction analyses were carried out as described above for the analyses of 16S rRNA genes.

Phylogenetic incongruence and G+C comparison based on 16S rRNA and *merA* genes sequences.

Two approaches were employed to investigate the possible evolution of *merA* by horizontal gene transfer (HGT) events among OR isolates. The first was a comparison of the phylogenies of the 16S rRNA gene with the deduced MerA sequences to determine incongruencies between the trees as reflected by cluster groupings (Lawrence and Ochman, 2002, Coombs and Barkay, 2004). The second approach was applied to the MerA sequences for which a phylogenetic incongruence was detected by the first approach. The ranges of the genomic G+C content of the recipient organisms were found in *The Prokaryotes* (2006) and the G+C content of

merA was calculated using the OligoCal tool (www.basic.northwestern.edu/biotools/oligocalc.html) (Kibbe, 2007). Finally the presence of plasmids and/or positive PCR amplifications of the *merA* gene using plasmid DNA of the isolates, was also considered evidence for HGT events.

Results

Soil Characteristics:

The Organic Carbon (OC) content of the soil sample was 4.47% (Table 2.2). It falls below the reported 8% OC content of Anderson County, where the ORR is located (Capri 1998), and in between the previously reported OC range for the EFPC area which was 0.62-6.4% (deLipthay, 2008). Soil moisture was 17.5% and the Water Holding Capacity (WHC) was 82.06%, while the field capacity was 79.3%. Comparing the results presented in WHC figures one can conclude that the WHC of the experimental soil lies in between the Loam and Silt Loam soil standards and that the soil was rich in organic matter as evidenced by the high WHC level (http://www.agviselabs.com/tech_art/whc.php).

The pH of the Oak Ridge soil was 8.11, which lies on the higher end of known pH values for soils from that area ranging from 6-8 (USDA, Anderson County). The sedimentation technique was used to determine the texture of the soil sample. The exact distribution of soil particles was: 75% sand, 15% silt and 10% clay, characteristic texture of a sandy loam soil based on the USDA soil texture triangle (<http://soils.usda.gov>).

Bacterial counts and isolations:

Cultured bacterial counts under oligotrophic conditions (0.01X TSA medium) ranged from 6.4×10^5 CFU/g on the 0 μ M Hg plate, to 1.8×10^5 CFU/g on the 10 μ M

Hg plate (Table 2.3). A biphasic response to mercury stress was observed in this medium. The 0 μM Hg plate had lower counts than plates between Hg concentrations of 0.2 to 2.4 μM . This stimulation of growth may be explained by the hormetic effect, whereby toxic substances at low concentration stimulate rather than inhibit the growth of organisms (Hotchkiss, 1923). Under copiotrophic conditions (0.2X TSA medium), the cell counts ranged from 10.8×10^5 CFU/g to 1.9×10^5 CFU/g, on the 0 μM and 100 μM Hg plates respectively (Table 2.4). Regression analysis determined that there was a significant inverse relationship between the Hg concentration and the CFU under both oligotrophic ($r^2 = 0.87$, P-value = 0.0001) and copiotrophic ($r^2 = 0.83$, P-value = 0.0015) conditions. The counts for the Hg^R soil bacteria on both oligotrophic and copiotrophic conditions are comparable to the $2.5 \pm 1 \times 10^5$ CFU/g reported by Rasmussen et al (2008) working with surface soil samples from the same area, yet the Hg concentration that they employed was only 4 μM , less than half of the lowest mercury concentration used in this study.

Based on cell counts, 28% of the total culturable oligotrophic community and 17.6% of the total culturable copiotrophic community were Hg^R (Tables 2.3 & 2.4). Finally, a total of 84 Hg^R bacterial isolates were obtained in this study: 37 oligotrophs growing on 10 μM 0.01X TSA (LS isolates), and 47 copiotrophs growing on 100 μM 0.2X TSA (FS isolates) (Figure 2.2).

16S rRNA gene sequence based analyses:

Taxonomic associations.

Based on the sequencing effort, a total of 36 and 47 16S rRNA gene sequences were obtained from the LS and FS isolates, respectively (Appendix Tables 1 & 2). The size range of the sequenced 16S rRNA gene of the LS isolates was 386 to 873 nucleotides, with the majority of amplicons in the 800s, and for the FS isolates

the range of the sequenced gene size was 500 to 828 nucleotides with the majority of amplicons in the 700s.

BlastN queries revealed that both LS and FS isolates belonged to genera of the Gram-positive, High G+C phylum Actinobacteria, and the Gram-negative *alpha*, *beta* and *gamma* classes of Proteobacteria. Under oligotrophic conditions, Actinobacteria (75%) are selected over Proteobacteria (25%), while under copiotrophic conditions, the two Phyla are equally represented (53% to 47%) (Figures 2.3, 2.4, 2.5).

At the genus level, the LS group is dominated by *Streptomyces* spp. and *Arthrobacter* spp., while in the FS group, an even distribution is observed for species of *Streptomyces*, *Arthrobacter*, *Nocardia* and *Mycobacterium* (Appendix Tables 1 & 2). In the case of gene sequences affiliated with the Proteobacteria, the FS group has 3 times more sequences belonging to the *alpha*, and *gammaproteobacteria* than the LS group. The FS group is dominated by species of the *alphaproteobacterial* *Aminobacter* spp., while the LS group contains no representatives from this genus. Both groups are genetically affiliated with the *Sinorhizobium/Ensifer* genus. The *Rhizobium* genus is found only among the LS isolates' group and the *Bradyrhizobium* only in the FS group. The *betaproteobacterial* genus *Alcaligenes* is found in a 2:1 ratio in the FS and LS groups respectively, and the *gammaproteobacterial* genus *Lysobacter* is only observed in the FS group.

At the species level, twenty seven 16S rRNA gene sequences of the LS isolates that belonged to the Actinobacteria, are 98-100% similar to 7 different species of the genus *Arthrobacter* and 99-100% similar to 20 species of the genus *Streptomyces* (Appendix Table 1). As for the *alpha* class of the Proteobacteria, LS gene sequences are 97% similar to 2 species of the genus *Sinorhizobium*, 98-99% similar to 2 *Rhizobium* spp. and 100% similar to *Ensifer adhaerans*. Two LS isolate sequences are 99% similar to the *betaproteobacterial* *Variovorax* spp. and

Alcaligenes spp., and 100% similar to the *gammaproteobacterium* *E. coli*. Finally, for one LS strain, there is a 99% sequence similarity to an uncultured soil clone.

The 16S rRNA gene sequences of the FS isolates most closely related to genera of the Actinobacteria, are 97-100% similar to 9 species of *Arthrobacter*, 99% similar to 2 *Mycobacterium* spp., and 96-100% similar to 10 species of the genus *Streptomyces* (Appendix Table 2). Three gene sequences are most similar by 98-99% to an uncultured actinobacterium clone and one sequence is 98% similar to *Nocardia alba*. The 15 sequences most closely related to *alphaproteobacteria* are distributed among 8 *Aminobacter* spp. (97-100% sequence similarity), 2 species of the Bradyrhizobiaceae family by 98-99%, 3 *Sinorhizobium* spp. by 98%, and finally to 2 *Ensifer adhaerans* strains by 99%. As for the sequences most similar to *betaproteobacteria*, one is 98% similar to *Stenotrophomonas maltophilia* by 98%, and 2 are similar by 99% to *Alcaligenes* sp. strain HI-ABCE2. Finally, there are 3 sequences most closely related to species of *Lysobacter* by 99% and one to *E. coli* by 100%, all belonging to the *gammaproteobacterial* class.

Phylogenetic analyses.

The phylogenetic tree based on alignments of the 16S rRNA gene sequences of LS isolates and the reference organisms they are closely related to is dichotomized between the Actinobacteria and the *alpha*, *beta*, and *gamma* Proteobacteria (Figure 2.6). The Actinobacteria clade appears basal to the Proteobacterial clade, with the *Streptomyces* genera branching deeper than *Arthrobacter* in the Actinobacterial node. The *Streptomyces* group forms 7 distinct clusters. In three of them, reference strains cluster together with LS isolates and in 4 of them the isolates form clusters on their own. LS 26 and LS 4 form 2 separate clusters with *Streptomyces flavotricini* and *Streptomyces gelaticus*, respectively, and isolates LS 16 and 10 with its clonal sequence (16S rRNA sequences sharing 100% similarity) shown in parentheses, form

one cluster with *Streptomyces scabiei* and *Streptomyces* sp. SCP-2 (Figure 2.6). The *Arthrobacter* group contains 2 clusters, breaking in two the isolates associated with *Arthrobacter* species. LS 3 and its clonal 16S rRNA sequences cluster with *Arthrobacter* sp. HSL-2, and LS 27 and LS 14 with its clonal sequences form another cluster with *Arthrobacter* sp. 16.43.

The deepest branching cluster in the Proteobacteria is that of *gamma*, and the *alpha/beta* groups branch out together at a later stage. The *gammaproteobacteria*, are represented by the reference strain *E. coli* which shares a single cluster with LS 40. The reference strains *Alcaligenes* and *Variovorax* with their associated isolates LS 21 and 8, form 2 distinct and associated clusters, and share the branch node with the *alpha* branch. Two clusters divide that branch; one of the genus *Ensifer* and LS 22, and another of the reference strains belonging to the genera *Sinorhizobium* and *Rhizobium* with all the isolates that are most similar to the latter genera (LS 6, 9, 15, 19) interspersed within this cluster. It is of interest that *Sinorhizobium* clusters with the *Rhizobium* strains instead of the *Ensifer* ones, since *Ensifer* and *Sinorhizobium* are of the same genus (780 and 821 nucleotides of the 16S rRNA gene were analyzed for LS 22 *Ensifer* and LS 6 *Sinorhizobium* respectively) (Chen, 1982, Young, 2003).

In the phylogenetic tree of the FS isolates (Figure 2.7), one can observe a dichotomy between the members of the 3 classes of the Proteobacteria and 4 genera of High G+C Actinobacteria. The High G+C Actinobacteria, are separated in well-defined clusters of isolates belonging to the Genera *Arthrobacter*, *Streptomyces*, and *Nocardia/Mycobacterium* which form a common node. The reference strain of an uncultured Actinobacterial clone clusters together with other *Arthrobacter* reference strain and its associated FS isolates. The other 2 clusters contain only FS isolates. A similar situation is found in the *Streptomyces* clusters, where one cluster contains only FS isolates 25 and 28 with their clonal gene sequences, and the other contains

reference strain among the isolates (FS 1, 9, 14, 27, 36 and its clonal sequence 53). The *Mycobacterium* reference strain clusters together with FS isolate 19 and FS isolate forms its own cluster sharing the same node with the above sequences. Finally, *Nocardia alba* clusters together with FS isolate 4, sharing a common node with the *Mycobacterium* related sequences.

The Proteobacterial part of the tree is divided between earlier evolving mixed clusters of *beta* and *gamma* genera, and genera belonging to the *alphaproteobacteria* (Figure 2.7). FS 48 and its closest relative *E. coli*, are basal to all the other Proteobacteria and form a distinct cluster. The *betaproteobacterial* group of isolates, with the reference strains of the genera *Stenotrophomonas/Alcaligenes* form one cluster and Isolate FS 2 clusters on its own. The *gammaproteobacterial* clade of *Lysobacter* and FS isolates 35 and 41 clusters together with a reference *Stenotrophomonas* strain. Finally, the *alphaproteobacteria* form 3 distinct and associated clades, of the earlier evolving *Aminobacter*, *Ensifer/Sinorhizobium* and *Bradyrhizobium*.

Sample coverage and estimates of diversity.

To estimate how much of the cultured bacterial diversity present in the soil sample was captured in the 2 groups of isolates, rarefaction or collector's curves were calculated at the species and genus level distance cutoffs for the 16S rRNA gene sequence. The accumulation curves (Figures 2.8 & 2.9), plotted as the cumulative number of OTUs versus the number of sequences collected, for the 0.03 (>97% gene sequence identity) and 0.05 (>95% gene sequence identity) cutoff for both groups of isolates were leveling off approaching an asymptote. The singlet accumulation curves, 0.00 cutoff, on the other hand, were increasing in a linear fashion. There is no 0.05 cutoff curve for the LS isolates because there was no

significant difference in the DNA sequences between the 0.04 and the 0.05 cutoff curves. These results taken together, demonstrate that both isolate groups were equally well sampled at the higher cutoffs (corresponding to species and genus levels) (Konstantinidis and Tiedje, 2004, Schloss and Handelsman, 2004), as opposed to the lower 0.00 cutoff when they are treated at the strain level (Figures 2.8 & 2.9).

For the LS group, there were a total of 36 gene sequences of which 23 were unique phylotypes based on the operational taxonomic units (OTU) definition grouping of 16S rRNA sequences sharing at least 97% similarity (Table 2.4). The FS group had a total of 47 gene sequences of which 36 were unique phylotypes. To estimate the diversity for both groups of isolates, the nonparametric accumulation-based coverage (ACE) and Chao1 estimators were used (Hughes, 2001), as well as the Shannon diversity index. Within group based Chao1 and ACE were in agreement, for both LS (13 and 12) and FS (25 and 25) groups, yet between group comparisons show that the FS group has higher values for these estimators. The Shannon index and the evenness measure show the same trend, further substantiating that a higher diversity and more equal distribution of species are found among the FS isolates than the LS isolates, which translates into greater organismal diversity supported by the higher nutrient content medium (Table 2.4).

***merA* gene sequence and MerA amino acid sequences analyses.**

Taxonomic associations.

Thirty *merA* amplification products were obtained from LS isolates while such products could not be obtained for 6 of the isolates. In the case of the FS isolates, there were 8 out of the 47 isolates for which none of the primer sets produced a

product with the expected size. In other words, at least 83.3 % of the Hg^R LS isolates and 85.1 % of the FS isolates have a copy of the *merA* gene implying a potential for Hg detoxification by the *mer*-operon mediated mechanism (Appendix Tables 2.3 & 2.4). The inability to obtain *merA* amplification products from 14 isolates could signify that their *merA* genes were too divergent to be captured by the primers used or another equally plausible explanation could be that these isolates may not use the *mer*-mediated Hg detoxification mechanism.

The majority of the *merA* genes were successfully amplified using primer set 3, which targets *merA* genes common among the Proteobacteria, the Firmicutes and Actinobacteria/Deinococcus-Thermus phyla (Table 2.5). A total of 50 *merA* amplification products were obtained for the LS and FS isolates using this primer set. The resulting *merA* gene sequences related to those from organisms representing all the above Phyla, except Deinococcus-Thermus, thus exhibiting high specificity of target groups. The case is the same for the *alphaproteobacterial* specific primers (primer set 4) which produced 10 amplifications of *merA* genes, all from DNA extracts of strains belonging to the *alphaproteobacterial* lineage as determined by 16S rRNA gene similarity. Amplifications with primer sets 1 and 2, where primer set 1 is nested within the primer set 2 product (Wang et al, 2011), which target *merA* of Proteobacteria and Firmicutes, gave 9 positive amplifications (Data not shown). The 3 positive amplifications with primer set 1 produced a small sequence (310 bp) and thus no meaningful identification was possible. Based on the observation that primer set 2 gave positive amplifications to *merA* belonging to Proteobacteria, Firmicutes and Actinobacteria, one can conclude that this set goes beyond the specificity of its original design and captures a broader diversity of *merA* than was intended, equaling the diversity of *merA* captured with primer set 3.

merA gene sequences were translated into amino acid sequences and used to carry out BLASTP searches to identify taxonomic associations between the isolates'

MerA protein and those in the database. This effort revealed the same pattern to that observed with the 16S rRNA gene. Namely, that under oligotrophic conditions accompanied by Hg stress the abundance of loci common among the Proteobacteria was reduced (~20%) as compared to the abundances of the same loci in bacteria that were obtained in copiotrophic conditions (45%) (Figures 2.10, 2.11 & 2.12, Appendix Tables 3 & 4). The LS group contained MerA most closely related to those of the *alphaproteobacterial* genera *Rhizobiales* (4) and *Xanthobacter* sp. (1), which contribute ~17% of the total abundance (Figure 2.11). Loci related to *betaproteobacteria*, contribute 3.3% of the total abundance, and originate from *Ralstonia* sp. No sequences most closely related to *gammaproteobacterial* MerA were observed. The FS group, exhibits a wider variety of MerA sequences most closely related to the *alphaproteobacteria* accounting for 25% of the total abundance (Figures 2.10 & 2.12). *Bradyrhizobium* spp. MerA sequences, are closely related to organisms isolated from the same Oak Ridge site by other workers (Øregaard and Sørensen, 2007), and are more abundant in the FS group rather than the LS group (Appendix Table 3 & 4). MerA loci most closely related to *Aurantimonas* spp. are doubletons, and those related to *Rhizobium* and *Oligotropha* spp. are singletons. The *betaproteobacterial* class, has 4 MerA representatives in the FS group, related to *Ralstonia* spp. (1), *Polaromonas* sp. (1) and *Stenotrophomonas* sp. (1). Finally, 4 MerA are related to *gammaproteobacterial* genera *Pseudomonas* and *Salmonella*.

As for the loci most closely related to Actinobacteria, a higher abundance was observed for the LS group (~77%) than the FS group (50%) and MerA closely related to the genera *Streptomyces*, *Arthrobacter* and *Acidotherrmus* are the major players in both groups (Figures 2.11 & 2.12, Appendix Tables 3 & 4). In addition to those, the LS group has 3 singleton loci related to the *Pseudonocardia*, *Nocardiodides* and *Micrococcus* genera. The FS group contains 2 MerA sequences related to *Bacillus cereus* of the Low G+C phylum Firmicutes.

Sample coverage and estimates of diversity.

For the *merA* genes of the LS isolates, 3 rarefaction curves were calculated based on 0.00, 0.01 and 0.05 cutoffs (Figure 2.13). The 0.00 cutoff accumulation curve has a steeper slope than the 0.01 and 0.05 cutoff accumulation curves, testifying to a worse sample coverage in the higher cutoffs, yet the absence of an asymptote in the curves signifies the need for a bigger sampling effort.

The rarefaction curves calculated for *merA* genes found in the FS isolates had a similar trend to the LS ones (Figure 2.14). The 0.00 and 0.02 cutoffs were used, as there was no significant difference between the 0.02 and 0.05 cutoffs, and the 0.00 cutoff curve had a steeper slope. Taken together, these results are indicative of the insufficiency of the sampling effort to estimate the actual richness of *merA* genes in either nutrient level. It is also of interest that the rarefaction curves based on the *merA* gene are steeper than those observed for the 16S rRNA genes for both groups of isolates which may attest to the fact that *merA* genes diverge faster than the more conserved 16S rRNA genes (Figures 2.8, 2.9, 2.13 & 2.14)

For the LS group, there were a total of 30 *merA* amplification products, yet only 16 of these sequences could be used for the distance matrix created and further inputted in MOTHUR (Schloss et al, 2009) to assess diversity with the non-parametric estimators and the Shannon diversity index (Table 2.6). A possible explanation is that partial gene sequences were not overlapping and thus an all-inclusive alignment was not possible for the distance matrix to be created. Likewise, only 33 of the 40 *merA* gene sequences of the FS group were used for this analysis.

Of the 16 LS *merA* gene sequences used, 8 were unique phylotypes based on the operational taxonomic units (OTU) definition grouping sequences sharing 99% similarity (Table 2.6). The FS group had a total of 33 gene sequences of which 21 were unique phylotypes. The nonparametric Chao1 estimator (Hughes, 2001), the diversity index Shannon and the evenness measure, were in agreement, showing

higher diversities and equality in distribution of individuals achieved in the FS group of isolates as compared to the LS group.

Horizontal gene transfer analyses.

To investigate the role of HGT in the evolution of *merA* in the 2 communities isolated from the soil environment, gene phylogenies were examined for congruency. A neighbor-joining phylogenetic species tree was constructed using the isolates' 16S rRNA gene sequences, with good bootstrap support for all nodes. Another neighbor-joining tree was created with the deduced amino acid sequences of the *merA* gene sequence of the same strains. In the cases where incongruence between the gene phylogenies was detected, the G+C mole% content of the genomes of recipient organisms, as published in *The Prokaryotes* and *Bergey's Manual*, was compared to the G+C mol% content of the *merA* genes, and used to support the identification of these HGT events (Dworkin et al, 2006, Holt et al, 2005, Lawrence and Ochman, 2002). Finally, the presence of plasmids and positive *merA* amplifications with plasmid DNA of these strains as target was used as another evidence for HGT.

This analysis revealed that HGT events are a common occurrence in the Oak Ridge isolates. In total, there were 27 incongruencies in the phylogenetic associations of the LS and FS isolates as evidenced by the difference in tree topologies constructed for closely related sequences of the 16 rRNA gene and the MerA protein (Tables 2.7, 2.8.1 & 2.8.2). In the case of the LS isolates; there were a total of 8 incongruencies in the gene phylogenies and of those 2 were further supported by G+C content differences between species' genomes and *merA* genes and only one strain carried a plasmid (LS40) (Figure 2.15, Tables 2.7 & 2.9). In the other 6 cases of phylogenetic incongruence, the G+C content of the *merA* gene fell in between the known range of the recipients' genomes and plasmids were detected in one strain (LS28).

More specifically, LS strains 7, 11 and 28 contained 16S rRNA genes, which cluster together with members of *Streptomyces*, and *merA* genes that cluster with *Acidothermus celluloliticus* (Figure 2.15). LS strain 24, clusters together with the *Streptomyces* in the 16S rRNA gene phylogenetic tree, but contains a *merA* gene that clusters with a *Nocardioides* species. These four instances of incongruence, suggest the possibility of intra-phylum cross-family HGT events among 3 different families of the Actinobacteria. The other 2 cases where probable HGT events were observed, involve 2 LS strains that belong to the *beta* and *gamma* classes of the Proteobacteria. LS strain 40, clustered with the *gammaproteobacterial E. coli* based on the 16S rRNA gene phylogeny, whereas in the MerA amino acid phylogeny, it clustered with the *alphaproteobacterial Xanthobacter autotrophicus*. The LS strain 21, forms a cluster with the *betaproteobacterium Alcaligenes* sp. in the 16S rRNA phylogenetic tree and in the MerA protein tree with another *betaproteobacterium, Ralstonia pickettii*. These incongruencies are corroborated with the G+C mole % contents of the genome and *merA* for these strains (Table 2.7). The genome of the *E. coli* related strain LS 40, ranges from 48.5 to 50, falling below the G+C mole % content of the *merA* gene of the donor *Xanthobacter autotrophicus* (61 mole%). The G+C content of the recipient's genome of LS 21, is again lower than that of the *merA* gene of the donor, ranging from 56 to 60 mol% as compared to 65 mol%. These findings, suggest an event of an inter-class transfer from an *alphaproteobacterial merA* gene to a *gammaproteobacterial* recipient and an intra-class transfer between 2 *betaproteobacteria* belonging to 2 different genera.

Among the FS group, there were 19 incongruencies based on close relative associations between the 16S rRNA genes and MerA proteins and 13 of these were further supported by differences in the G+C content between the species genomes and the *merA* gene (Tables 2.8.1 & 2.8.2). There were 16 instances of plasmid presence and 14 positive *merA* amplifications with the organismal plasmid DNA

(Tables 2.10.1 & 2.10.2). I was unable to construct of a phylogenetic tree based on the deduced amino acid sequence of *merA* genes, as partial gene sequences amplified with the 4 primer sets were not overlapping and an all-inclusive alignment was not possible. Thus the information presented here for the FS group, is solely based on discrepancies between taxonomic affiliations based on the two genes.

Isolates FS 7, 18, and 33 cluster together with the *betaproteobacterium* *Aminobacter* in the 16S rRNA tree, while based on MerA sequences, they are affiliated with *Aurantimonas* (an *alphaproteobacterium*), *Bradyrhizobium* (*alpha*) and *Bacillus* (Gram positive Firmicutes) (Figure 2.7, Tables 2.8.1 & 2.8.2). FS isolates, 17 and 42 cluster with *Alcaligenes* (*beta*) in the 16S rRNA tree and their MerA is related to *Ralstonia* (*beta*). In the case of FS 7, 17, 33 and 42 but not for FS 18, the phylogenetic incongruencies are further supported with G+C content incongruencies as well as positive amplifications of the *merA* gene from plasmid DNA. FS 3 clustered with the *alphaproteobacterium* *Bradyrhizobium* in the 16S rRNA tree and with the MerA of *betaproteobacterium* *Oligotropha*, a discrepancy supported by positive plasmid *merA* amplification. FS 54, clustered with *alphaproteobacteria* in the 16S rRNA based tree, and with *Bacillus cereus* (Gram positive Firmicutes) according to their MerA taxonomy. All inter-phylum incongruencies between 16S rRNA gene sequences and MerA amino acid sequences, are supported by both G+C incongruencies and plasmid DNA amplifications of the *merA* gene. FS 4 clusters with *Nocardia alba* in the 16S rRNA tree, while its MerA is taxonomically associated with *Streptomyces* sp. FS 14, 27, and 28, cluster with *Streptomyces* at the species level, while based their MerA are closely related to *Acidothermus* species.

Discussion

Mercury contamination in exposed floodplain banks poses a persistent stress to resident bacterial communities as riverine systems contaminated more than 60 years ago, still exhibit high concentrations of the toxic metal. Through the abiotic processes of bank erosion and flooding events, Hg is mobilized and migrates into the associated soils and waters of the river system (Brooks and Southworth, 2011, Campbell et al, 1998). In the soils there is a metabolic potential for the reduction of Hg (Olson and Thorton, 1982), as amino and sulfhydryl groups of humic acids essential for heterotrophic biosynthetic pathways are bound to Hg(II) (Han et al, 2006, Grigal, 2003).

In this study I investigated the effect of Hg contamination on the diversity and evenness of bacterial communities that in their natural environment inhabit niches of differing levels of nutrient and Hg availability. Analysis of soil samples from the EFPC by direct cultivation, revealed a dramatic reduction in the number of colony forming units of both oligotrophic and copiotrophic indigenous bacterial populations in response to increasing Hg levels (Tables 2.2 & 2.3). The total population numbers were higher for copiotrophs, which grew at nutrient levels 20X higher than the oligotrophs. Fifty percent mortality, a common measure of toxicity, occurred at 7.5 μM Hg under oligotrophic conditions, which is 10X lower than the 50% mortality observed for copiotrophs (75 μM). At the highest concentrations of the lab-controlled Hg-gradient, the Hg^R population size was 28% of the total oligotrophs and 17.6% of the total copiotrophic counts.

In comparison, de Liphay et al (2008), working with samples from the floodplains of the Lower East Fork Poplar Creek, reported that only 1% of the total heterotrophic community was Hg^R at 50 μM of HgCl₂. This difference in the

population of Hg^R bacteria between the two studies can be attributed to the use of different culture media. Rich media such as R2A (de Liphay et al, 2008) have been shown to bind Hg(II), decreasing its bioavailability by 30-40% (Chang et al, 1993, Ramamoorthy and Kushner, 1975). Consequently, selection of Hg^R bacteria to detoxify the environment was decreased. On the other hand, in this study, to ensure Hg bioavailability and avoid its loss to organic carbon complexations, TSA medium was diluted and amended with appropriate Hg concentrations (Chang, 1993). Thus increased Hg availability may explain the higher selection of Hg^R populations observed in this study.

Phylogenetic analyses based on results from PCR amplifications and sequencing of 16S rRNA gene, showed that the bacterial communities isolated in both nutrient levels were dominated by the *alpha*, *beta* and *gamma* classes of the Gram negative Proteobacteria and by members of the Gram positive Actinobacteria (Figures 2.6 & 2.7). At copiotrophic conditions the proportion of organisms belonging to the two phyla, were equally distributed, while under oligotrophic conditions, there was a shift in community composition and genera belonging to Actinobacteria, achieved 75% of total abundance (Figures 2.3 & 2.4). This is in accord with previous culture-dependent studies performed with soil samples of the EFPC, where actinobacterial isolates under oligotrophic conditions (0.1X TSA) made up 98% of the total community (Rasmussen, 2008), and Ranjard et al (1997) observations that under copiotrophic conditions (Plate Count Agar medium compares to full strength TSA), Hg contamination in soil samples resulted in a pronounced increase in the abundance of Hg^R isolates related to Gram negative bacteria (Ranjard et al, 1997).

A number of diversity estimators, used to calculate the evenness and species richness of the communities as that is manifest in the 16S rRNA gene sequences similarity, showed that copiotrophic conditions supported higher levels of diversity and evenness (Table 2.4), and selected against the fast-growing Genus *Rhizobium* of

alphaproteobacteria, while slow-growing N₂ fixers made up 32% of the total community (Figure 2.4). These two observations are in contrast to findings of other studies, where oligotrophic environments have higher evenness and spp. richness than copiotrophic environments (Torsvik et al, 2002, McCaig et al, 2001, Finkel and Kolter, 1998), and that under oligotrophic conditions in metal contaminated river systems, *alphaproteobacteria* outcompete other resident populations (Rubin 2007, Pinhassi 2003). A recent study profiling the communities from soil samples of the EFPC using a culture-independent method, showed that *alphaproteobacteria* did indeed dominate the community, and that Actinobacteria were always a minority across samples, and not present in the most contaminated point source (Vishnivetskaya et al, 2011). Taken together, these results show that description of community composition, even when studies are performed in the same ecosystem, heavily relies on the methodologies used to assess it as well as on the nature of Hg-contamination.

To determine the specific mechanism of Hg detoxification employed by the LS and FS isolates and to capture the broad diversity of the gene, 4 different primer sets were used that target Phyla of Actinobacteria, Firmicutes, Proteobacteria and Deinococcus-Thermus. It was shown that at least 83.3 % of the Hg^R LS isolates and 85.1 % of the FS isolates have a copy of the *merA* gene, further attesting to the high acclimatization of these communities to life under the stress of Hg (Appendix Tables 3 & 4). The diversity of the *merA* gene sequences was lower under oligotrophic than copiotrophic conditions, as was the case for the 16S rRNA gene sequences, further supporting that nutrient limiting conditions in the environment have a lower ceiling in the diversity of organisms that they can hold (Tables 2.4 & 2.6). Another interesting finding, is that between the gene pools of the LS and FS isolates, loci affiliated to *alphaproteobacteria* were a common occurrence, whereas using a culture-independent technique to assess *merA* diversity in surface soils of the Lower East

Fork Poplar Creek, Øregaard and Sørensen (2007) observed that only one *merA* sequence was affiliated to this class. Additionally, they were the first to report an *alphaproteobacterial*-type *merA* gene, while Vetriani et al (2005), had isolated a Hg^R *alphaproteobacterium* from hydrothermal vent fluids. To date no *mer* system from an *alphaproteobacterium* has been characterized even though there are many *merA* homologues in complete genomes of *alphaproteobacteria* (Barkay, personal communication).

HGT plays a major role in the enhancement of genetic diversity in bacterial communities, and *merA* determinants isolated from organisms affiliated to a wide range of taxonomic groups, show phylogenetic incongruencies, when compared to the 16S rRNA genes, further supporting that HGT influences the evolution of this gene (Lal and Lal, 2010, Osborn et al, 1997). In this study, I used phylogenetic incongruencies, G+C content anomalies, and presence of plasmid and/or positive PCR amplifications of *merA* genes using plasmid DNA, to assess the role of HGT in the observed diversity of *merA* genes and in the adaptation of 50 isolates to long-term Hg stress. In total there were 27 phylogenetic incongruencies among LS and FS isolates (Tables 2.7, 2.8.1 & 2.8.2).

In the case of LS isolates, only one phylogenetic incongruence was further supported by irregular G+C content between the host genome and the *merA* gene, and positive *merA* amplification from plasmid DNA extracted from the isolate, while in FS isolates 12 phylogenetic incongruencies were supported based on the same reasoning (Tables 2.9, 2.10.1 & 2.10.2). In the other cases, the G+C content of the *merA* genes found in these isolates were within the known G+C ranges of their genomes. Since the discrepancy between the recipient's genome and the functional gene is only valid for recent transfer events (Lawrence and Ochman, 1997), the lack thereof does not necessarily contradict the HGT occurrence. It might just be suggestive of an early transfer event where the transferred genes have, through

time, ameliorated to the G+C content of the transcriptional/translational machinery of the new host for superior function. An additional explanation for this phenomenon is that members of the Actinobacteria have a very similar genomic G+C content, thus horizontally transferred genes cannot be distinguished based on this criterion. Furthermore, one of the conditions that have been shown to accelerate HGT events, is shared genome size, G+C content, and carbon utilization, which may mask molecular evidence for HGT events (Jain et al, 2003).

Isolate LS 40 is most closely related to *gammaproteobacterial E. coli* at the species level, whereas in the MerA amino acid phylogeny, it clustered with the *alphaproteobacterial Xanthobacter autotrophicus*, suggesting an event of an inter-class transfer from an *alpha* Proteobacterial *merA* gene to a *gammaproteobacterial* recipient (Figure 2.15). It has been shown that *gammaproteobacteria* preferentially exchange genes with *alphaproteobacteria* which may further support the findings of this study (Beiko, 2005). As for the FS isolates, there was evidence for 6 instances of HGT events among the classes of Proteobacteria, and one between Firmicutes to an *alphaproteobacterium* (Tables 2.10.1 & 2.10.2). Furthermore, there were 5 instances of intra-phyllum HGT events among genera of the Actinobacteria.

The results of this study, suggest that the response of soil bacterial communities to Hg stress, when that is combined with a nutrient stress, is tripartite, affecting phylogeny, function and metabolism of the community thus highlighting the complexity of the impact of Hg-toxicity on microbial communities in long-term contaminated soils.

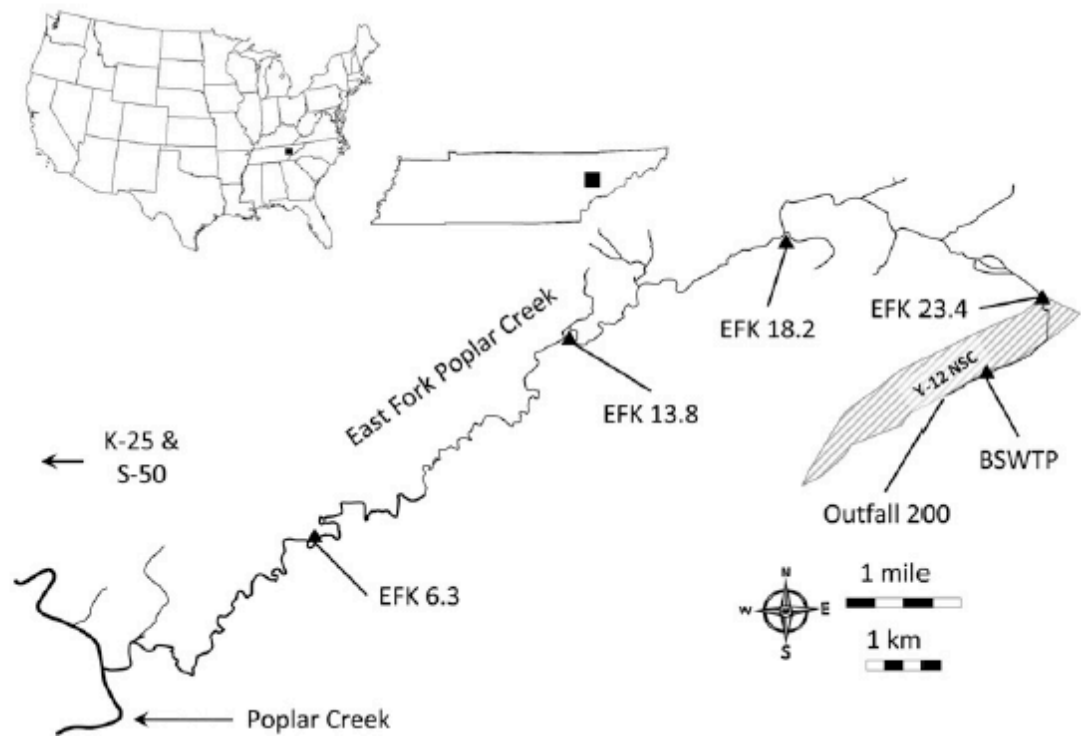


Figure 2.1. Map of the Oak Ridge Reservation (ORR) in Oak Ridge, Tennessee. East Fork Poplar Creek (EFPC) originates at the Y-12 National Security Complex (Y-12 NSC) and spans for 24 Km from East to Northwest flowing into the Poplar Creek, a tributary of that Clinch River (Taken from Brooks and Southworth, 2011).

Table 2.1. Summary of analyses of the physical/chemical properties of the Oak Ridge soil sample.

Parameters	Average	StDev^a
Soil Moisture (% by mass)	17.5%	± 0.0063
Soil Mass at Field Capacity	20.55 g	± 0.56
Water at Field Capacity	79.3%	N/A ^b
Water in Saturated Soil	52.48 g	± 0.73
Water Holding Capacity (WHC)	82.06 %	± 0.46
LOI ₅₅₀ ^c	8.94%	± 0.04
Organic Carbon	4.47%	± 0.02
LOI ₉₅₀ ^d	1.98%	± 0.09
Inorganic Carbon	0.54%	± 0.024
pH	8.1	
Soil Texture:		
Sand	75%	N/A
Silt	15%	N/A
Clay	10%	N/A

^a ± 1 standard deviation from the mean of three replicates

^b N/A = Not Determined

^c Loss On Ignition at 550 °C

^d Loss On Ignition at 950 °C

Table 2.2. Bacterial counts from dilution series plated on 0.01X TSA medium supplemented with a range of mercury concentrations.

HgCl₂ (μM)	0	0.2	0.4	0.8	1.2	2.4	5	7.5	10
Average^a (cells g⁻¹ x 10⁵)	6.4	9.02	7.77	8.81	6.75	6.69	4.87	2.7	1.8
Std Deviation^b	± 0.5	± 1.7	± 2.6	± 2.2	± 0.9	± 2.1	± 1.3	± 0.4	± 0.3

^a The average of dilutions 10² and 10³ were used for the cell counts for each mercury level.

^b ± 1 Std Dev from the mean.

Table 2.3. Bacterial counts from dilution series plated on 0.2X TSA medium supplemented with a range of mercury concentrations.

HgCl₂ (μM)	0	2	5	10	20	50	75	100
Average^a (cells g⁻¹ x 10⁵)	10.8	10.64	9.65	7.69	5.28	6.18	4.03	1.9
Std Deviation^b	± 4.2	± 6.1	± 4.4	± 4.4	± 0.7	± 1.4	± 0.3	± 0.4

^a The average of dilutions 10² and 10³ were used for the cell counts for each mercury level.

^b ± 1 Std Dev from the mean.

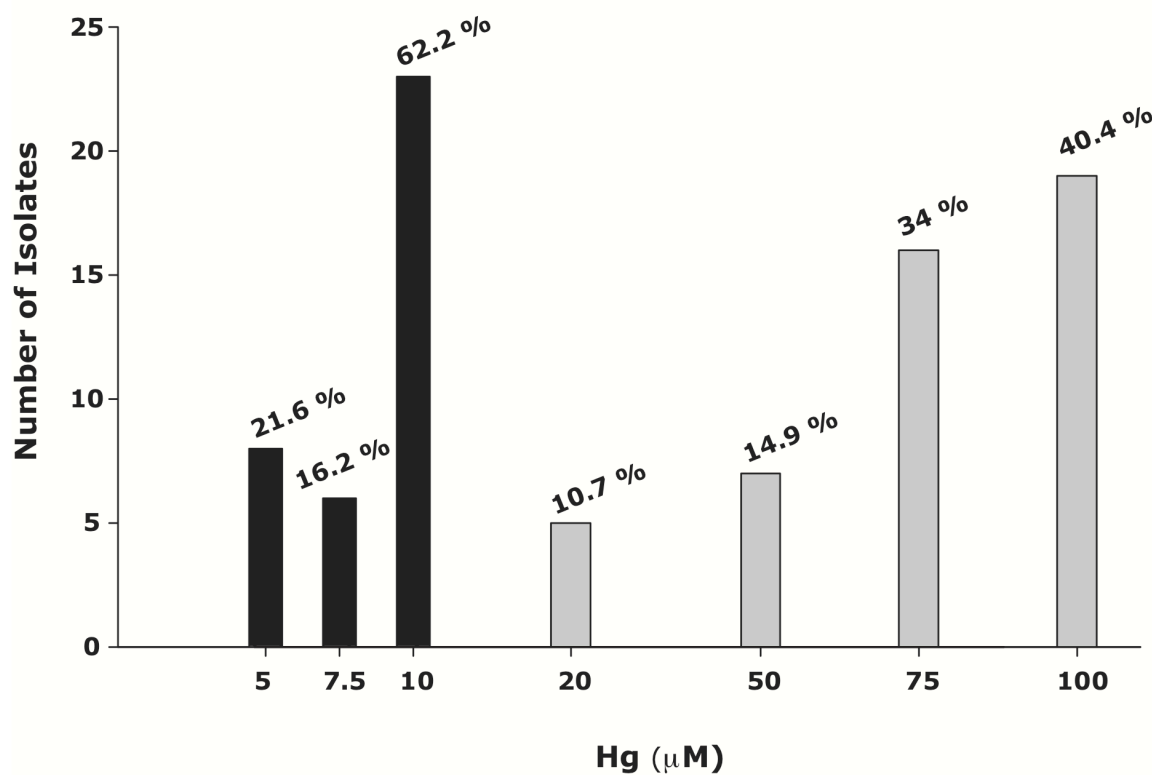


Figure 2.2. Bar graph of LS (black bars) and FS (grey bars) isolates indicating the original Hg concentration on which the isolates were obtained. Percentile distribution of isolates that were obtained at each Hg concentration, are displayed on top of each bar.

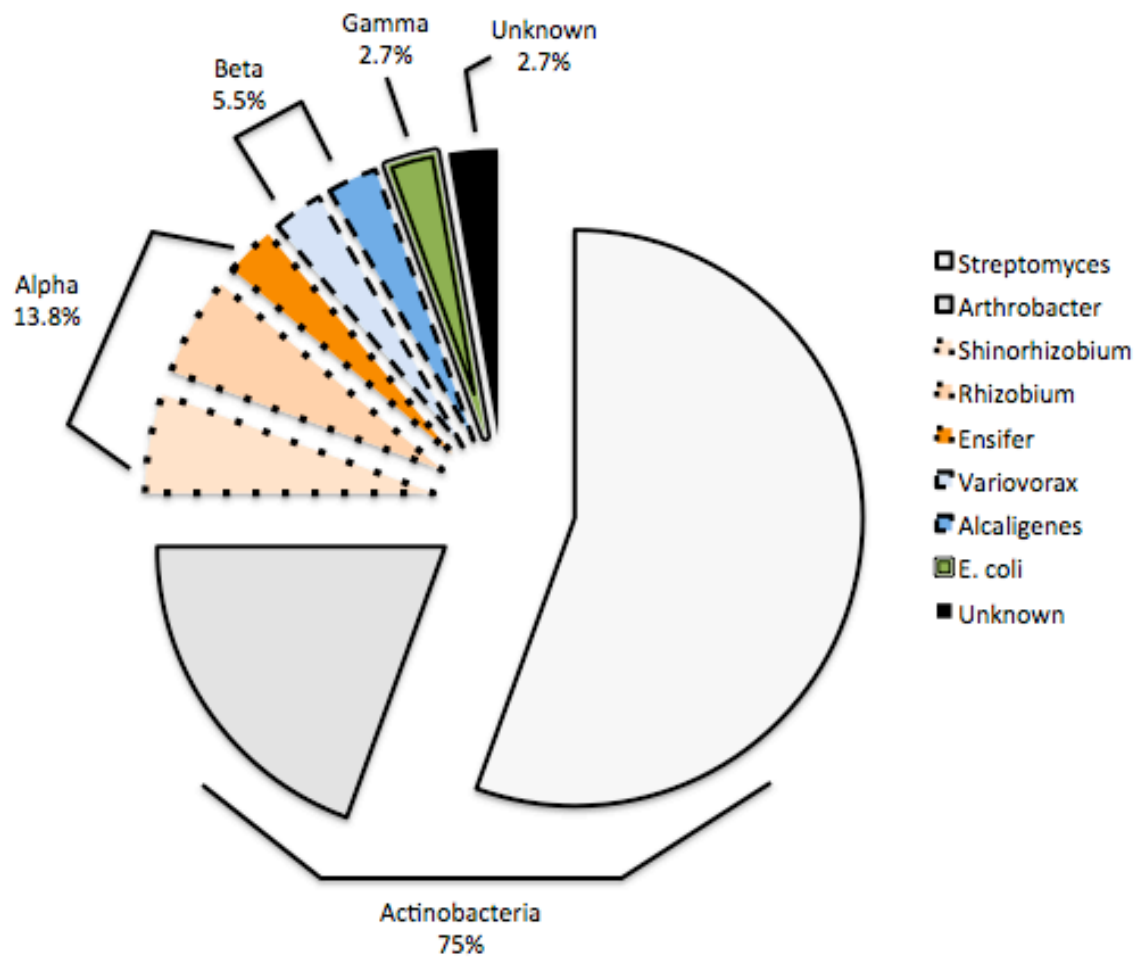


Figure 2.3. Pie chart of taxonomic associations of LS isolates based on 16S rRNA gene sequence BLASTN searches. The Actinobacteria are shown with solid perimetric lines. The Proteobacteria have dotted lines for the *alpha*, dash lines for the *beta*, and double lines for the *gamma*. Sequences that were similar to uncultured clones are marked as unknown and have a solid black fill.

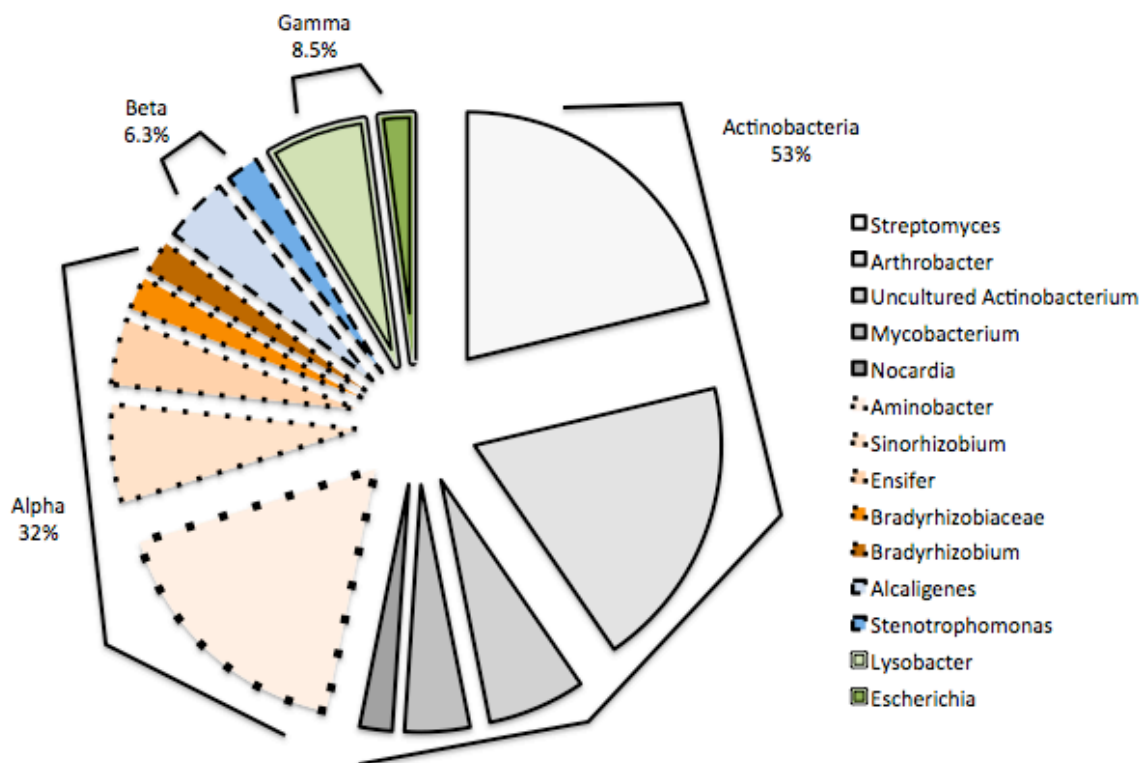


Figure 2.4. Pie chart of taxonomic associations of FS isolates based on 16S rRNA gene sequence BLASTN searches. The Actinobacteria are shown with solid perimetric lines. The Proteobacteria have dotted lines for the *alpha*, dash lines for the *beta*, and double lines for the *gamma*.

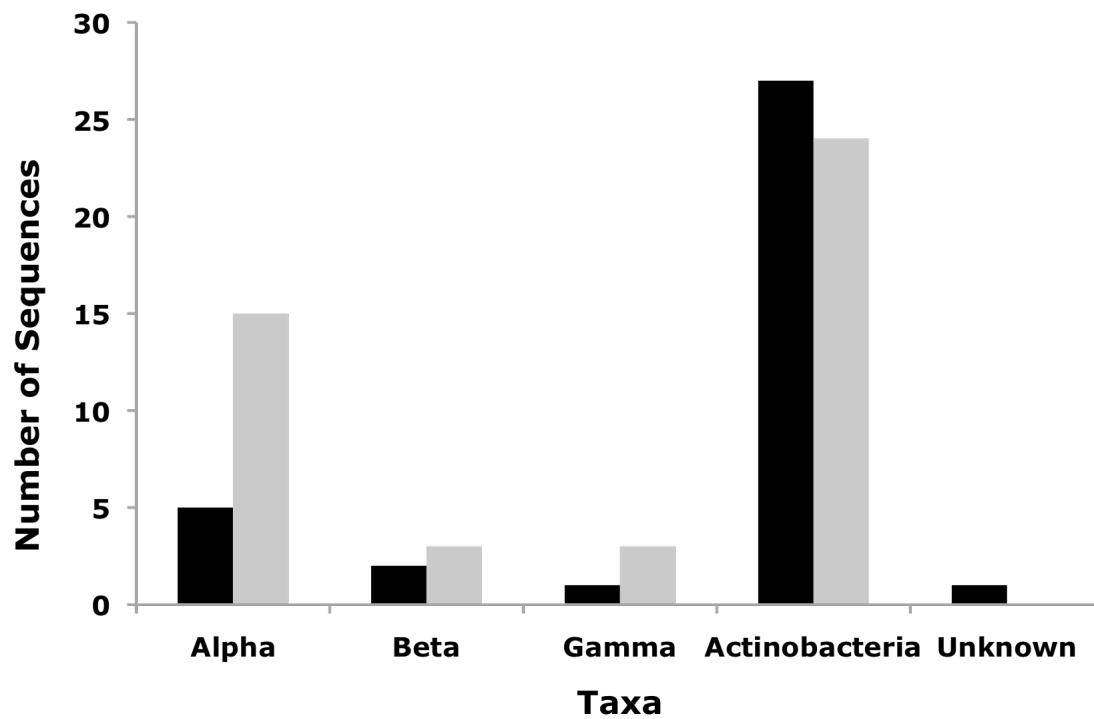


Figure 2.5. Class and phylum level taxonomic distribution of LS (black bars) and FS (grey bars) isolates based on 97% 16S rRNA gene sequence similarity (species level). *Alpha*, *beta* and *gamma*, refer to classes of the Gram negative Proteobacteria. Actinobacteria are High G+C, Gram positive organisms.

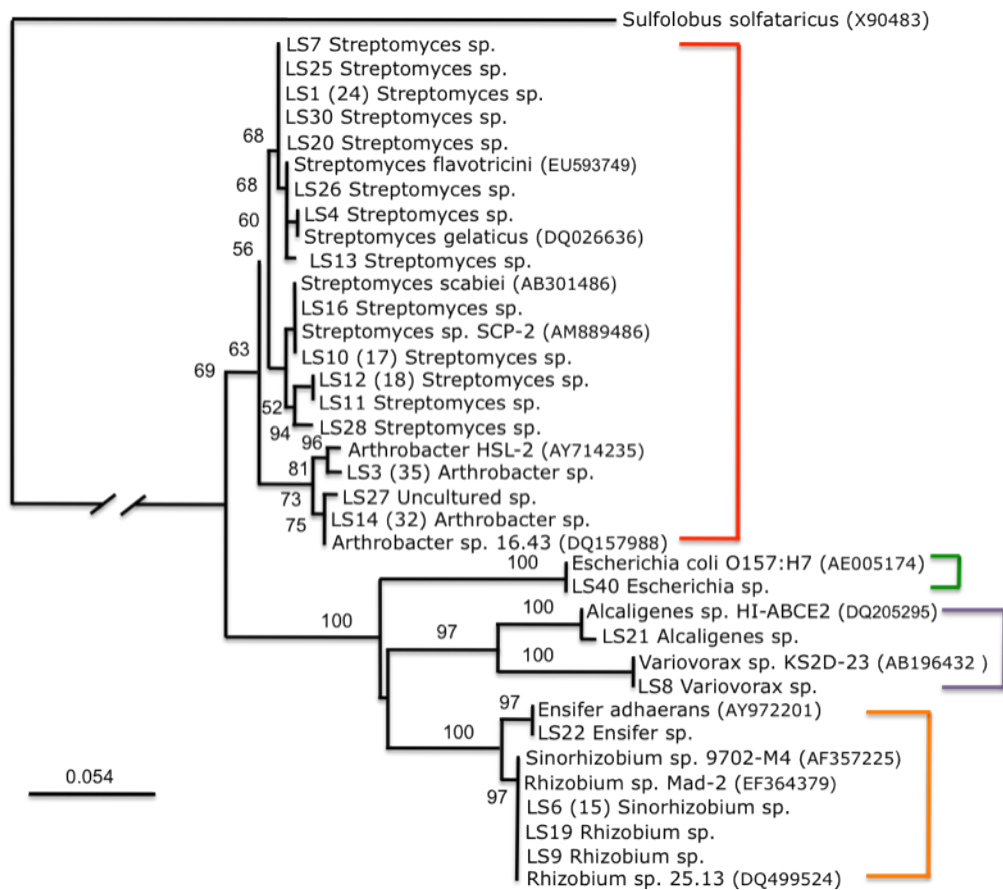


Figure 2.6. Phylogenetic tree of LS isolates and their closest relatives (accession numbers) based on 16S rRNA gene sequences. The Neighbor-Joining tree was constructed using Phylo_Win and the Bootstrap values higher than 50 are shown. Bar indicates 5% estimated nucleotide substitution per site. Color of bracket indicates taxonomic affiliation. Red: Actinobacteria, Green: *gammaproteobacteria*, Purple: *betaproteobacteria*, Orange: *alphaproteobacteria*. Numbers in parentheses indicate clonal sequences. *Sulfolobus solfataricus* was used as an outgroup.

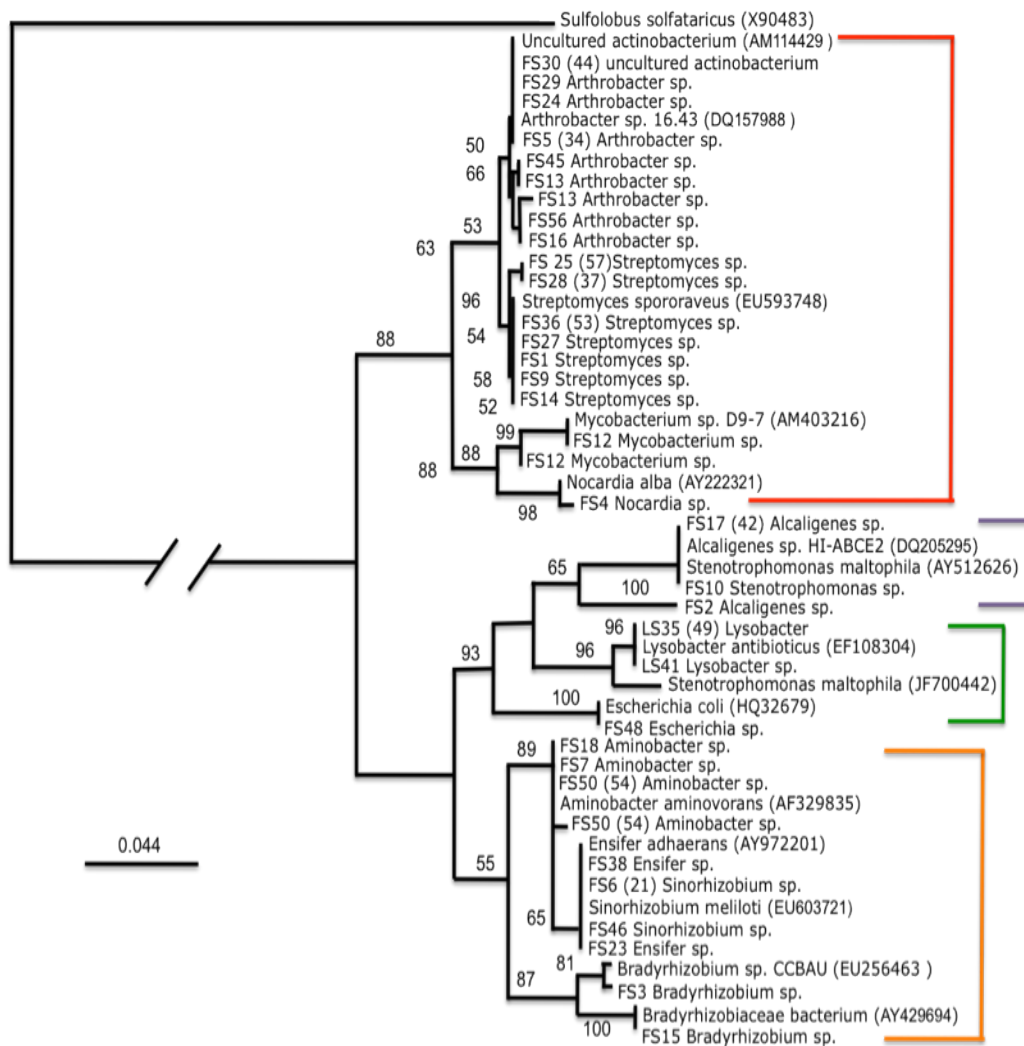


Figure 2.7. Phylogenetic tree of FS isolates and their closest relatives based on 16S rRNA gene sequences. The Neighbor-Joining tree was constructed using Phylo_Win and the Bootstrap values higher than 50 are shown. Bar indicates 4% estimated substitution. Color of bracket indicates taxonomic affiliation. Red: Actinobacteria, Green: *gammaproteobacteria*, Purple: *betaproteobacteria*, Orange: *alphaproteobacteria*. Numbers in parentheses indicate clonal sequences. *Sulfolobus solfataricus* was used as an outgroup.

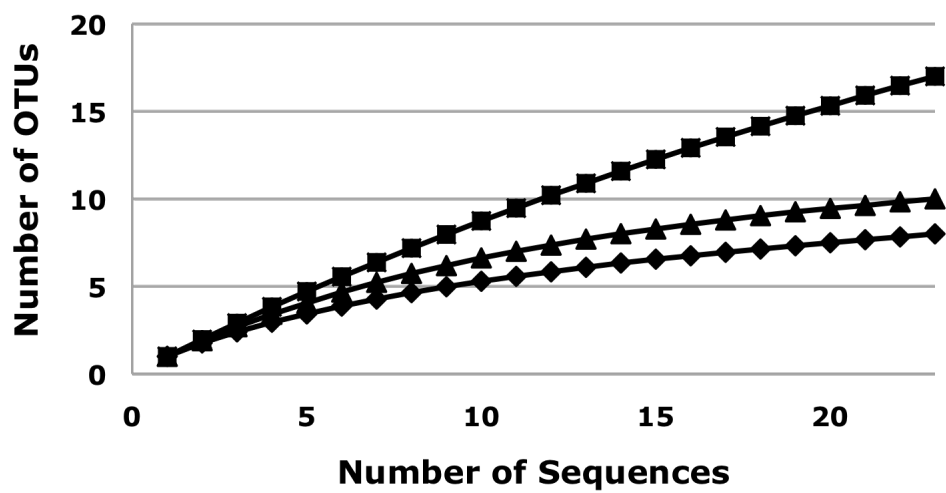


Figure 2.8. Rarefaction curves calculated for the LS isolates, using different grouping criteria. (■) 100%, (▲) 97%, (◆) 96-95% percent 16S rRNA gene sequence similarity.

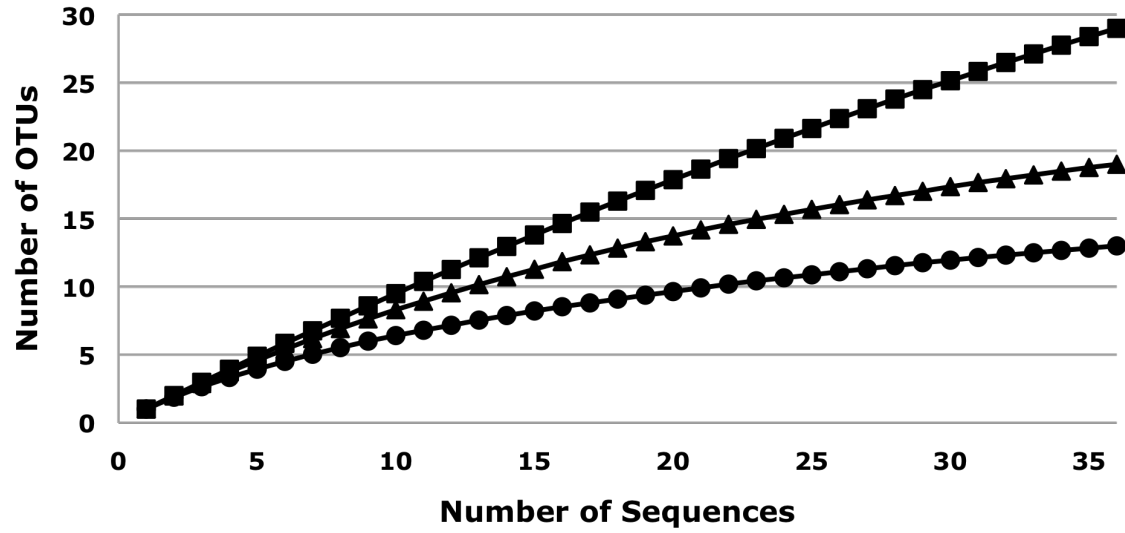


Figure 2.9. Rarefaction curves calculated for the FS isolates, using different grouping criteria. (■) 100%, (▲) 97%, (●) 95% percent 16S rRNA gene sequence similarity.

Table 2.4. Diversity of LS and FS isolates' groups based on 16S rRNA gene sequences.

Isolates' Group	Number of sequences	Number of phylotypes ^a	ACE ^b	Chao1	H' ^c	J ^d
LS	36	23	13 (10-28) ^e	12 (10-26)	2.11 (1.81-2.42)	0.73
FS	47	36	25 (20-46)	25 (20-46)	2.8 (2.57-3.04)	0.81

^a Diversity indices were based on 97% sequence similarity

^b Nonparametric estimates of diversity ACE and Chao1

^c Calculated Shannon Diversity index

^d Evenness measure

^e Numbers in parentheses indicate the 95% confidence intervals

Table 2.5. Primer sets used to amplify the *merA* gene from LS and FS isolates.

Primer Set	Target Organisms	Annealing ¹	Extension	Primer name: sequence (5' to 3')	Amplicon size
1 ^a	Proteobacteria, Firmicutes,	59 °C, 30 s	72 °C, 30 s	Nsf: ATC CGC AAG TNG CVA CBG TNG G rev: CGC YGC RAG CTT YAA YCY YTC RRC CAT YGT	310 bp
2 ^a	Proteobacteria, Firmicutes	61 °C, 30 s	72 °C, 90 s	Nif: CCA TCG GCG GCA CYT GCG TYA A rev: CGC YGC RAG CTT YAA YCY YTC RRC CAT YGT	1249 bp
3 ^a	Proteobacteria, Firmicutes, Actinobacteria Deinococcus-Thermus	64 °C, 60 s	72 °C, 90 s	4 highGC-for: CGT SAA CGT SGG STG CGT GCC STC CAA G 4 highGC-rev: CGA GCY TKA RSS CYT CGG MCA KSG TCA GGT AGG	1246 bp
4 ^b	Alpha-Proteobacteria	52 °C, 30 s	72 °C, 60 s	AI-Fw: TCC AAG GCG MTG ATC CGC GC AI-Rv: TAG GCG GCC ATG TAG ACG AAC TGG TC	800 bp

¹ All PCR programs had 1X cycle of 95 °C, 5 min and 30 X cycles of a 95 °C denaturation step followed by the listed annealing and extension conditions. The program was completed by a final step of extension at 72 °C for 10 min.

^a Primer set designed by Wang et al, (2011).

^b Primer set designed by Øregaard and Sørensen (2007).

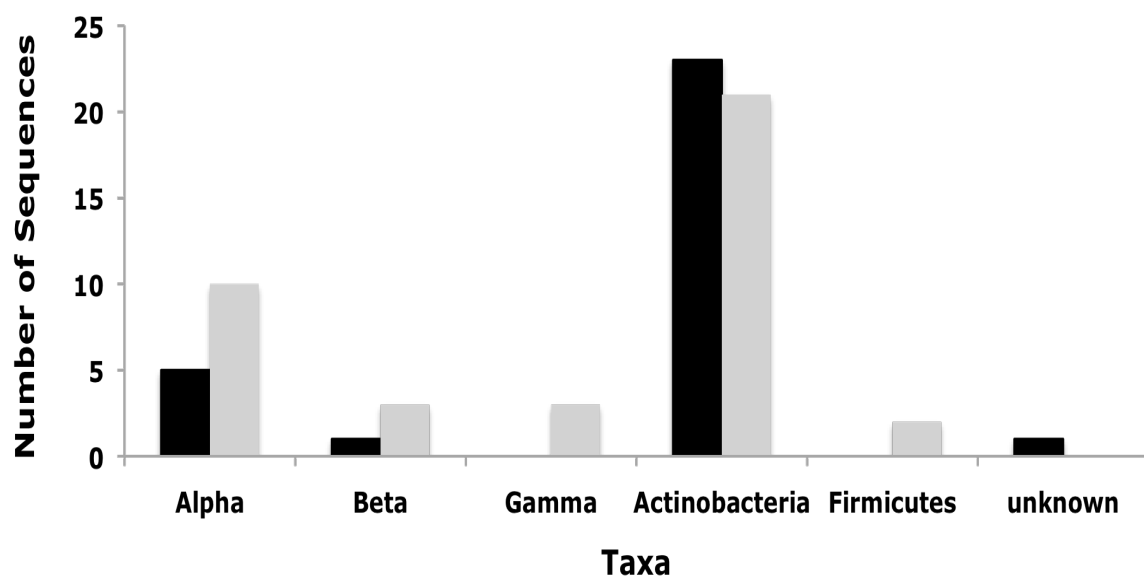


Figure 2.10. Taxonomic distribution of LS (black bars) and FS (grey bars) isolates based on the *merA* gene sequence similarity. *Alpha*, *beta* and *gamma*, refer to classes of the Gram negative Proteobacteria. Actinobacteria and Firmicutes are High and Low G+C Gram positive organisms, respectively.

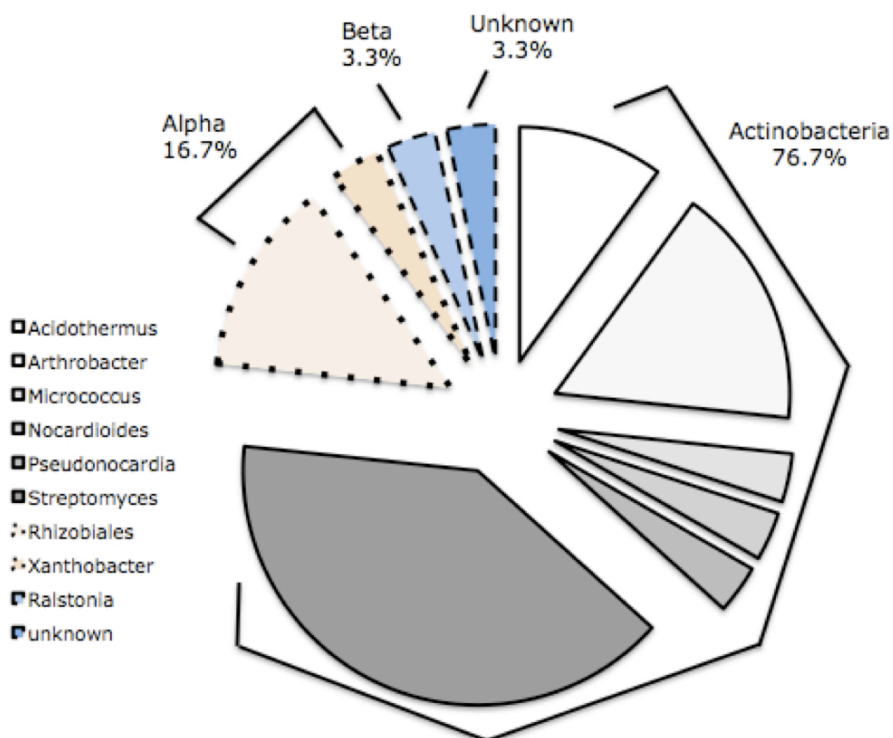


Figure 2.11. Pie chart of taxonomic associations of LS isolates based on MerA amino acid sequence BLASTP searches. The Actinobacteria are shown with solid perimetric lines. The Proteobacteria have dotted lines for the *alpha*, dash lines for the *beta*, and double lines for the *gamma*. Sequences that were similar to uncultured clones are marked as unknown and have a solid black fill.

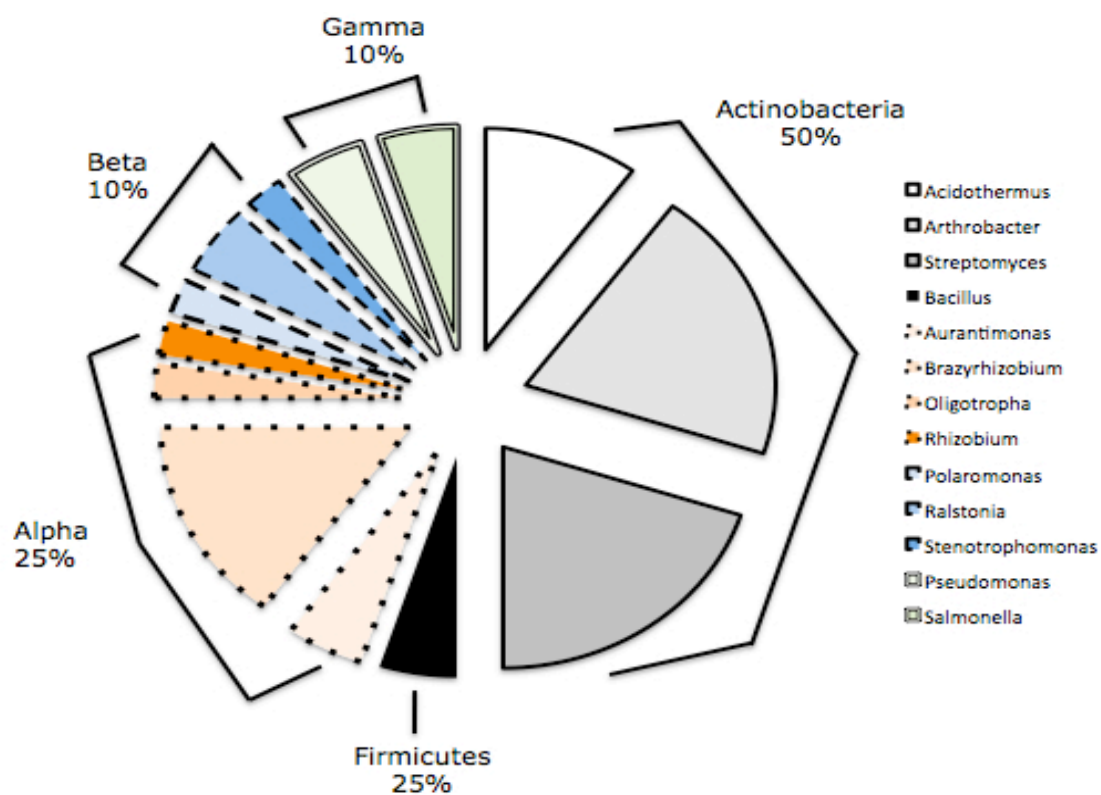


Figure 2.12. Pie chart of taxonomic associations of FS isolates based on MerA amino acid sequence BLASTP searches. The Actinobacteria are shown with solid perimetric lines. The Proteobacteria have dotted lines for the *alpha*, dash lines for the *beta*, and double lines for the *gamma*. Firmicutes are shown in solid black.

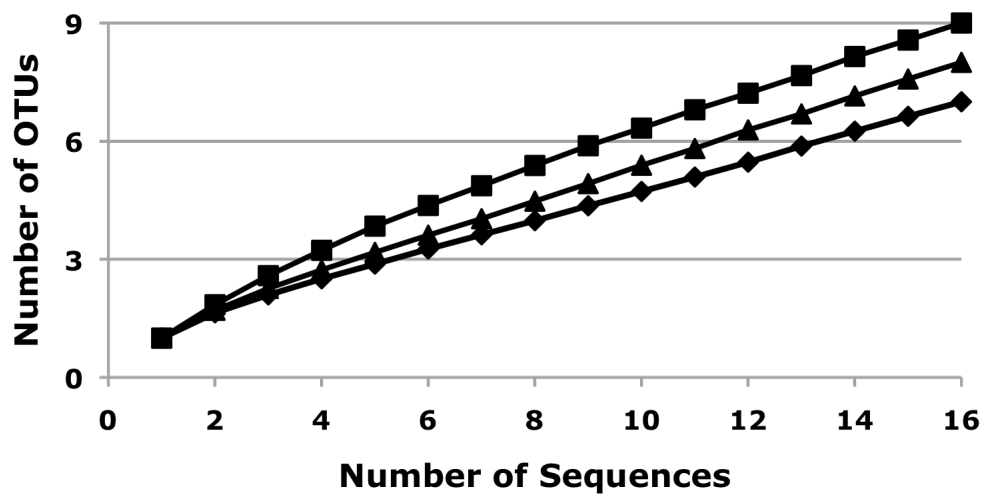


Figure 2.13. Rarefaction curves calculated for the LS isolates, using different grouping criteria. (■) 100%, (▲) 99% and (◆) 95% percent *merA* gene sequence similarity.

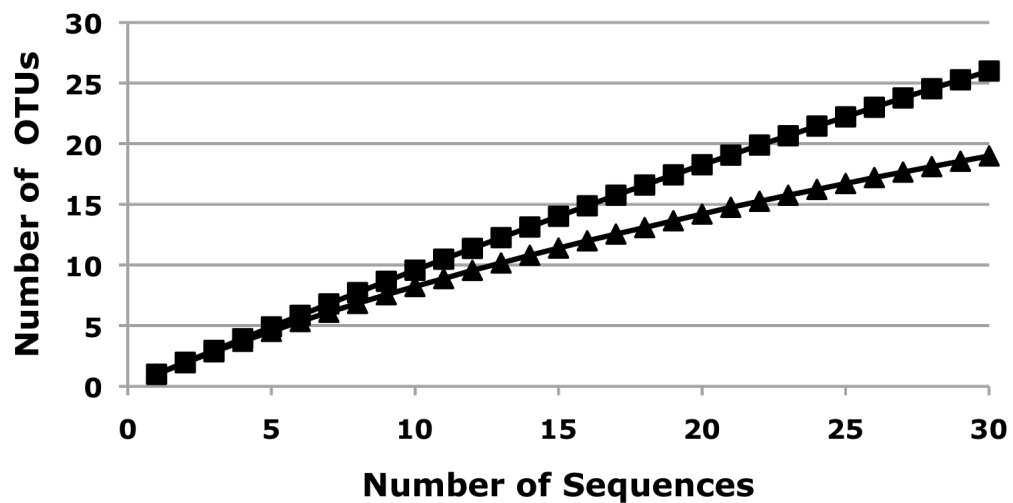


Figure 2.14. Rarefaction curves calculated for the FS isolates, using different grouping criteria. (■) 100%, (▲) 98% percent *merA* gene sequence similarity.

Table 2.6. Diversity LS and FS isolates' groups based on *merA* gene sequences.

Isolates' Group	Number of sequences	Number of phylotypes ^a	Chao1 ^b	H' ^c	J ^d
LS	16	8	22 (10-75) ^e	1.64 (1.1-2.2)	0.85
FS	33	21	36 (25-74)	2.9 (2.7-3.2)	0.92

^a Diversity indices were based on 99% sequence similarity

^b Nonparametric estimates of diversity Chao1

^c Calculated Shannon Diversity index

^d Evenness measure

^e Numbers in parentheses indicate the 95% confidence intervals

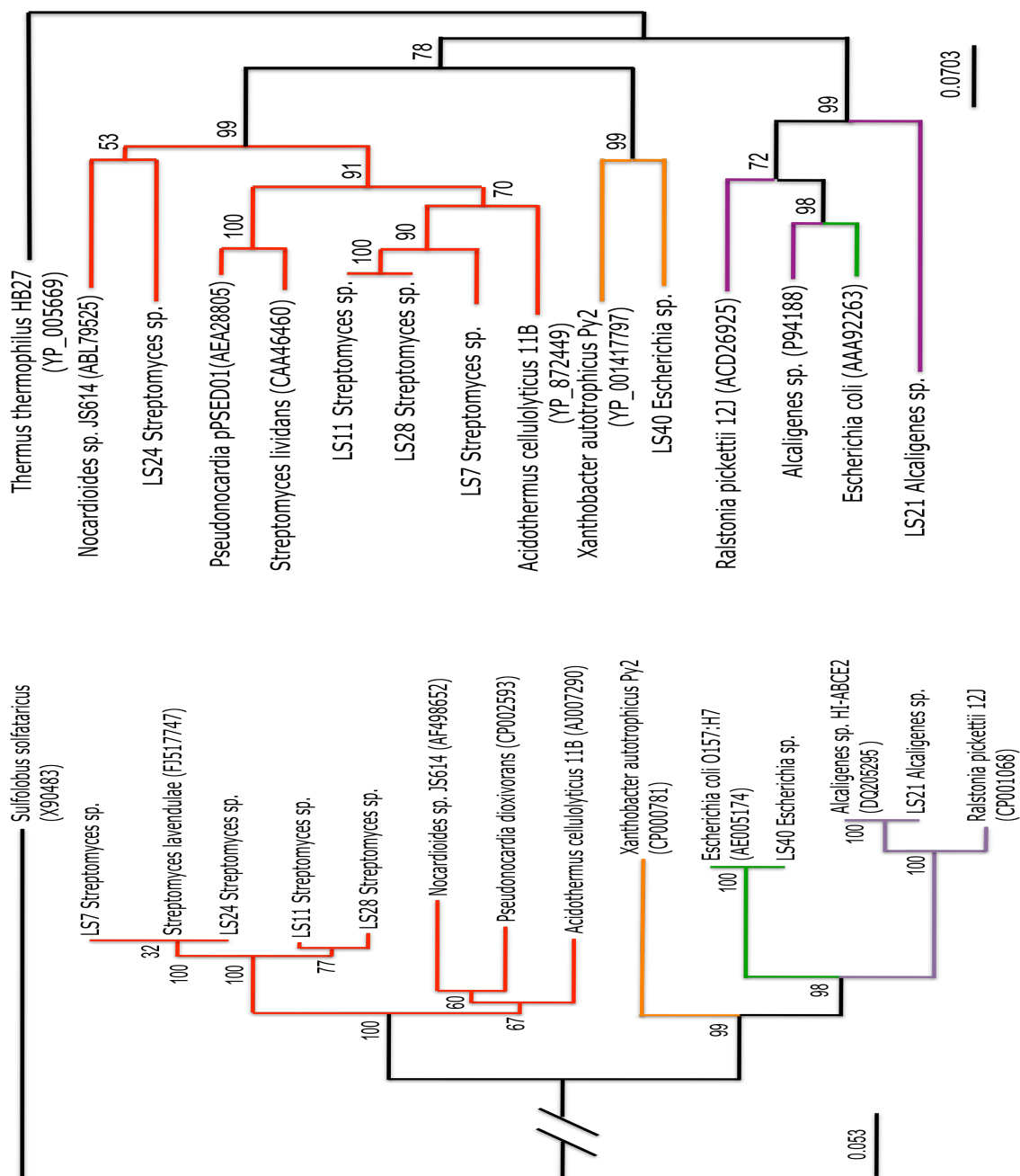


Figure 2.15. Neighbor-joining analysis of 16S rRNA gene and MerA protein sequences of selected LS isolates that show incongruencies and of reference strains. The names of the isolates in both trees correspond to organism's phylogenetic group (16S rRNA gene). Bootstrap values higher than 50 are shown. Bar indicates 5% and 7% estimated substitution. Color indicates taxonomic affiliation. Orange: *alphaproteobacteria*, Purple: *betaproteobacteria*, Green: *gammaproteobacteria*, Red: Actinobacteria. *Sulfolobus solfataricus* was used as an outgroup for the 16S rRNA tree and *Thermus thermophilus* for the MerA tree.

Table 2.7. Comparison of G+C mole% content between recipient strains' genomes and donor *merA* genes among LS Isolates.

Org. Name	Recipient 16S rRNA gene sequence most closely related to:	G+C mole% content genome ^a	G+C mole% content <i>merA</i> ^b	Donor <i>merA</i> gene sequence most closely related to:
LS 7	<i>Streptomyces sp. MJM8416</i> (Actinobacteria)	66-73	72	<i>Pseudonocardia dioxanivorans CB1190 pSED01</i> (Actinobacteria)
LS 11	<i>Streptomyces umbrinus</i> (Actinobacteria)	66-73	70	<i>Acidothermus cellulolyticus 11B</i> (Actinobacteria)
LS 14	<i>Arthrobacter sp. 16.43</i> (Actinobacteria)	64-73	66	<i>Streptomyces lividans</i> (Actinobacteria)
LS 24	<i>Streptomyces sp. SCP-2</i> (Actinobacteria)	66-73	67	<i>Nocardioides sp. JS614</i> (Actinobacteria)
LS 28	<i>Streptomyces sp. Lz531</i> (Actinobacteria)	66-73	70	<i>Acidothermus cellulolyticus 11B</i> (Actinobacteria)
LS 21	<i>Alcaligenes sp. HI-ABCE2</i> (beta)	56-60	65	<i>Ralstonia pickettii 12J</i> (beta)
LS 33	<i>Streptomyces sp. SCP-2</i> (Actinobacteria)	66-73	67	<i>Micrococcus luteus NCTC 2665</i> (Actinobacteria)
LS 40	<i>E. coli</i> (gamma)	48.5-52	61	<i>Xanthobacter autotrophicus</i> (alpha)

^a The genomic G+C mole% content ranges were found in *The Prokaryotes* and Bergey's manual.

^b The G+C mole% content of the *merA* genes was calculated using the OligoCal tool at: www.basic.northwestern.edu/biotools/oligocalc.html

Table 2.8.1. Comparison of G+C mole% content between recipient strains' genomes and donor *merA* genes among Proteobacterial FS Isolates.

Org. Name	Recipient 16S rRNA gene sequence most closely related to:	G+C mole% content genome ^a	G+C mole% content <i>merA</i> ^b	Donor <i>merA</i> gene sequence most closely related to:
FS 2	<i>Aminobacter aminovorans</i> (<i>alpha</i>)	62.5	64	<i>Bradyrhizobium</i> sp. Is-D308 (<i>alpha</i>)
FS 3	<i>Bradyrhizobium</i> sp. CCBAU 85057 (<i>alpha</i>)	64.1	64	<i>Oligotropha carboxidovorans</i> OM5 (<i>alpha</i>)
FS 6 & 21	<i>Sinorhizobium</i> sp. CAF63 (<i>alpha</i>)	57-66	64	<i>Bradyrhizobium</i> sp. Is-D308 (<i>alpha</i>)
FS 7	<i>Aminobacter aminovorans</i> DSM7048T (<i>alpha</i>)	62.5	66	<i>Aurantimonas manganooxydans</i> SI85-9A1 (<i>alpha</i>)
FS 18	<i>Aminobacter</i> sp. MSH1 (<i>alpha</i>)	62-64	64	<i>Bradyrhizobium</i> sp. Is-D308 (<i>alpha</i>)
FS 23	<i>Ensifer adhaerens</i> S-30.7.5 (<i>alpha</i>)	62.1	66	<i>Aurantimonas</i> sp. SI85-9A1 (<i>alpha</i>)
FS 33	<i>Aminobacter aminovorans</i> (<i>alpha</i>)	62.5	57	<i>Bacillus cereus</i> (Firmicutes)
FS 54	<i>Aminobacter</i> sp. C4 (<i>alpha</i>)	57-63	57	<i>Bacillus cereus</i> (Firmicutes)
FS 10	<i>Stenotrophomonas maltophilia</i> (<i>beta</i>)	66	66	<i>Salmonella enterica</i> (<i>gamma</i>)
FS 17	<i>Alcaligenes</i> sp. HI-ABCE2 (<i>beta</i>)	56-60	69	<i>Ralstonia pichettii</i> 12J (<i>beta</i>)
FS 42	<i>Alcaligenes</i> sp. HI-ABCE2 (<i>beta</i>)	56-60	69	<i>Ralstonia pichettii</i> 12J (<i>beta</i>)
FS 35	<i>Lysobacter</i> sp. 13-1 (<i>gamma</i>)	65-70	64	<i>Pseudomonas aeruginosa</i> (<i>gamma</i>)
FS 41	<i>Lysobacter antibioticus</i> (<i>gamma</i>)	66.2-69.2	68	<i>Polaromonas</i> sp. (<i>beta</i>)
FS 49	<i>Lysobacter</i> sp. 13-1 (<i>gamma</i>)	65-70	64	<i>Stenotrophomonas maltophilia</i> K279a (<i>beta</i>)

^a The genomic G+C mole% content ranges were found in *The Prokaryotes* and Bergey's manual.

^b The G+C mole% content of the *merA* genes was calculated using the OligoCal tool at: www.basic.northwestern.edu/biotools/oligoCalc.html

Table 2.8.2. Comparison of G+C mole% content between recipient strains' genomes and donor *merA* genes among Actinobacterial FS Isolates.

Org. Name	Recipient 16S rRNA gene sequence most closely related to:	%G+C genome ^a	%G+C <i>merA</i> ^b	Donor <i>merA</i> gene sequence most closely related to:
FS 4	<i>Nocardia alba</i> (Actinobacteria)	72	67	<i>Streptomyces</i> sp. CHR28 pRJ28 (Actinobacteria)
FS12	<i>Mycobacterium</i> sp. MOLA 520 (Actinobacteria)	59-66	68	<i>Acidothermus cellulolyticus</i> 11B (Actinobacteria)
FS 14	<i>Streptomyces</i> sp. 10-3 (Actinobacteria)	70-72	68	<i>Acidothermus cellulolyticus</i> 11B (Actinobacteria)
FS 27	<i>Streptomyces ederensis</i> strain 174483 (Actinobacteria)	70-72	68	<i>Acidothermus cellulolyticus</i> 11B (Actinobacteria)
FS 28	<i>Streptomyces</i> sp. HBUM87110 (Actinobacteria)	70-72	68	<i>Acidothermus cellulolyticus</i> 11B (Actinobacteria)

^a The genomic G+C mole% content ranges were found in *The Prokaryotes* and Bergey's manual.

^b The G+C mole% content of the *merA* genes was calculated using the OligoCal tool at: www.basic.northwestern.edu/biotools/oligoalc.html

Table 2.9. Indications of HGT of *merA* among LS Isolates.

Isolate	Phylogenetic incongruence ^a	G+C mole% content ^b	Plasmid presence/Positive <i>merA</i> amplification
LS 7 <i>Streptomyces sp.</i> <i>MJM8416</i> (Actinobacteria)	+	-	-/-
LS 11 <i>Streptomyces umbrinus</i> (Actinobacteria)	+	-	-/-
LS 14 <i>Arthrobacter sp.</i> <i>16.43</i> (Actinobacteria)	+	-	ND ^c
LS 24 <i>Streptomyces sp.</i> <i>SCP-2</i> (Actinobacteria)	+	-	-/-
LS 28 <i>Streptomyces sp.</i> <i>Lz531</i> (Actinobacteria)	+	-	+ / ND
LS 21 <i>Alcaligenes sp.</i> <i>HI-ABCE2</i> (beta)	+	+	ND/ND
LS 33 <i>Streptomyces sp.</i> <i>SCP-2</i> (Actinobacteria)	+	-	-
LS 40 <i>E. coli</i> (gamma)	+	+	+ / ND

^a Phylogenetic incongruencies between the 16S rRNA gene sequences and MerA amino acid sequences.

^b G+C mole% content comparison between genomic and *merA* gene sequences.

Table 2.10.1. Indications of HGT of *merA* among Proteobacterial FS Isolates.

Isolate	Phylogenetic incongruence ^a	G+C mole% content ^b	Plasmid presence/ Positive <i>merA</i> amplification
FS 2 <i>Aminobacter aminovorans</i> (<i>alpha</i>)	+	+	+/ND ^c
FS 3 <i>Bradyrhizobium</i> sp. CCBAU 85057 (<i>alpha</i>)	+	-	+/+
FS 6 & 21 <i>Sinorhizobium</i> sp. CAF63 (<i>alpha</i>)	+	-	+/+ +/ND
FS 7 <i>Aminobacter aminovorans</i> DSM7048T (<i>alpha</i>)	+	+	+/+
FS 18 <i>Aminobacter</i> sp. MSH1 (<i>alpha</i>)	+	-	-
FS 23 <i>Ensifer adhaerens</i> S-30.7.5 (<i>alpha</i>)	+	+	-
FS 33 <i>Aminobacter aminovorans</i> (<i>alpha</i>)	+	+	+/+ (Primer Set 2)
FS 54 <i>Aminobacter</i> sp.C4 (<i>alpha</i>)	+	-	ND
FS 10 <i>Stenotrophomonas maltophila</i> (<i>beta</i>)	+	-	+/+
FS 17 <i>Alcaligenes</i> sp. HI-ABCE2 (<i>beta</i>)	+	+	+/+
FS 42 <i>Alcaligenes</i> sp. HI-ABCE2 (<i>beta</i>)	+	+	+/+
FS 35 <i>Lysobacter</i> sp. 13-1 (<i>gamma</i>)	+	+	+/+
FS 41 <i>Lysobacter antibioticus</i> (<i>gamma</i>)	+	-	+/+
FS 49 <i>Lysobacter</i> sp. 13-1 (<i>gamma</i>)	+	+	+/+

^a Phylogenetic incongruencies between the 16S rRNA gene sequences and MerA amino acid sequences.

^b G+C mole% content comparison between genomic and *merA* gene sequences.

^c ND: Not determined.

Table 2.10.2. Indications of HGT of *merA* among Actinobacterial FS Isolates.

Isolate	Phylogenetic incongruence ^a	G+C mole% content ^b	Plasmid presence/ Positive <i>merA</i> amplification
FS 4 <i>Nocardia alba</i> (Actinobacteria)	+	+	+/+
FS12 <i>Mycobacterium</i> sp. MOLA 520 (Actinobacteria)	+	+	+/+
FS 14 <i>Streptomyces</i> sp. 10-3 (Actinobacteria)	+	+	+/+
FS 27 <i>Streptomyces ederenis</i> strain 174483 (Actinobacteria)	+	+	+/+
FS 28 <i>Streptomyces</i> sp. HBUM87110 (Actinobacteria)	+	+	+/+

^a Phylogenetic incongruencies between the 16S rRNA gene sequences and MerA amino acid sequences.

^b G+C mole% content comparison between genomic and *merA* gene sequences.

Chapter 3 - Biogeographical Patterns of Bacterial Communities Along the Mercury Contaminated Floodplains of South River, Virginia.

Introduction

Hg contamination in Virginia's South River (SR) is attributed to the use of mercuric sulfate as a catalyst in the production of acetate fiber. The industrial process was carried out in the DuPont facility located on the banks of SR in the town of Waynesboro (Carter, 1977). Hg contamination in the floodplain sediments, is thought to have originated from unreported spills during the catalyst recycling process, and by virtue of flooding and bank erosion events, carried throughout the SR ecosystem.

In this riverine system, Hg contamination is a persistent problem that doesn't seem to attenuate with the passing of time. Sixty years after the cessation of Hg use, Hg concentrations are still high, severely impacting the associated aquatic and terrestrial food chains (Cristol et al, 2008). Fish, arthropods and birds, all were found to have Hg levels that exceed the EPA standards (0.3 mg/Kg) (EPA). Fish consumption is also prohibited as Hg exceeds the FDA action levels of 0.5 mg/Kg for marketed fish, restricting fishing activities to recreational catch/release (FDA).

To identify the causes and consequences of Hg contamination in SR, a consortium of scientists from different agencies and corporations, called the South River Science Team, was formed in 2000. The specific objectives of this team were: (1) to evaluate specific factors contributing to the Hg contamination, (2) to determine the reasons why Hg concentration in the fish and wildlife biota remains elevated despite the 60-year natural recovery, and (3) to identify and propose remedial strategies (Flanders et al, 2010, Carter, 1977).

Understanding the microbial contribution to the Hg contamination problem in this riverine system is of particular importance because microbial communities

occupy the base of the food chain and the way they transform Hg has bottom-up effects to all trophic levels (Barkay et al, 2003, Clarkson, 2002). Furthermore, microorganisms are far more sensitive to heavy-metal stress than animals and plants, thus they can be used as indicators of stress in the environment (Giller et al, 2009). Bio-indicators are a very useful tool in assessing pollution levels, especially when the endpoint of management is to protect and conserve biological and ecological resources and functions (White et al, 1998). Finally, a microbial remedial action is an attractive proposition as it bypasses the use of engineering or chemical based-remediation (Barkay and Schaefer, 2001). Simple induction of local microbial communities is not very likely to impact the ecosystem negatively, whereas dredging and capping (Wessels Perelo, 2010), removal and incineration of contaminated sediments disturb the environment gravely (Whicker et al, 2004).

For these reasons, there is a pressing need to study and understand the microbial contribution to the Hg contamination problem in SR. In other words, how does the choice of Hg transformations employed by microbes to detoxify their own milieu influence the bioavailability of Hg to the food chain and to the environment itself?

Bacterial resistance to methylmercury (MeHg) is encoded by the mercury resistance (*mer*) operon, which is tightly regulated by the Hg(II) bioavailability in the environment (Barkay et al, 2003). This mechanism involves expression and co-ordination of the organomercurial lyase (MerB) protein, that cleaves the C-Hg bond, and the mercuric reductase (MerA) which further reduces Hg(II) to Hg(0), a volatile form that escapes to the atmosphere. This two-step detoxification process is in competition with Hg methylation, which converts Hg(II) into MeHg thus increasing Hg toxicity by virtue of transfer of the neurotoxic substance into the food chain. MeHg demethylation undoes methylation, as MerB degrades the MeHg reducing its environmental pool and accumulation in sediments and biomagnification in the food

chain (Schaefer et al, 2004). The reduction mechanism indirectly competes with methylation, as Hg(II) is a shared substrate for both processes and high reduction rates of Hg(II) to its volatile form (Hg[0]), by MerA, decreases its bioavailability to the methylation process and may lower the rates of the methylation/demethylation cycle. Studies performed in other aquatic ecosystems showed that Total Mercury (THg) concentrations are inversely proportional to MeHg concentrations (Barkay and Wagner-Dobler, 2005 and References therein). This trend was attributed to the induction of the more efficient mechanisms of detoxification, carried out by the Mer proteins, when THg concentrations were high (Schaefer et al, 2004).

The contribution of microbial communities to the production of MeHg in South River sediments was recently studied (Yu et al, 2011). It was shown that in anaerobic riverine sediment incubations, the potential methylation rates were higher than those observed in other riverine ecosystems, and that active microbial guilds in sediment incubations that methylated Hg were phylogenetically related to sulfate-reducing bacteria (SRB) and to iron reducing bacteria (IRB). The detoxification mechanism of MeHg-demethylation was also found to be significant, but at lower rates than those found in other studies, and it best correlated to MeHg as opposed to THg, sulfate and iron concentrations (Yu et al, 2011). Together the results suggested a high metabolic potential for the production of MeHg in South River sediments.

Scope of study

No previous research has been conducted to study the biogeographical patterns of bacterial communities along the contaminated SR in response to Hg and other abiotic factors. In this study I examined the development and composition of soil bacteria in samples collected from forest-covered floodplains across the SR using a culture-dependent method and their diversity based on culture-independent

methods. The specific method used was terminal restriction length polymorphism (t-RFLP), which allows quantification of sequence variability of 16S rRNA gene sequences directly extracted from environmental samples (Liu et al, 1997). The DNA fingerprints produced from each bacterial community are based on fragment length representing unique phylotypes and their abundance within that community.

This method is suited for analysis of a large number of samples and for quantitatively detecting differences in diversity and composition of soil bacterial communities (Shutte, et al 2008). This is a valuable tool providing a reliable assessment of bacterial abundance, and is an alternative to clone libraries, which do allow for a more detailed analysis of phylogenetic information, but demand large scale sequence efforts to capture the same levels of diversity to those captured with t-RFLP (Kitts, 2001 and references therein, Liu et al, 1997). Also, t-RFLP results have been shown to be consistent with results from clone libraries (Mannisto et al, 2009).

I also report the development of a new functional gene t-RFLP method, for the estimation and quantification of *merA* determinant diversity and spatial distribution in soil samples across the SR. *merA* gene encodes for MerA, a part of the reductive Hg detoxification mechanism. The choice of primers in the method design, was based on their ability to amplify *merA* genes from organisms belonging to a wide array of taxonomic groups, including but not limited to the phyla Deinococcus-Thermus, Actinobacteria, Firmicutes and classes of the Proteobacteria (Wang et al, 2011). To the best of our knowledge, this is the first report of a functional *merA*-t-RFLP procedure, yet functional gene t-RFLP has been used successfully by other workers to assess the spatial variability of genes encoding functions such as nitrification (Siripong and Rittmann, 2006), methane oxidation (Hoffmann et al, 2002) and chitin degradation (Ikeda et al, 2006).

Finally, to assess biogeographical patterns of bacterial communities and determine which environmental variables are good predictors of diversity, I used a

number of univariate and multivariate ordination techniques and cluster analyses based on both 16S rRNA- and *merA*- gene fingerprints (Shutte, et al 2008, Fierer and Jackson, 2006). Univariate and cluster methods of analysis were used to determine the influence on diversity, one variable at a time. To obtain a more resolved picture on the interplay of abiotic and biotic variables, the multivariate method was used as it ordines variables in multi-dimensional space and can infer cross-correlations among them at a time (Cao et al, 2006, terBraak 1986).

Materials & Methods

1. Hg gradient sampling site

The South River (SR) originates south of Staunton, Virginia, and flows northward through Waynesboro, to the confluence with North and Middle Rivers at Port Republic (Figure 3.1). These three rivers are tributaries to the South Fork Shenandoah River. For sampling purposes, the SR has been sub-divided in six reaches, with each reach being the distance between 2 bridge crossings along the 24 miles between the DuPont site in Waynesboro and the Port Republic. The DuPont site is the beginning of the gradient as it is thought to be the source of Hg to the SR ecosystem. The soil samples used in this study were collected from forested areas of the floodplain with an average flooding frequency (FP) of 2-years (Figure 3.2). The THg levels for this specific land use and flooding frequency combination are the highest as compared to other land uses (open space and pastureland) and flooding frequencies (5-year and 60-year). The THg in these samples ranged from 0.026 to 70.7 mg/Kg (Flanders, J. R. Personal Communication).

Samples were collected in duplicate from each reach, between 2/19/2008 to 3/18/2008, from the surface (0 cm) to a depth of 15 cm and sieved down to 2 mm. Chemical analyses for THg concentration, moisture, soil texture and organic carbon

content (LOI), were performed by J. R. Flanders (URS Corporation and the DuPont Corp.) (Table 3.1). Soil samples were then dried and stored at room temperature. Upon receipt at Rutgers, on April 2009, the soil samples were stored at 4 °C for chemical, microbial, and molecular analyses.

To determine the pH, 20 g of soil was mixed with 20 ml of 2 mM pyrophosphate buffer and stirred for 30 min. The slurry was allowed to sit for 2 h to allow the particles to settle before a reading was taken using a Fisher Scientific Accumet pH meter (Fisher Scientific Inc., Pittsburg, PA) (Hartman et al, 2008).

2. Day of colony appearance protocol

To examine the viable Hg^R bacteria present in the soil samples of the gradient, soil samples were serially diluted and plated on 0.2X TSA amended with 100 µM HgCl₂. I used this nutrient and Hg concentration because these same conditions selected for resistant bacteria and promoted the growth of both slow and fast growers of the r & K continuum when applied to soil samples from the EFPC (See Materials & Methods section in Chapter 2).

The plating protocol followed the one that is presented in the Materials & Methods section of Chapter 2, except for the addition of a pre-treatment step. This treatment, applied to two of the soil samples, relative river mile (RRM) 9.1 and RRM 19.7, consisted of a 24 hrs exposure to 10 µg/g HgCl₂ prior to plating. This step was included to test whether pre-treatment with Hg has an effect on the Hg^R bacteria when compared to the same sample that was not pre-treated.

Colonies were counted on day 3, 10, and 17 so as to see the progression of the r- and K-continuum. I used the assumption that organisms that grow after 24-48 h are fast-growing r-strategists and those appearing on the 10th and 17th day readings are considered slow growing K-strategists (Deleij, 1993). Finally, all incubations were carried out in the dark and at 28 °C.

3. 16S rRNA/t-RFLP analysis of the soil samples

a- Sample preparation protocol

To determine the trends of the phylogenetic diversity among the microbial communities of the soil samples of the gradient, the culture-independent terminal Restriction Fragment Length Polymorphism (t-RFLP) technique was used. In general terms, in the t-RFLP community analysis, the chromatogram that has the most peaks represents the most diverse community and vice versa (Avaniss-Aghajani, et al, 1994).

In more detail, total genomic DNA, from each soil sample, was successfully extracted, except for the RRM 1.7 sample, using the UltraClean™ Microbial DNA isolation kit, according to the manufacturer's instructions (MoBio Laboratories, Solana Beach, CA, USA). To quantitate the concentration of DNA, samples were loaded and ran in a 1% agarose gel against 100 ng of the λ *HindIII* marker. Ten nanograms of total DNA was added to a PCR reaction mix containing: 15.25 μ l H₂O, 2.5 μ l 10x PCR buffer, 1.5 μ l of 25 mM MgCl₂, 0.5 μ l of 10 μ M dNTPs, 0.5 μ l of universal primer 27F carrying 6-FAM fluorescent tag on the 5' end (Gibco Life Technologies, Gaithersburg, MD), 0.5 μ l of universal primer 519R, and 0.25 μ l of Taq polymerase to a final volume of 25 μ l per reaction. The PCR program includes 1x cycle of denaturation at 95 °C for 5 min, 28X cycles of denaturation at 95 °C for 1 min, primer annealing at 53 °C for 20 sec, extension at 72 °C for 30 sec, and a final cycle of extension at 72 °C for 10 min.

To produce a mixture of variable length, end-labeled fragments, 15 ng of DNA were digested with the restriction enzyme *MnI* (New England Biolabs® Inc., Ipswich, MA) for 6 h at 37 °C in a reaction mix containing: 2 μ l of NEB buffer 2, 2 μ l of 10x BSA, 0.2 μ l of *MnI*, and 10.8 μ l of H₂O for a final volume of 20 μ l per reaction. To clean up the digested DNA, 1.9 μ l of 3 mM sodium acetate and 37 μ l of 95% ethanol

were added to the digests and tubes were incubated at room temperature for 15 min. The reactions were centrifuged at maximum speed for 15 min at 4 °C, the supernatant was removed and 125 µl of 70 % ethanol were added to wash the DNA pellet. The pellets were left to dry at room temperature and dissolved in 19.7 µl of deionized formamide and 0.3 µl of GeneScan®-500 [ROX][™] (Applied Biosystems, South San Francisco, CA) and denatured at 95 °C for 2 min. The end-labeled DNA fragments were electrophoretically separated on a polyacrylamide gel in an ABI model 373 automated sequencer (Applied Biosystems, Foster City, CA) (Kerkhof et al, 2000).

b- Analysis of 16S rRNA/t-RFLP results

The resulting t-RFLP fingerprints of the 11 soil samples were analyzed using the Genescan Software (Perkin-Elmer, Foster City, CA) with a peak size detection of 50-495 base pairs (bps) and peak area detection of ≥ 50 arbitrary fluorescent units. Peak presence is used as a species richness measure, and peak area as a measure of abundance of each peak in the sample (McGuinness et al, 2006, Scala and Kerkhof, 2000, Liu et al, 1997).

Peaks that differed by >0.5 bps in different fingerprints were considered unique operational taxonomic units (OTU) (Dunbar et al, 2001). To allow for a comparison among the samples, all peak areas of a fingerprint were normalized to the total area of that sample. Peaks contributing $\geq 1\%$ of the total areas of all the samples were considered the most abundant/dominant peaks (Mannisto et al, 2009, McGuinness et al, 2006).

4. Development of a *merA*-t-RFLP method

To determine the trends in functional diversity among the microbial communities of the soil samples along the Hg gradient, the t-RFLP method was

applied using Primer set 3 (see Chapter 2). This degenerate PCR primer set, targets *merA* determinants of the Phyla Proteobacteria, Firmicutes, Actinobacteria and Deinococcus-Thermus. The resulting amplified PCR product is 1,205 bp long (Wang et al, 2011). The 5'-end of forward primer of this set was labeled with 6-carboxylfluorescein (6-FAM) (Applied Biosystems, Foster City, CA) for the t-RFLP purposes.

The EnzymeX program (<http://www.mekentosj.com/science/enzymex>) was used to determine which endonucleases will produce a mixture of variable length end-labeled fragments desired for fingerprinting. The *merA* sequences used to determine the *in silico* digestion were the *mer* operons, of the *gammaproteobacterial* Tn501 (Z00027), Tn21 (AF071413) and pPB20 (U80214) of the *P. stutzerii* strain OX, those of the actinobacterial *Rubrobacter xylanophilus* (YP644538), *Streptomyces lividans* (X65467), and *Streptomyces* sp. CHR28/pRJ28 (AF222792), and Deinococcus-Thermus *Thermus thermophilus* HB27 (YP004762), based on which the Primer set 3 was designed (Wang et al, 2011). *merA* sequences belonging to the *alphaproteobacteria* *Oligotropha carboxidovorans* OM5 (NC_011386.1) and *Xanthobacter autotrophicus* Py2 (NC_009720.1), the *betaproteobacteria* *Ralstonia pickettii* 12J (CP001068.1) and *Alcaligenes* sp. pMER610 (Y08993.1), and the Firmicutes *Bacillus cereus* AH820 (CP001283.1), were also digested *in silico*, as it has been shown that they can be amplified by this primer set (See Chapter 2).

The endonucleases *Mbo*II and *M*s/I were selected as their combined cutting pattern allows distinction among the major subclasses of amplicons produced by the Primer set 3. The size ranges of *merA* sequences doubly digested with these restriction enzymes was 115 to 466 bps, which is within the size detection limits of the ABI model 373 automated sequencer (Applied Biosystems, Foster City, CA).

Whole DNA was amplified in 50- μ l reaction mixtures with 20 pmol of primer

set with PCR condition as follows; 95 °C for 5 min and then 30 cycles of 95 °C for 1 min, 64 °C for 1 min, and 72 °C for 90 sec, with a final extension at 72 °C for 10 min. Fluorescently labeled PCR products were ran on a 1% agarose gel electrophoresis, and the product was quantified by image analysis. Fifteen nanograms of PCR product were digested with *Mbo*II and *Msi*I endonucleases (New England Biolabs® Inc., Ipswich, MA). All digests were in 20- μ l volumes, incubated for 6 h at 37 °C. The digested reactions were processed and the resulting *merA*-t-RFLP fingerprints were analyzed as described in section 3b. Only 3 samples were analyzed using this method from sites RRM 4.6, 5.2, 8.6.

5. Diversity analyses of the samples based on species abundance (area under the peak) and species richness (number of peaks)

The following analyses were applied to the fingerprints of both 16s rRNA gene and *merA*-t-RFLP data to examine the taxonomic and functional diversity of the SR soil microbial communities:

a- Shannon

The Shannon diversity index (H') (Shannon, 1948) was calculated as a function peak presence/absence and the area under the peak (Equation 1). P_i is the proportion that each peak area contributes to the total area in the i^{th} peaks and S is the total number of peaks. An evenness measure (J') was also calculated for each sample based on observed to maximum H' ratio values (Equations 2 and 3) (Hewson and Fuhrman, 2004).

Equation 1:

$$H' = -\sum_{i=1}^S P_i \ln(P_i)$$

Equation 2:

$$H'_{max} = \ln(S)$$

Equation 3:

$$J' = H'/H'_{max}$$

b- Sorensen and Bray-Curtis analyses with COMPAH

The binary system of peak presence or absence was used to calculate the Sorensen Similarity index, and the normalized relative abundance of each peak was used to calculate the Bray-Curtis Similarity index. Two independent rooted trees (dendrograms) were constructed based on both similarity indices using the Un-weighted Pair Group Mean Average (UPGMA). Similarity indices' calculations and clustering analyses were performed using the COMbinatorial Polythetic Agglomerative Hierarchical clustering package (<http://alpha.es.umb.edu/faculty/edg/files/edgwebp.htm#COMPAH>) (McGuinness et al, 2006, Girvan et al, 2003, Scala and Kerkhof, 2001).

c- Cluster Analysis: The Relationship of Nearest Neighbor- Shannon Diversity Index to Soil Total Hg Concentration.

Nearest Neighbor was the clustering method used to relate community diversity to the soil THg concentration in South River samples. This is a single linkage clustering method, where clusters form based on the dissimilarity of each entity to each cluster and to its nearest neighbor. It is a space-conserving strategy and it is best used when data structure is discrete and not continuous. (McGarigal, et al, 2000)

The Shannon diversity index and the THg concentration served as the variables ordered based on distance away from the source of contamination. The SAS statistical package was used, to run the protocols modified by Peter Morin from the manufacturer's manual. (Morin, 2009, Personal Communication, SAS Institute Inc., 1999)

6. Canonical Correspondence Analysis (CCA) based on 16S rRNA-t-RFLP peaks and abiotic factors.

Canonical Correspondence Analysis (CCA) was used as the direct gradient analysis technique to relate and rank the abiotic factors with the 16S rRNA and *merA*-t-RFLP fingerprint patterns (Cao et al, 2006, Ter Braak, 1986). The PC-ORD™ software (McCune and Mefford, 1999) was used to run the analysis. The t-RFLP data (data not shown) were the main matrix, and the abiotic factors were the second matrix (Table 3.1).

t-RFLP fingerprint data were represented as a 1 or a 0 for the presence or absence of the sample's peak at a specific size (bps). Peaks that had at least one representative in a given size in at least one sample were used and those peaks of a size not represented in any of the samples' t-RFLP fingerprints, were omitted from the analysis.

The abiotic factors included in this analysis were: distance from the point source in miles, THg concentration, moisture content, soil texture (silt/sand/clay), pH, and organic carbon content (LOI) (Table 3.1). A multi-co-linearity with components of the soil texture (silt/sand/clay) caused no tolerance for any axis in 999 randomized iterations, thus silt was removed from the second matrix and the data sets were re-analyzed.

To compare the % variation explained using the whole community (all peak abundances) and the dominant peak abundances ($\geq 1\%$ of the total area cutoff), two

additional CCA analyses were performed using relative abundances instead of the binary presence absence.

To determine the correlation between the biotic and abiotic variables, two correlations were used: the parametric Pearson correlation and the non-parametric Kendall rank correlation. The Pearson correlation assumes normal distribution of the linear related variables, while Kendall rank correlation ranks groups with no assumptions about distribution.

Results

Cultivation and Characterization of Bacterial Communities

To obtain an estimate of the Hg^R viable populations within the bacterial communities in all soil samples of the SR gradient, serially diluted soil suspensions were plated on 0.2X TSA amended with 100 µM HgCl₂, and incubated in the dark, at 28 °C. The specific medium strength and Hg concentration level were chosen as it has been shown that they indeed select for both slow- and fast-growing Hg^R bacteria (See Chapter 2). In this experiment incubation lasted for 17 days and CFU readings were obtained on day-3, day-10 and day-17. The intent of these 3 separate readings, was to monitor the development of the r & K continuum in the Hg^R populations, and thus get an insight on community assembly and structure (Deleij, 1993). Colonies appearing on day-3 represent fast growing organisms, or r-strategists, as they are better fitted to unstable environments of no crowding and high substrate availability. On the other hand, slow growers, or K-strategists, appeared on day-10 and day-17, as they have a competitive advantage in high crowding and in low substrate availability situations.

Hg^R colony forming units (CFU) were observed on plates inoculated with soil suspensions from sites RRM 1.7, 3.2, 9.1, 19.7 and 23.8, on day-10 and day-17, but not on day-3 (Figure 3.3). The THg concentration in these sites ranges from 10.3 to 70.7 mg/Kg, with an outlier of 3.05 mg/Kg in site RRM 23.8 (Table 3.1). Interestingly, the site that produced the highest Hg^R CFU count was the one closest to the source of contamination and not site RRM 3.2 in which the THg concentration was the highest among the samples tested. Direct cultivation of soil samples from sites RRM 9.2, 13.2, 14.5, 19.6 and 21.5 did not produce any Hg^R CFU throughout the 17-day incubation period. The THg concentration in these sites is lower when compared to sites where Hg^R CFU were produced, and it ranges from 0.026 to 9.16 mg/Kg. These results suggest, that communities chronically stressed by high THg, are adapted to toxicity by virtue of their Hg^R populations, whereas these populations are not maintained in communities that experience chronically low concentrations of THg, with the exception of the indigenous communities in site 23.8.

As no Hg^R CFU appeared on day-3, it can be concluded that Hg^R populations were mainly composed of K-strategists. This may further support the adaptation to Hg toxicity of communities subjected to chronic Hg-stress, since K-strategists are indicative of late successional communities, close to carrying capacity and usually at equilibrium. Another factor contributing to the exclusion of Hg^R r-strategists in this setting might be decreased substrate availability as their other 2 requirements for growth, i.e., no crowding and environmental instability, are met. If this is true, then an acute "recent" stress would disrupt the equilibrium, as lysis of sensitive cells leads to an increase in substrate availability, and gives a competitive advantage to Hg^R r-strategists. This would manifest in changes of the development and composition in the r & K continuum.

To experimentally test this hypothesis, I selected 2 soil samples from sites RRM 9.1 and 19.7, which had produced colonies only on day-10 and day-17,

respectively, in the previous experiment. To mimic a “recent” Hg-stress, soil suspensions in water were spiked with 10 µg/g HgCl₂ and incubated in the dark to avoid Hg photoreduction, at 28 °C for 24 h before being serially diluted and plated. Upon the completion of the 17-day long incubation, it was observed that both spiked samples developed more total Hg^R CFU on earlier time points than their un-spiked counterparts (Figure 3.4). In the case of site RRM 19.7, the Hg-spiked sample showed about 30x higher Hg^R CFU counts on day-10, a week before the non-spiked control, and only on that day. As for the Hg-spiked RRM 9.1 site, Hg^R CFU first appeared again a week before the un-spiked sample, on day-3. This is the only sample among these tested showing r-strategists’ growth. The number of CFU that appeared on day-10 were comparable to those of the un-spiked sample, and neither sample produced colonies on day-17.

In summation, this experiment provides evidence to support the hypothesis that “recent” Hg-stress does disrupt the equilibrium attained by communities adapted to chronic Hg-stress. This was manifest in an earlier development of the r & K continuum. In terms of the continuum’s composition, r-strategists were selected by exposure to “recent” Hg, resulting in a 3:2 ratio with the K-strategists, whereas no r-strategists were observed in un-spiked samples.

Characterization of Bacterial Community Structure

16SrRNA- and *merA*-t-RFLP fingerprint Analysis

The day of colony appearance is very fitting when it comes to understanding the communities’ development and composition, but it too has the inherent limitation shared by all culture-based methods, namely that unculturable but viable bacteria (UBVB) might be selected against by the controlled laboratory conditions that don’t necessarily reflect the conditions in their natural habitat. To circumvent this

limitation, I used the culture-independent method t-RFLP. DNA directly extracted from SR soil samples, was used as a template for PCR-amplifications of the 16S rRNA and *merA* genes. These amplicons were digested, and the resulting DNA-fingerprints were used to calculate soil bacterial diversity and evenness at the taxonomic- and functional-gene levels. Finally, I used both univariate and multivariate statistical models to relate biodiversity patterns to local environmental factors, and determine which factors are good predictors of the observed diversity.

T-RFLP fingerprints of the 16S rRNA gene generated were used to assess the composition of the overall community (all individual OTUs) as well as the composition of communities when only the dominant OTUs are considered. The total species richness (number of all the peaks) for all 9 sites analyzed, was 404 (Table 3.2). There were 118 peaks representing individual OTUs observed with fragment size range of 63-450 bps. Of those, 85 OTU were shared (≥ 2 samples) and 35 were unique (singletons) among sites (Data not shown). There was a high percentage of unique observed OTU between samples with close proximity, ranging from 84% for sites RRM 19.6 & 19.7 to 96% for sites RRM 21.5 & 23.8. In contrast, dominant OTUs, with abundance levels of $>1\%$ of the total abundance observed in all the samples, were evenly distributed among sites (Figures 3.5 & 3.6). Twenty-seven out of the 118 individual OTUs qualifying as dominant, accounted for $\sim 70\%$ of the total abundance observed in all the samples. Two OTUs are present in all 9 sites and 4 OTUs in 8 sites, together accounting for 25% of the total abundance. The fact that these OTUs are well represented in most samples at high abundance levels suggests that essential functions are carried out by species represented by these OTUs in their natural environment.

The t-RFLP analysis based on the 16S rRNA gene gives a snapshot of the diversity exhibited by the local communities at the taxonomic level. To assess the diversity of the community at the functional level, I designed a t-RFLP method using

primers that capture divergent *merA* determinants. Based on the *merA*-fingerprint analysis, the species richness was 153 in all 3 sites tested (Figure 3.7). A total of 93 individual OTU were observed, of which 41 were shared among sites and 52 were unique. The 37 most abundant OTUs account for ~ 80% of the total abundance in all sites, and their size range was 56-492 bps. They were well distributed among sites (23.8-28.5%), with the exception of 5 singletons found in sites RRM 5.2 (56, 67 and 492 bps) and 8.6 (439 and 482 bps) accounting for 6.1% and 3%, respectively, of the total abundance.

To determine whether community composition exhibits spatial patterns at the taxonomic level, a dendrogram was constructed with similarity values generated with Sorensen index based on species richness (peak number per fingerprint), along the miles gradient (Figure 3.8). This analysis revealed no clustering based on geography, as the highest similarity values were observed between sites separated by 5 miles (RRM 3.2 and 19.7) and 16 miles (RRM 14.5 and 19.6). Instead, these 4 sites clustered based on identical species richness, a trend that was not observed in any of the other clusters. An analogous dendrogram was constructed with Bray-Curtis similarity values generated from normalized peak abundances, and this time 2 sites (RRM 1.7 and 3.2) did cluster based on geography, albeit at medium similarity levels (Figure 3.9). Sites RRM 14.5 and 19.6, clustered together in this dendrogram as well, as their diversity levels were the same. Thus, these findings further substantiate that community composition is not dictated by the spatial structure of these sites. In the case of *merA*-t-RFLP fingerprints, dendrograms constructed based on similarity values generated with Sorensen index based on species richness and Bray-Curtis index based on OTU abundance, show that sites do cluster based on geography, with sites located 0.6 miles apart showing higher similarity values (Figure 3.10).

To investigate how other factors affect the diversity of these communities, I calculated Shannon diversity index (H'), and evenness (J') based on the 16S rRNA-t-RFLP OTU abundance results and ran univariate models to correlate them (Table 3.2). As was the case for species richness, H' and J' followed the same trend: the highest values were found in sites RRM 9.2, 14.5, 19.6, where no Hg^R CFU developed (Table 3.2, Figure 3.3). Site RRM 21.5 is the only exception, exhibiting low S and H' , but high evenness. Percent moisture and silt were the only environmental factors that showed low levels of correlation ($r^2 = 0.34$ and $r^2 = -0.33$, respectively) only with Hg^R CFU counts, but with none of the other measures of heterogeneity tested (Table 3.3). Interestingly, soil THg concentration was not a good predictor of heterogeneity either. This was exhibited both in the univariate model and in the clustering analysis generated using H' and THg. Nearest neighbor cluster analysis, separated the sites into 2 distinct clusters (Figure 3.11). One cluster is made up of a single site (RRM 3.2), which had the highest THg (~ 70 mg/Kg), and all the rest, whose THg ranged from 0.027 to 15.6 mg/Kg, into another cluster. This observation is contradictory to findings of Hg gradients created in laboratory settings, where measures of heterogeneity and Hg^R CFU counts are highly correlated to Hg levels in the culture medium (See Chapter 2). Finally, it was shown that Shannon diversity index and evenness measures calculated based on *merA*-t-RFLP fingerprints were high and at very similar levels among the sites tested (Table 3.2).

Since my study is ecologically-based, where not all factors can be efficiently controlled as in a lab setting, I used multivariate statistics to obtain a better resolved picture on the interplay of biotic and abiotic variables. The method used, CCA, is a direct gradient analysis technique combined with ordination, whereby environmental variables are optimally summarized into axes, in as many dimensions as the variables studied, and species are ordered against these variables based on correlation values. Thus one can determine simultaneously the pattern of variation in

community composition accounted by each environmental variable and the distribution of species along these variables. This multidimensional space, can be better visualized as an aleph (Borges, 1970), where all the different variables co-exist at one given moment, and species are distributed at the interface of the niches that allow for optimal growth.

The CCA analysis performed using environmental variables and the dominant 16S rRNA-t-RFLP OTUs ($\geq 1\%$ of total abundance), which contribute $\sim 70\%$ of the total OTUs observed (see above), indeed gave better correlations between environmental variables and community composition as compared to the univariate models of analysis (Table 3.4). The 3 environmental variables that could best predict community composition were: pH, moisture content, and clay content. The parametric Pearson Correlation and the Kendall Rank Correlation for the species-environment correlation are high for all three axes, ranging from 0.944 to 1.

The highest variance (29%) is explained by Axis 1, representing a pH gradient, with a correlation coefficient of - 0.33. Only one community from site RRM 21.5 aligns to this Axis, and it is the one that shows the lowest similarity value to all the other sites based on the Sorensen and Bray-Curtis indices (Figures 3.8 & 3.9). Sites RRM 1.7 and 3.2, which are the closest to the source, aligned on a moisture gradient (Axis 2), which explains 17.6% of variance with a correlation coefficient of 0.71. These are the only sites that show a spatial pattern based on the Sorensen and Bray-Curtis indices. Except for site RRM 21.5, all other sites where no Hg^R CFU developed (Table 3.2), aligned to the clay-Axis 3 (RRM 9.2, 14.5, 19.6), which explains 15.6% of variance with a correlation coefficient of - 0.55. In terms of individual OTUs within the communities, the majority aligned to pH-Axis 1 (55.5%), and 22.2% and 30% aligned with the moisture-Axis 2 and clay-Axis 3, respectively.

Even though distance away from the source of contamination and THg concentration are not good predictors of community composition, they show high

associations with the variables that do explain variation, and they are negatively correlated to each other (-0.61) (Table 3.5). Moisture is positively correlated to THg (0.54) and negatively correlated to distance from the source (-0.85). THg shows a weak correlation to pH (0.29), but no significant correlation to clay content (0.057), and intermediate negative correlation with distance away from the source (-0.61). The variable that correlates best with THg is LOI (0.78), and distance away from the source correlates well but negatively (-0.8) with this variable. Thus, LOI, and moisture can be used as proxies to THg concentrations in the environment. When the statistical analysis was expanded from the most abundant peaks ($\geq 1\%$ of total abundance) to include all peaks observed in all the sites, the % variance explained decreased by $\sim 20\%$ (Data not shown). This may be an indication that peaks contributing $\leq 1\%$ of the total abundance create a background noise that masks trends that explain the total variation in the SR ecosystem.

Discussion

Many riverine ecosystems across the United States have been contaminated as a result of gold mining operations, where Hg was used for the amalgamation of gold from its ore, and/or from disposal of toxic effluents from industrial operations where Hg was used as a catalyst (EPA). Mercury contamination in riverine ecosystems doesn't attenuate with the passing of time and clean-up efforts are a priority for EPA and local federal governments as potential methylation of Hg increases its toxicity due to bioaccumulation and biomagnification in aquatic food chains, thus posing a public health risk and leading to the deterioration of ecosystems' health (Barkay and Wagner-Dobler, 2005). The remedial actions that are usually proposed and studied for Hg contaminated systems are of an engineering nature, whereby contaminated sediments are capped on site or removed and

incinerated in a different location. At present, microbial remedial actions are not employed, as our understanding of the microbe-Hg interactions is not sufficient (Yu et al, 2011, Barkay and Schaefer, 2001).

In this study I investigated the impact of Hg on microbial communities and their potential to reduce Hg(II) to Hg(0) in floodplain soil samples taken along a 24-mile reach of the South River in Virginia. As is the case for other riverine ecosystems with Hg contamination legacy, in the SR Hg levels remain high, especially close to the source of contamination (Flanders et al, 2010, Carter, 1977). Direct cultivation of soil samples from the Hg gradient showed that the highest Hg^R CFU were found in samples closest to the source and that bacterial communities that experience THg at low levels in their natural environment did not contain any Hg^R CFU (Table 3.1, Figure 3.3). This finding is in accordance with previous studies where increased occurrence of Hg^R bacteria was highly related to Hg concentration (Muller et al, 2001), and indicative of the communities' adaptation to chronic Hg-stress (Barkay, 1987).

Investigation on Hg^R community assembly and development (DeLeij, et al, 1993), revealed that Hg^R communities from the highly contaminated samples of the gradient (RRM 1.7-9.1) were exclusively composed of K-strategists (Figure 3.3), and that "recent" Hg-stress changed the development and composition in the r & K continuum, selecting for r-strategists as well (Figure 3.4). Furthermore, sites within 1.7-9.1 miles away from the source exhibited lower levels of species richness, evenness and diversity than sites RRM 9.2-19.6, which experience low THg levels and where no Hg^R CFU developed (Tables 3.1 & 3.2). These findings further support the acclimation of soil bacterial communities to chronic Hg-stress in the SR ecosystem, since K-strategists are indicative of late successional communities, close to carrying capacity and usually at equilibrium (Sandaa, 1999, Pianka, 1970, Dobzansky, 1950), and suggest that community composition is influenced by the

nature and intensity of Hg-stress to which it is exposed (Muller et al, 2001, Ranjard et al, 1997).

While it has been shown in both laboratory and field experiments that bacterial species can react differently over temporal and spatial gradients (Riemann & Middleboe, 2002), the physical, chemical, and biological drivers, which influence microbial diversity and activity are still unclear. Furthermore, a heated debate exists in microbial ecology on whether factors that determine geographical patterns are shared between macro- and microorganisms (Falkowski et al, 2008, Whittaker et al, 2003, Fenchel et al, 1997). In this study, clustering analyses based on both species richness (Sorensen index) and diversity (Bray-Curtis) generated using 16S rRNA-fingerprints, showed that sites do not cluster based on geographical proximity (Figures 3.8 & 3.9). Thus, the soil microbial communities didn't exhibit biogeographical patterns at a scale of 24 miles. The best predictors of diversity in these communities are pH, moisture and soil texture, together explaining 62.3% of the total variance observed (Table 3.4). These results suggest that soils that share environmental characteristics and not geography, support similar bacterial communities, and corroborate the findings of previous studies where these 3 factors were the best predictors of the observed diversity in soil bacterial communities (DeBruyn et al, 2011, Fierer and Jackson, 2006, Girvan et al, 2003). Interestingly, THg was not a good predictor of diversity, even though it was clearly shown that chronic high levels of Hg influence the abundance of Hg^R culturable bacteria (see above) (Table 3.5).

To determine functional composition and diversity of communities in samples from the SR, a new t-RFLP method was designed using primers that target a broad range of *merA* genes of both Gram positive and negative microorganisms (Wang et al, 2011). Clustering analyses based on both species richness (Sorensen index) and diversity (Bray-Curtis) of the *merA*-t-RFLP-fingerprints, revealed that SR

communities do cluster based on geographical proximity (Figure 3.10). A geographical pattern of functional diversity, estimated based on the diversity of another *mer*-determinant (*merA* encoding for the *mer* operon major regulator, MerR) has been shown in communities from another riverine system along a 6 meter gradient (Bruce, 1997), while denitrification in aquatic systems shows spatial patterns at the centimeter scale (Scala and Kerkhof, 2000). Also, both the diversity and evenness was similar among sites and comparable to diversity and evenness levels observed at the taxonomic species level determined with 16S rRNA-fingerprints (Table 3.2). These findings corroborate with the hypothesis that environments chronically contaminated with Hg, can maintain a high diversity of *mer*-determinants similar to my observations for the 16S rRNA gene (see Chapter 2), as long-term selective pressure allows for divergence (Øregaard and Sørensen, 2007). Finally, the data suggest that the newly created *merA*-based t-RFLP method is a promising tool for rapid and reliable detection of *mer*-determinants in soil samples, and for assessing functional composition and diversity of Hg^R communities.

In summation, my results show that bacterial communities in the SR ecosystem are adapted to chronic Hg-stress and that the Hg-reduction potential, as suggested by the number of Hg^R CFU, is the highest closest to the source. Spatial patterns in bacterial communities, based on 16S rRNA-fingerprints, were best predicted by local environmental factors and not by geography. The lack of geographic patterns may indicate that the 24-mile scale used in this study was not appropriate to discern geographical distribution of the soil bacterial communities, which live in pores of microsites and respond more acutely to changes in the environment as compared to animals and plants (Giller et al, 2009, vanElsas et al, 2007). Thus investigation on spatial patterns of distribution of microbes in soils should be conducted at the micro-scale (1-3 mm) (Nunan et al, 2003). Alternatively, lack of observable spatial patterns, may imply that interpretation of taxonomic

patterns in terms of how they are affected by geographical patterns is difficult, as microorganisms sharing 16S rRNA genes have a broad variation in the functions they perform in the environment, thus use of functional genes (trait-based analysis) would allow for a better resolution (Green et al, 2008). Indeed, functional analysis based on *merA*-fingerprints, performed here on a small number of samples, showed biogeographical patterns at a 4-mile scale and may further support the notion that geographical patterns should be based on core metabolic machineries as these are maintained and unperturbed over evolutionary times (Falkowski et al, 2008, Weiher and Keddy, 1995). This function-based investigation of microbial spatial patterns is especially attractive for it bypasses the need for a distinct species concept for prokaryotes, which do not fit the biological (Mayr, 1942), ecological (Van Valen, 1976) and morphological (Cronquist, 1988) species concepts.

Tables & Figures

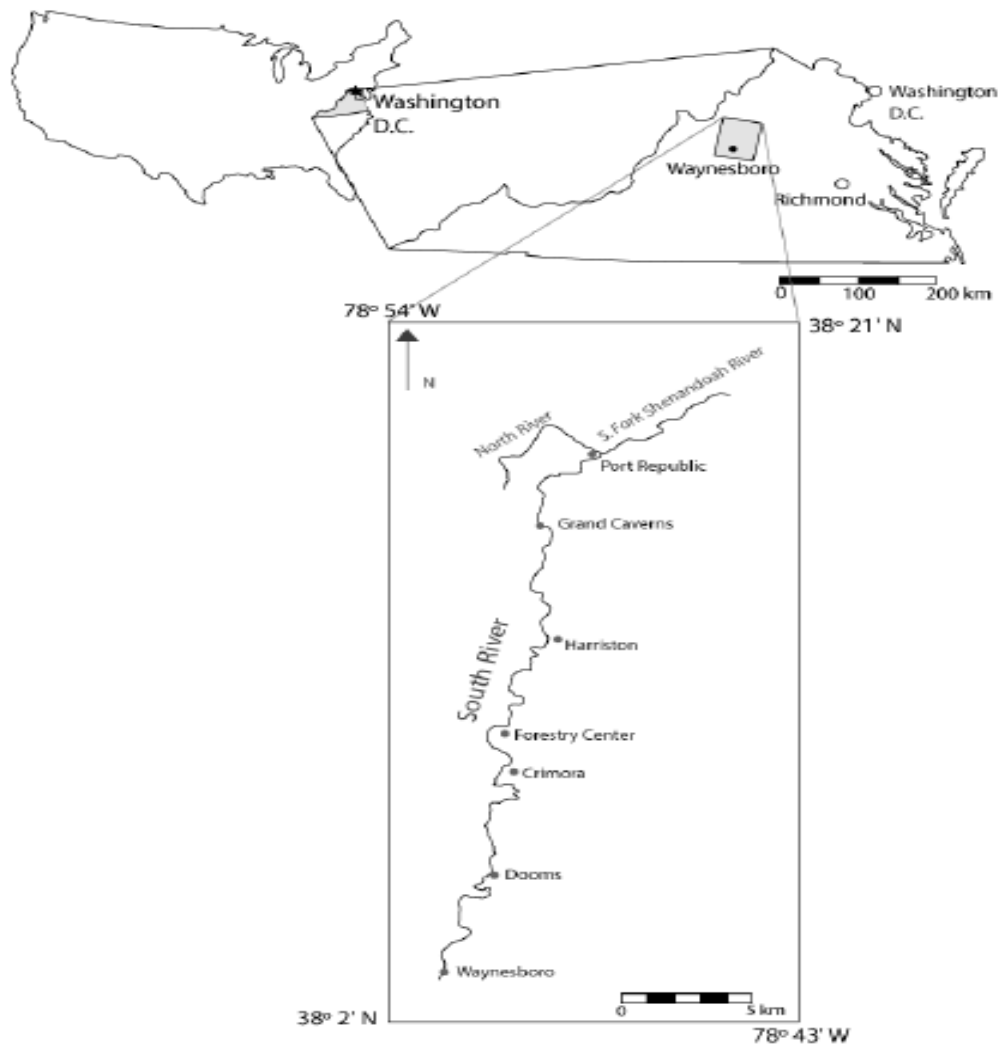


Figure 3.1. Map of the South River, which originates south of Staunton, Virginia and flows northward through the town of Waynesboro where the DuPont site sits, to the confluence with North River at Port Republic. These rivers are tributaries to the South Fork Shenandoah River (Reproduced from Flanders et al, 2010).

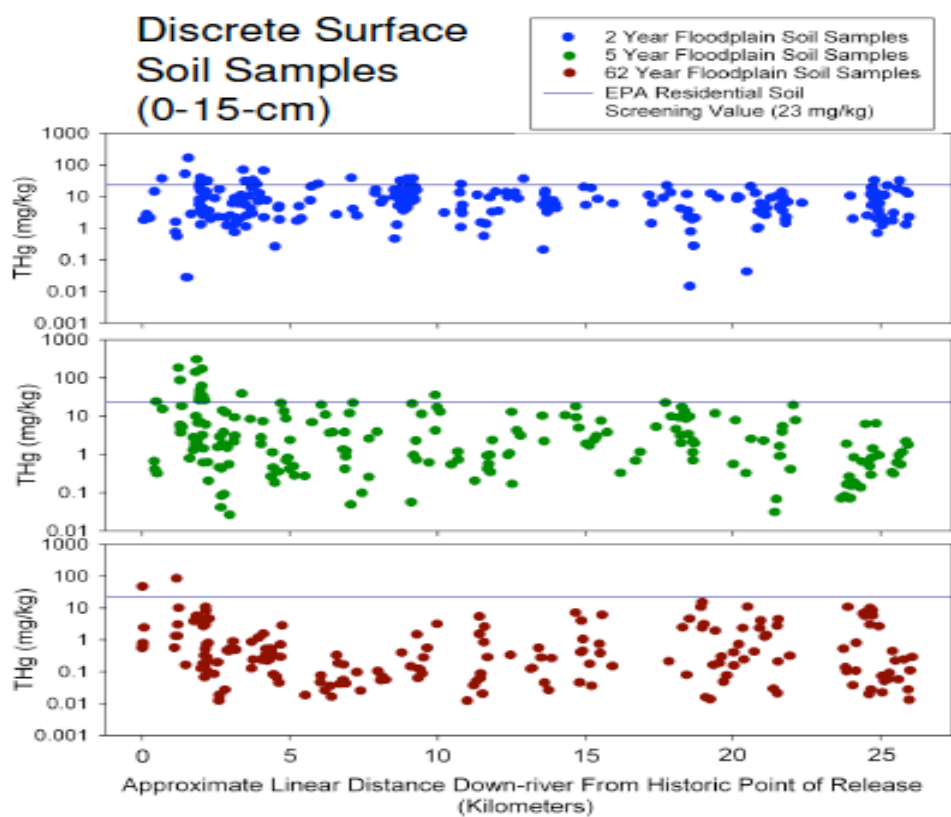


Figure 3.2. THg Concentrations in floodplain surface soil samples of 2-year (●), 5-year (●) and 62-year (●) flooding frequency (FP) along the South River as compared with the EPA Residential Soil Screening Value (—) (23 mg/Kg). At the point source the THg levels are the highest in all FP and the 2-year (●) (FP) exhibits the highest THg across the 26-Km of the gradient (Jordan et al, 2008).

Table 3.1. Physical and chemical characteristics of South River, VA, floodplain surface soils collected in February and March 2008. Samples were collected in forested areas of the floodplain with an average flooding frequency (FP) of 2-years.

RRM ^a	THg (mg/kg)	Moisture (%)	LOI (%)	% Sand	% Silt	% Clay	pH
1.7	15.6	23.7	4.2	53	32	15	7.93
1.8	20.4	26.4	4.5	51	34	15	7.97
3.2	70.7	22	5.9	38	46	16	7.7
9.1	13.9	18.3	4.2	52	35	13	6.77
9.2	6.98	20.5	4.8	56	35	9	6.91
13.2	4.79	13.8	2	66	26	8	7.62
14.5	0.0267	16.6	3.5	41	30	29	7.33
19.6	9.16	17.2	3.3	58	25	17	7.41
19.7	10.3	15.2	4	66	29	5	8.01
21.5	2.52	10.7	1.9	85	10	5	7.53
23.8	3.05	17	2.7	81	10	9	7.15

^a RRM refers to River Relative Mile distance away from the DuPont plant facility in Waynesboro, VA, which is the point source of Hg contamination in the SR.

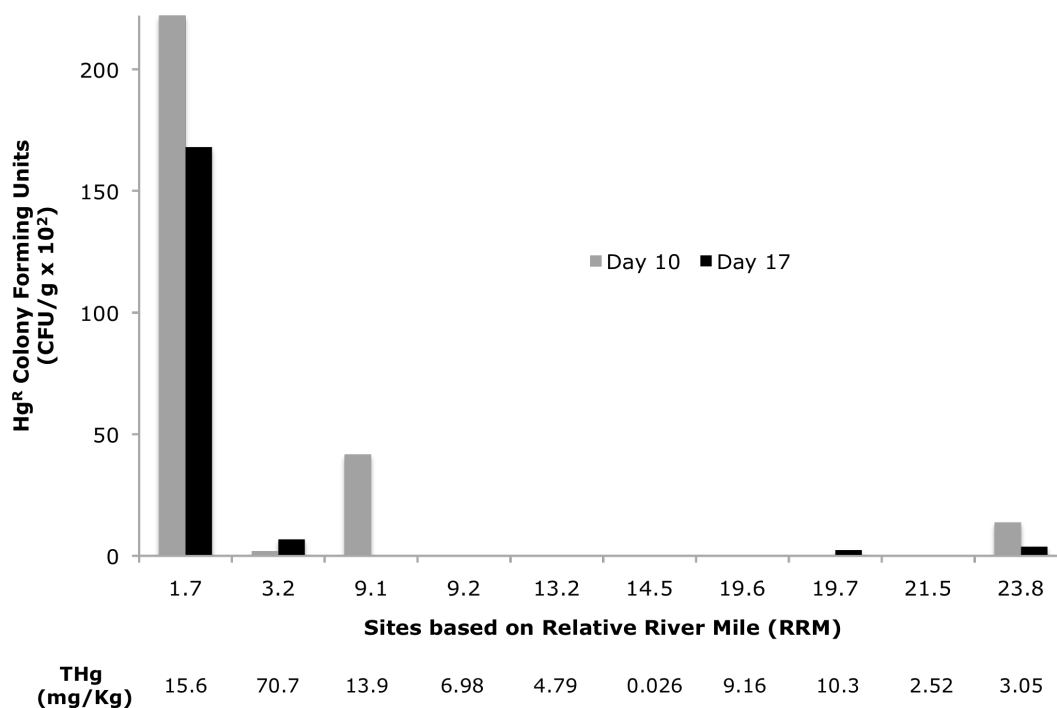


Figure 3.3. Number of Hg^R colony forming units per g⁻¹ soil that appeared on day 10 (grey bar) and day 17 (black bar) on 0.2X TSA amended with 100 μ M HgCl₂ and inoculated with 100 μ L of serially diluted soil suspensions of South River floodplain samples across the gradient. THg concentration at sampling is indicated below each site.

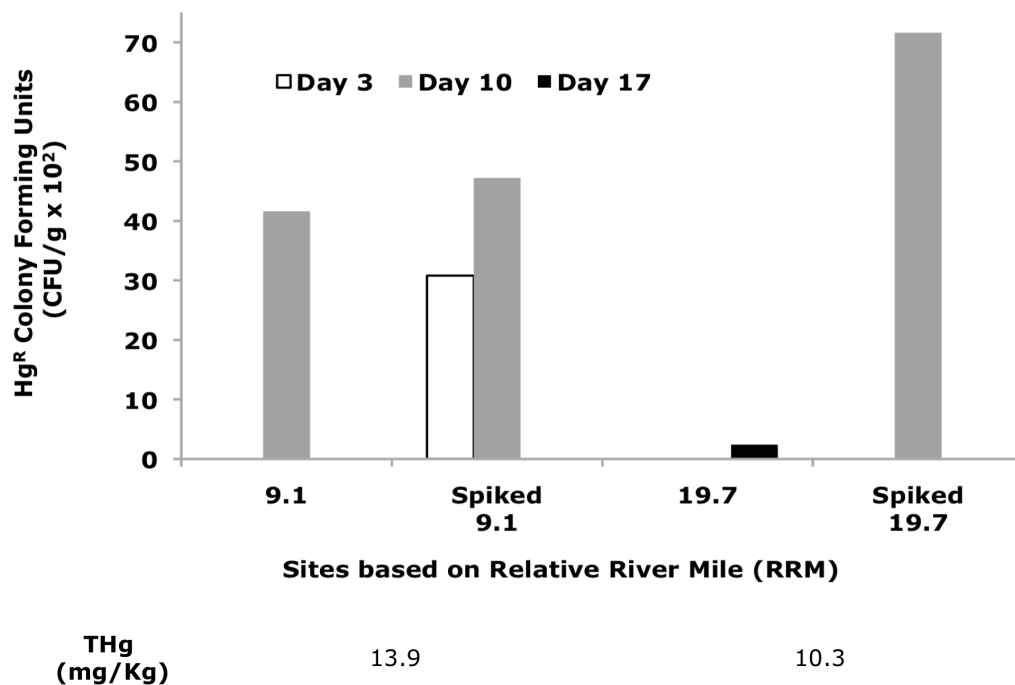


Figure 3.4. Comparison of Hg^R CFU per gram of soil⁻¹ between non-spiked and spiked samples from sites RRM 9.1 and 19.7, that appeared on day 3 (white bar), day 10 (grey bar) and day 17 (black bar) on 0.2X TSA amended with 100 μ M HgCl₂ and inoculated with 100 μ L of serially diluted soil suspensions. Spiked samples were exposed to 10 μ g/g HgCl₂ for 24 hrs prior to plating. THg concentration at sampling is indicated below each site.

Table 3.2. Measures of heterogeneity for 16S rRNA gene- and *merA* gene-t-RFLP fingerprints and direct plating methods.

Sites (RRM)	Species Richness ^a	Shannon Diversity Index ^b	Evenness ^c	Total Hg ^R CFU (10 ⁻² /g of soil) ^d
16S rRNA-t-RFLP fingerprints				
1.7	35	3.1	0.88	390
3.2	37	3.2	0.89	8.8
9.1	26	2.8	0.86	41.6
9.2	43	3.3	0.88	0
14.5	59	3.8	0.94	0
19.6	59	3.8	0.94	0
19.7	37	3.1	0.85	2.4
21.5	21	2.8	0.93	0
23.8	34	2.9	0.83	17.6
<i>merA</i> -t-RFLP fingerprints				
4.6	52	3.7	0.94	ND ^e
5.2	47	3.6	0.93	ND
8.6	54	3.7	0.93	ND

^a Species Richness (S) is the number of observed peaks per site

^b Shannon Diversity Index (H') was calculated based on total abundance of peaks per site (Shannon, 1948)

^c Evenness measure (J') for each site was calculated based on observed to maximum H' (LN(S)) ratio values

^d Total Hg^R CFU x 10⁻² per gram of soil⁻¹ of each site, is the sum of Hg^R CFU appearing on days 3, 10 and 17 of incubation on 0.2X TSA medium amended with 100 µM HgCl₂ and inoculated with 100 µL of serially diluted soil suspensions.

^e ND: Not Determined

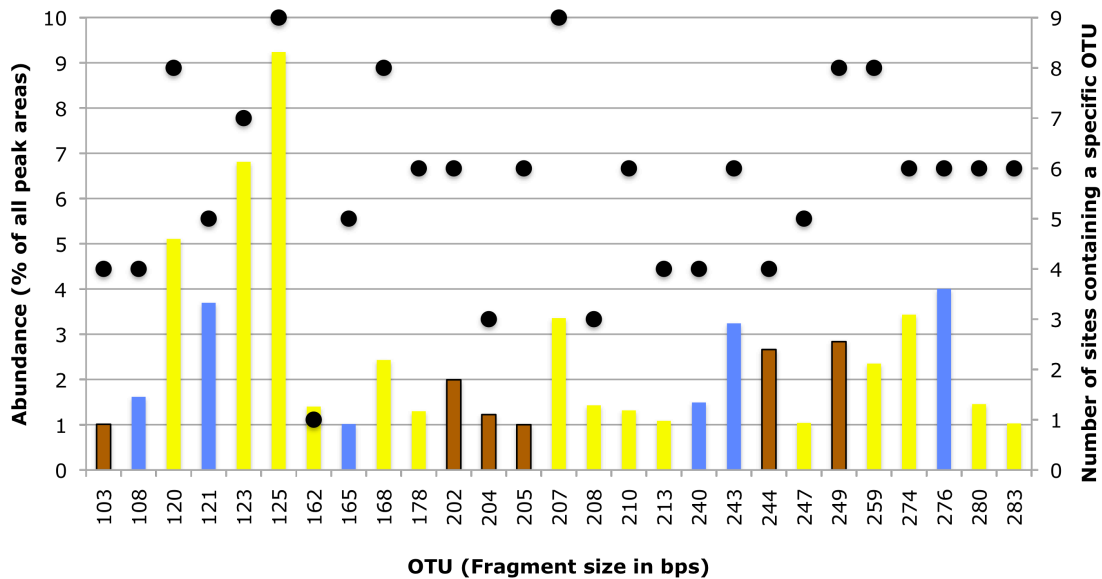


Figure 3.5. Percentile contribution of the most abundant OTUs to the total relative abundance observed in all sites. Only peaks contributing >1% of the total relative abundance in all sites based on 16S rRNA gene-t-RFLP fingerprints are included. The black circles (●) indicate the number of sites that contained this OTU in their fingerprints. Colors indicate the environmental variable, which influences their distribution. Brown bar: clay content, yellow bar: pH, and blue bar: moisture content.

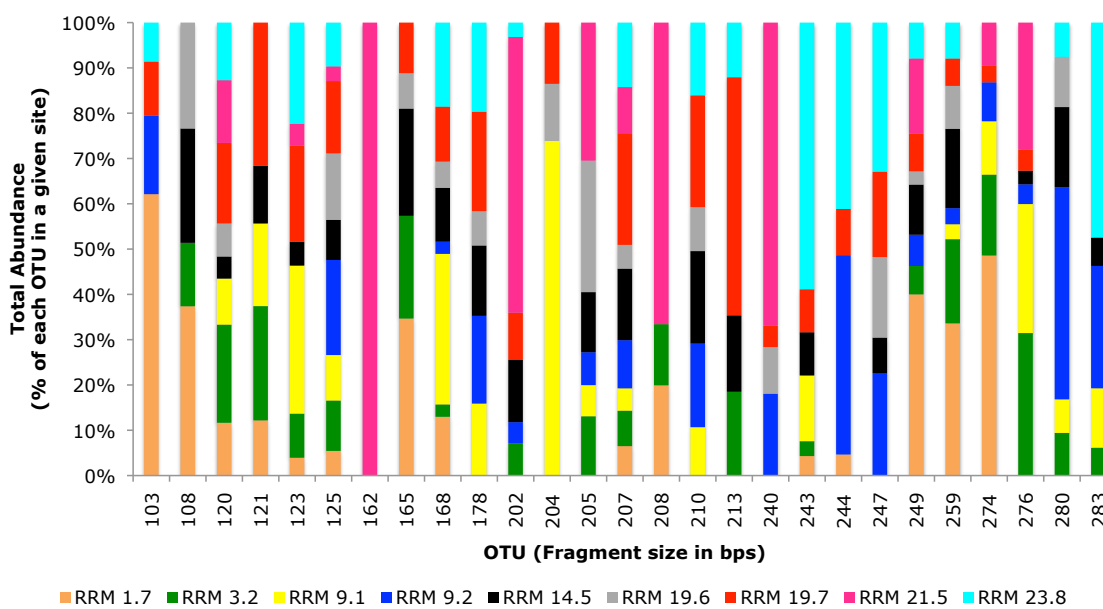


Figure 3.6. Percentile distribution of the most abundant OTUs per site (colors in each bar) along the mile gradient based on 16S rRNA-t-RFLP fingerprints. Only OTUs that represent >1% of the total relative abundance in all sites are included.

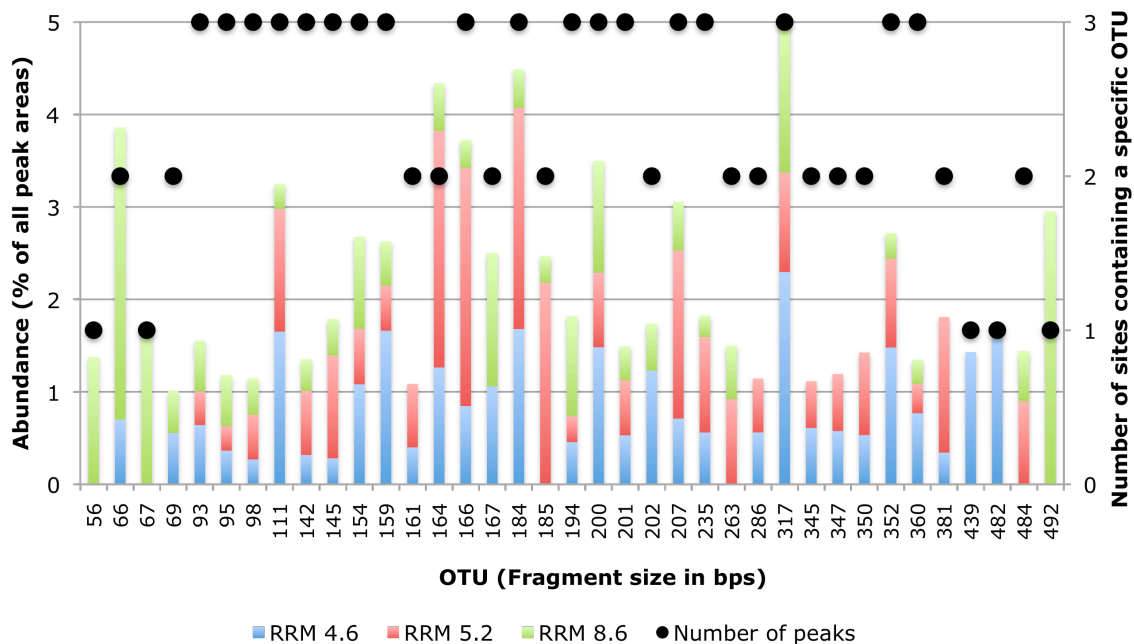


Figure 3.7. The percentile contribution of the most abundant OTUs. Only peaks contributing >1% of the total relative abundance in all sites based on *merA*-t-RFLP fingerprints are included. The black circles (●) indicate the number of sites that contained this OTU in their fingerprints.

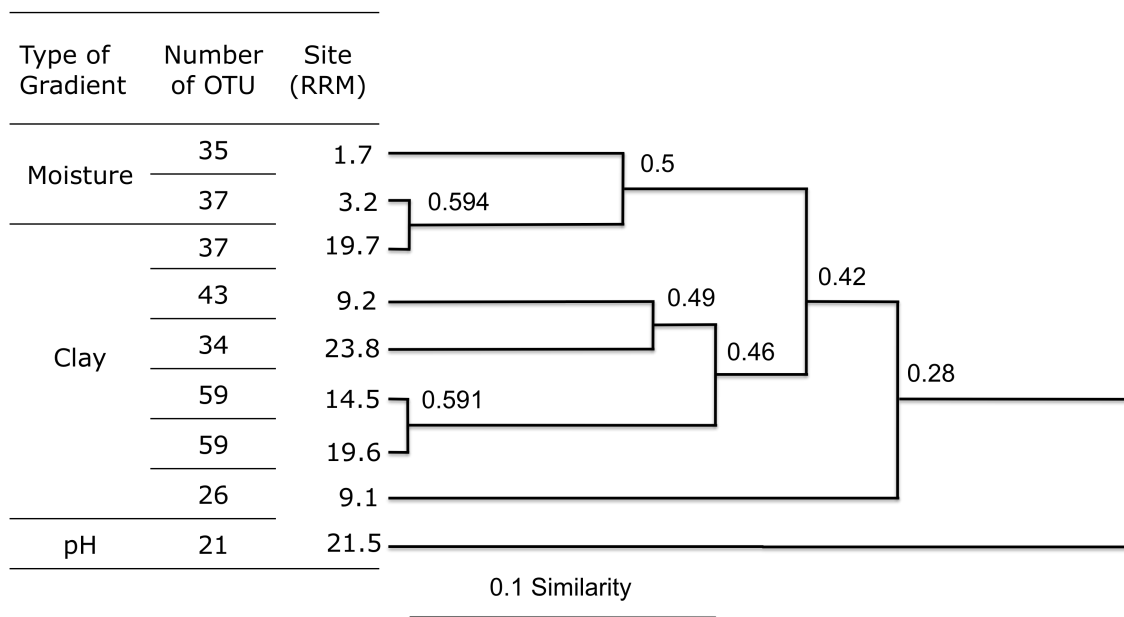


Figure 3.8. Rooted dendrogram of similarity values for South River samples. Similarity levels are indicated on each node. The Sorensen Similarity index was used to calculate similarity values based on peak presence/absence on the 16S rRNA gene-t-RFLP fingerprints. Clustering was done using the Un-weighted Pair Group Mean Average (UPGMA). The type of gradient refers to the variable that best explains the variation observed in these sites, based on the CCA.

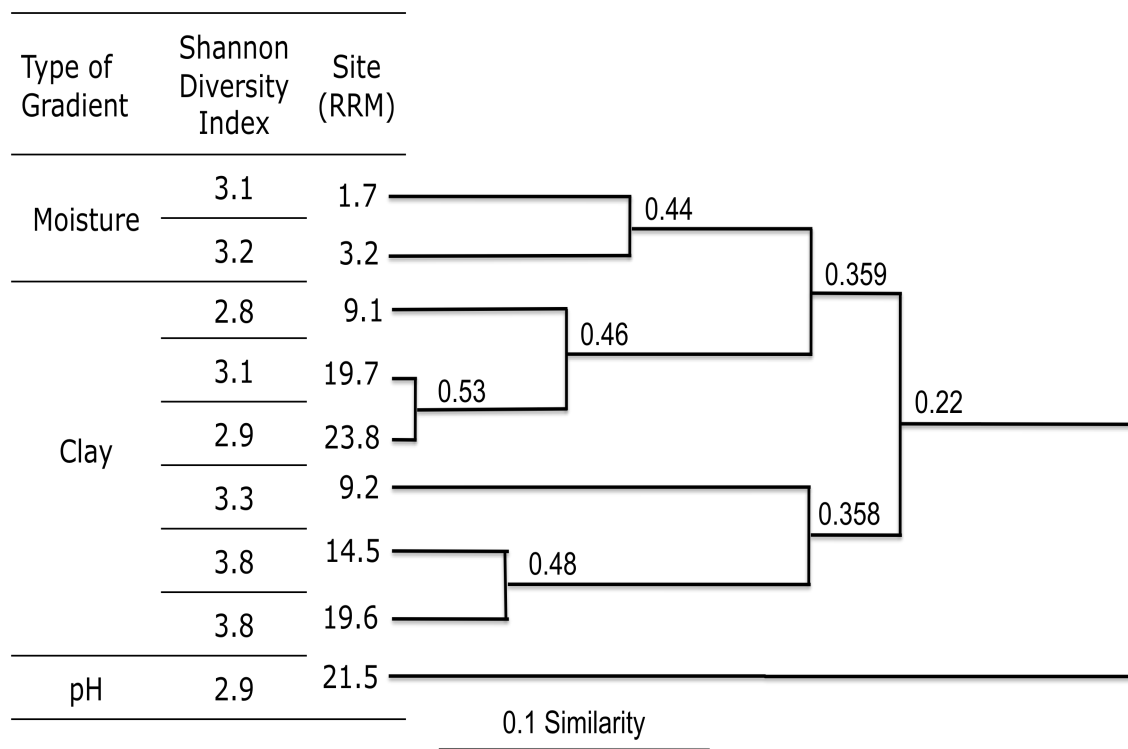


Figure 3.9. Rooted dendrogram of similarity values for South River samples. Similarity levels are indicated on each node. The Bray-Curtis index was used to calculate similarity values based on the normalized relative abundance of each peak on the 16S rRNA-t-RFLP fingerprints. Clustering was done using the Un-weighted Pair Group Mean Average (UPGMA). The type of gradient refers to the variable that best explains the variation observed in these sites, based on the CCA. Shannon Diversity Index (H') was calculated based on total abundance of peaks per site.

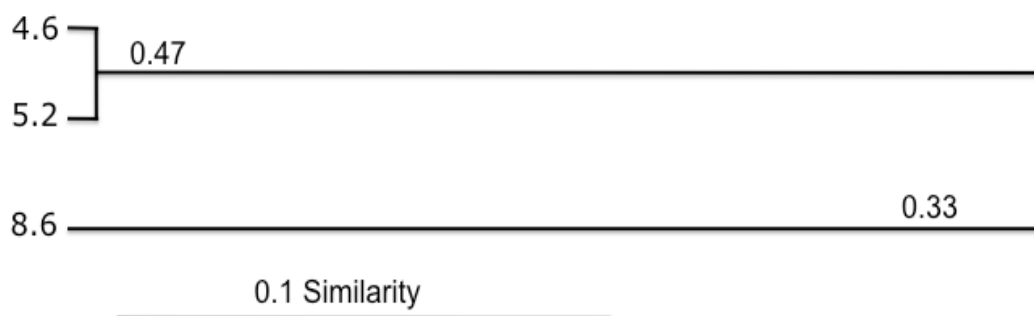


Figure 3.10. Rooted dendrogram of similarity values for South River samples. Similarity levels are indicated on each node. The Bray-Curtis index was used to calculate similarity values based on the normalized relative abundance of each peak on the *merA*-t-RFLP fingerprints. Clustering was done using the Un-weighted Pair Group Mean Average (UPGMA).

Table 3.3. Univariate analysis predicting diversity as a function of site and soil characteristics.

Variable	Species Richness ^a	Measures of Diversity		
		Shannon Diversity Index ^a	Evenness ^b	Total Hg ^R CFU (10 ⁻² /g of soil) ^c
THg (mg/Kg)	0.029	0.018	0.02	0.002
Distance (miles)	0.0014	0.0001	0.0007	0.16
Silt (%)	0.03	0.034	0.001	-0.33
LOI (%)	0.011	0.018	0.14	0.031
Moisture (%)	0	0.013	0.12	0.34
pH	0	0.018	0.035	0.13

In each case a fitted linear regression ($y = a + bx$) was used.

^a Shannon Diversity Index was calculated based on total abundance of peaks per site (Shannon, 1948)

^b Evenness measure (J') for each site was calculated based on observed to maximum H' (LN(S)) ratio values

^c Total Hg^R CFU $\times 10^{-2}$ per gram of soil⁻¹ of every site are the sum of Hg^R CFU appearing on days 3, 10 and 17 of incubation on 0.2X TSA medium amended with 100 μ M HgCl₂.

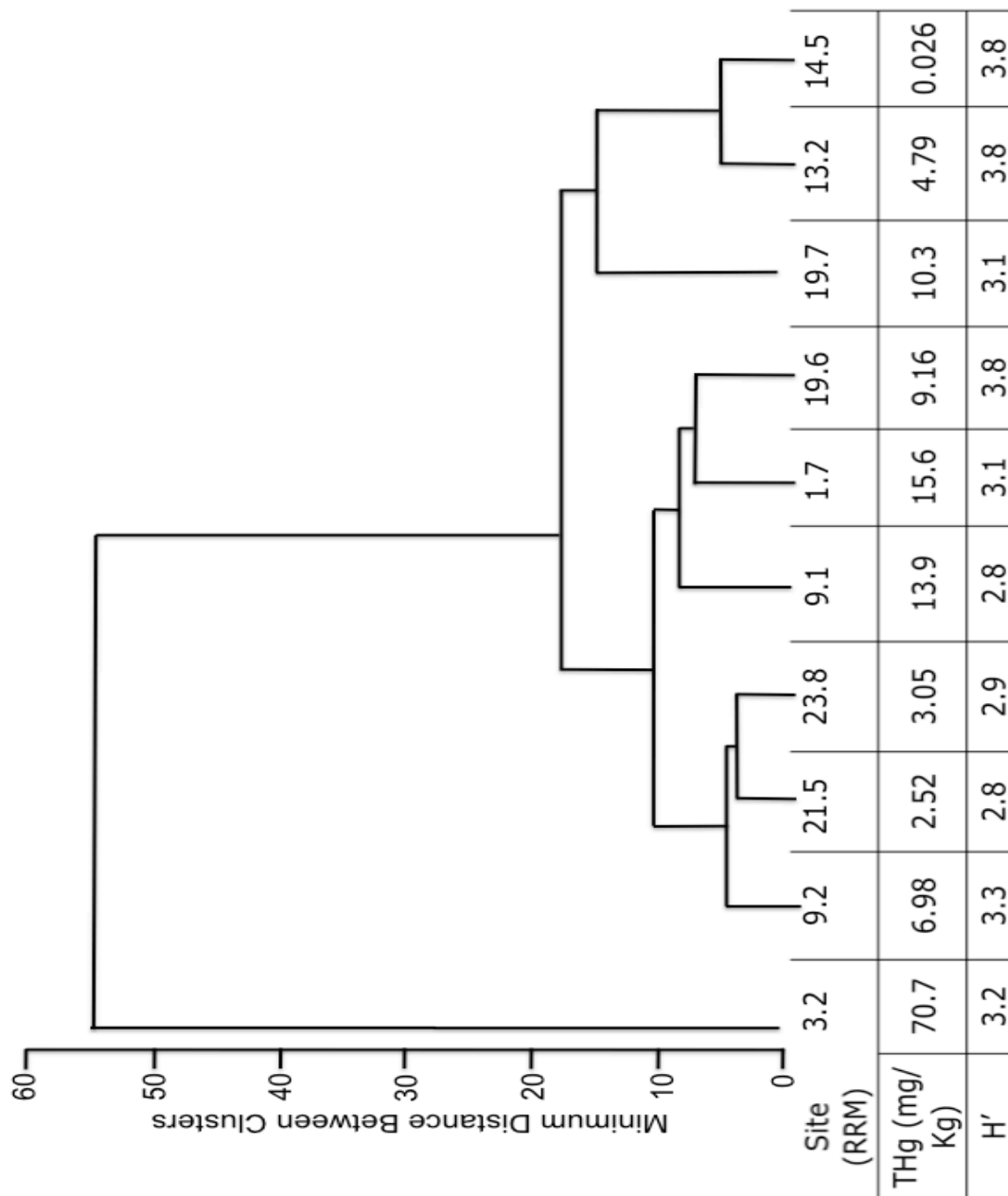


Figure 3.11. Cluster diagram of similarity values for South River samples. Similarity values were calculated based on Shannon diversity index values and THg concentration in each sample. Clustering was performed using the Nearest Neighbor method. THg concentrations present in each site are also listed as well as calculated Shannon index (H') based on total abundance of peaks per site

Table 3.4. Summary of results of Canonical Correspondence Analysis of the most abundant peaks ($\geq 1\%$ of the total area cutoff) in 16S rRNA-t-RFLP fingerprints of each site in relation to the environmental variables^a at that site.

Axis	Type of Gradient (Correlation Coefficient)	% Variance Explained by Axis	Species-Environment Correlations		Kendal Rank	% Sites (RRM) Aligned to Axis	% Peaks Aligned to Axis (% Positive Associations)
			Pearson				
Axis 1	pH (-0.33)	29%	0.98	0.94	11.1% (21.5)	55.5% (29.6%)	
Axis 2	Moisture (0.71)	17.6%	0.96	0.94	22.2% (1.7, 3.2)	22.2% (14.8%)	
Axis 3	Soil Texture: Clay (-0.55)	15.6%	1.0	0.94	66.6% (9.1, 9.2, 14.5, 19.6, 19.7, 23.8)	30% (14.8%)	

^a Environmental variable tested included: distance from the point source in relative river miles, THg concentration, moisture content (%), soil texture (silt/sand/clay) (%), pH, and organic carbon content (LOI) (%).

Table 3.5. Weighted correlations among tested environmental variables representing the SR contamination gradient. Variables were extracted from Canonical Correspondence Analysis.

Variable	THg (mg/Kg)	Distance (miles)	Clay (%)	LOI (%)	Moisture (%)	pH
THg (mg/Kg)	1	- 0.61	0.057	0.78	0.54	0.29
Distance (miles)	- 0.61	1	-0.29	-0.8	-0.85	-0.052
Clay (%)	0.057	-0.29	1	0.13	0.25	-0.12
LOI (%)	0.78	-0.8	0.128	1	0.77	0.1
Moisture (%)	0.54	-0.85	0.25	0.77	1	0.014
pH	0.29	-0.052	-0.12	0.1	0.014	1

Chapter 4 – Dissertation Conclusion

The broad scope of this dissertation was to determine the effects of Hg-stress on bacterial communities inhabiting floodplain soils in rivers contaminated chronically with Hg as a result of industrial processes. I incorporated microbiological, molecular, ecological and statistical methods, to investigate the consequences of the stress at resolution levels from genes to species to ecosystems. This dissertation demonstrates that soil bacterial communities are highly adapted to Hg-stress by virtue of the mercury resistance (*mer*) operon and that HGT plays a crucial role in the evolution of *mer*-determinants. It also demonstrates that local environmental factors play a critical role in shaping bacterial communities' diversity and composition rather than geography.

To estimate the abundance of culturable bacteria from soil samples of the EFPC (Brooks and Southworth, 2011), I set up Hg gradients using two different dilutions of the TSA medium to mimic oligotrophic and copiotrophic conditions, amended with appropriate concentrations to maintain bioavailability of Hg in the two media (Chang et al, 1993, Whang and Hitori, 1988). The total population counts under copiotrophic conditions in the absence of Hg, were higher than those achieved under oligotrophic conditions without Hg, suggesting that higher abundances are possible with increased nutrient availability. At the highest Hg-stress level (10 μM) under oligotrophy, 72% of the total community went extinct, and the cell counts were 2 – 6X lower than those observed under copiotrophic conditions at the same level of Hg. Copiotrophic communities suffered 82.5% losses in their populations at the highest Hg concentration (100 μM). A total of 37 Hg^R oligotrophic (LS) isolates and 47 Hg^R copiotrophic (FS) isolates were obtained from the highest Hg-gradient concentrations, based on phenotypic examination of their unique morphological characteristics.

The differential effect of Hg-stress concomitant with different nutrient levels was also apparent at the phylogenetic trends of the isolates assessed by PCR amplifications of the 16S rRNA gene. Although, both groups of isolates were taxonomically associated with genera of the Proteobacteria and the Actinobacteria, Hg^R copiotrophic community composition shows an even distribution among species belonging to these genera, while at oligotrophic conditions there is a selection for species of the Actinobacteria in a 3:1 ratio with the Proteobacteria. Further investigation on the functions performed by these species in the ecosystem, revealed that the majority of the Actinobacteria are organic matter decomposers and the alphaproteobacteria are N₂-fixers. This is in accord to previous research findings whereby free-living N₂-fixers rely on decomposers for readily available carbon sources and C-limitation selects for decomposers (Nemergut, 2008, Ventura et al, 2007, Craine et al, 2007). Finally, the species diversity was calculated using a number of diversity estimators based on 16S rRNA gene sequence similarity, and it was shown to be higher under copiotrophic conditions (Chao and Lee, 1992, Chao, 1984, Shannon, 1948). Taken together, these findings attest to the fact that Hg-stress affects the abundance, composition and diversity of communities isolated from soil samples of the EFPC environment, and that the stress is more pronounced under oligotrophic conditions. These observations expand our knowledge and corroborate with findings of previous researchers working with soil bacterial communities from the same ecosystem (Vishnivetskaya et al, 2011, Rasmussen et al, 2008).

To provide insight on the Hg detoxification mechanism employed by the Hg^R bacterial communities and to overcome primer limitations to capturing the whole gene diversity as is observed in many studies, I used a total of four primer sets that target *mer*-determinants from the phyla of Actinobacteria, Firmicutes, Proteobacteria, and Deinococcus-Thermus (Wang et al, 2011). It was shown that the vast majority of both LS (83.3%) and FS (85.1%) isolates contained a copy of the

merA gene, which further supports that these communities are acclimatized to chronic Hg-stress. *merA* gene diversity was lower than that observed for species-level diversity based on 16S rRNA gene sequences, yet the same trend was observed, whereby loci most closely related to the *alphaproteobacteria* are selected against under oligotrophic conditions.

Another goal of this study was to elucidate the effect of Hg-stress on the communication between bacterial communities, by investigating Horizontal Gene Transfer (HGT) events. HGT enhances the genetic diversity of bacteria as it promotes the spread of functional loci that increase fitness and survival under adverse conditions (DeLong et al, 2006, Tyson et al, 2004, Top and Springael, 2003). Twenty-seven phylogenetic incongruencies were observed between the 16S rRNA and *merA* genes from a total of fifty LS and FS isolates. In the case of the LS isolates, 1/8 phylogenetic incongruencies was further supported by anomalies in the G+C %mole content between the host genome and the *merA* gene as well as by the positive amplification of *merA* from plasmid DNA extracted from that isolate (Kibbe, 2007, Lawrence and Ochman, 2002, Coombs and Barkay, 2004). This was an inter-class transfer event, from an *alphaproteobacterial* locus to a *gammaproteobacterial* recipient. As for the FS group, based on the above reasoning, 12/19 phylogenetic incongruencies were supported. Six HGT events occurred among classes of the Proteobacteria, one between a Low G+C Firmicutes *merA* to an *alphaproteobacterial* recipient, and five inter-phylum transfers among genera of the Actinobacteria.

In summation, long-term Hg-stress has a strong impact on soil bacterial communities' composition, abundance, species and gene diversity. The stress is differentially felt in communities depending on their metabolic potential, corroborating with studies that observed Hg-resistance to be niche dependent (Chatziefthimiou et al, 2007, Vetriani et al, 2005). Hg-resistance was conferred by

the enzymatic activities of MerA, and copiotrophic conditions supported higher reduction potentials and they were more conducive to HGT events.

In the second part of this dissertation, I investigated the precise factors that influence the development, structure and distribution of bacterial communities at the ecosystem level. To that end, samples were obtained from the Hg-polluted South River in Virginia, along a gradient spanning 24 miles, starting at the DuPont facility in Waynesboro which is the point source, up to its confluence with the Middle and North Rivers at Port Republic (Flanders et al, 2010, Carter, 1977). Direct cultivation under copiotrophic conditions (0.2X TSA) in the presence of Hg-stress (100 μM HgCl_2), showed that Hg^{R} bacterial communities developed only in samples exposed to high Hg concentration levels (RRM 1.7-9.1), and that their abundance was higher closest to the source. It was also observed that the Hg^{R} communities were composed exclusively of K-strategists, while growth of r-strategists was promoted only when samples received an overnight spike of Hg (10 $\mu\text{g/g}$ HgCl_2) that mimicked a "recent" Hg-stress (Deleij, 1993). These results demonstrate that selection pressure of Hg has led to the emergence and maintenance of Hg^{R} bacterial populations and provide evidence that the resident communities are in late successional stages and possibly close to equilibrium (Sandaa, 1999, Pianka, 1970).

A primary objective of this study was to assess the composition and diversity of soil bacterial communities using a culture independent method, thus bypassing the limitations of direct cultivation techniques (Pace, 1997). Diversity and evenness measures calculated based on 16S rRNA-fingerprints, revealed that higher levels of diversity were achieved in communities experiencing low levels of THg, 9.2-19.6 miles away from the source, where no Hg^{R} CFU developed. Clustering analyses based on both species richness (Sorensen index) and diversity (Bray-Curtis) generated using 16S rRNA-fingerprints, showed that sites cluster based on geochemical characteristics rather than geographical proximity (Girvan et al, 2003). The

environmental factors that accounted for ~62% of the variation observed were pH, moisture and soil texture. On the other hand, functional diversity and evenness were comparable among sites, based on *merA*-fingerprints, and communities clustered based on geographical proximity. These findings provide evidence to support Baas-Becking's theory that in the case of microorganisms "everything is everywhere" but the local environmental conditions select and limit global species diversity (de Wit and Bouvier, 2006, Fenchel et al, 1997, Baas Becking, 1934, Beijerinck, 1913).

The findings of this study highlight the complexity of long-term Hg-stress on the development, composition and diversity of microbial communities inhabiting the floodplain ecosystems. The present study also provides further evidence to support the enrichment of *mer*-determinants in chronically contaminated environments and further our knowledge on the role of HGT in the evolution of this gene. Moreover, the new *merA*-based t-RFLP method can be employed as a tool by other workers in the field for rapid and reliable detection of *mer*-determinants in environmental samples. Finally, the results of this dissertation add to our understanding of the environmental factors that shape bacterial communities and provide a micro-ecological framework for future remedial actions in Hg contaminated sites.

Appendix – Supplementary Information on Phylogenetic and Functional Analyses in Chapter 2

Table A.1. LS isolates' phylogenetic associations based on 16S rRNA gene sequences.

Isolate	Closest relative	16S rRNA gene sequence % similarity	GenBank Accession number	Phylogenetic grouping
LS 1	<i>Streptomyces spororaveus</i>	100	AB184682	Actinobacteria (High G+C)
LS 3	<i>Arthrobacter</i> sp. HSL-2	98	AY714235	
LS 4	<i>Streptomyces gelaticus</i> strain NRRL B-2928	99	DQ026636	
LS 7	<i>Streptomyces</i> sp. GS11	100	GQ914733	
LS 10	<i>Streptomyces</i> sp. SCP-2	99	AM889486	
LS 11	<i>Streptomyces umbrinus</i>	99	AB184305	
LS 12	<i>Streptomyces phaeochromogenes</i> strain 174440	99	EU593667	
LS 13	<i>Streptomyces flavotricini</i> strain 173520	99	EU593749	
LS 14	<i>Arthrobacter</i> sp. 16.43	100	DQ157988	
LS 16	<i>Streptomyces scabiei</i>	99	AB301486	
LS 17	<i>Streptomyces</i> sp. SCP-2	99	AM889486	
LS 18	<i>Streptomyces phaeochromogenes</i> strain 174440	100	EU593667	
LS 20	<i>Streptomyces lavendulae</i> strain 7-1	99	FJ517747.1	
LS 23	<i>Streptomyces</i> sp. SCP-2	99	AM889486	
LS 24	<i>Streptomyces</i> sp. GS11	99	GQ914733	
LS 25	<i>Streptomyces</i> sp. FXJ2.004	100	EU677780	
LS 26	<i>Streptomyces</i> sp. 3-8	99	EU054350	
LS 28	<i>Streptomyces</i> sp. Lz531	99	EF125929	
LS 30	<i>Streptomyces nojiriensis</i>	99	AB184485	

LS 31	<i>Streptomyces spororaveus</i>	99	AB184682	Actinobacteria (High G+C)	
LS 32	<i>Arthrobacter</i> sp. 16.43	99	DQ157988		
LS 33	<i>Streptomyces</i> sp. SCP-2	99	AM889486		
LS 34	<i>Arthrobacter</i> sp. 16.43	99	DQ157988		
LS 35	<i>Arthrobacter</i> sp. HSL-2	98	AY714235		
LS 36	<i>Arthrobacter</i> sp. HSL-2	98	AY714235		
LS 38	<i>Arthrobacter</i> sp. 16.43	99	DQ157988		
LS 41	<i>Streptomyces</i> sp. SCP-2	99	AM889486		
LS 6	<i>Sinorhizobium</i> sp. 9702-M4	97	AF357225	D	Proteobacteria
LS 9	<i>Rhizobium</i> sp. 25.13	99	DQ499524		
LS 15	<i>Sinorhizobium</i> sp. 9702-M4	97	AF357225		
LS 19	<i>Rhizobium</i> sp. Mad-2	98	EF364379		
LS 22	<i>Ensifer adhaerens</i> strain P43	100	AY972201		
LS 8	<i>Variovorax</i> sp. KS2D-23	99	AB196432	B	
LS 21	<i>Alcaligenes</i> sp. HI-ABCE2	99	DQ205295		
LS 40	<i>Escherichia coli</i> O157:H7 EDL933	100	AE005174	Y	
LS 27	Uncultured soil clone W4Ba99	99	DQ643759	Unknown	

Table A.2. FS isolates' phylogenetic associations based on 16S rRNA gene sequences.

Isolate	Closest relative	16S rRNA gene sequence % similarity	GenBank Accession number	Phylogenetic grouping
FS 1	<i>Streptomyces spororaveus</i> strain 173981	99	EU593748	Actinobacteria (High G+C)
FS 4	<i>Nocardia alba</i>	98	AY222321	
FS 5	<i>Arthrobacter</i> sp. 16.43	100	DQ157988	
FS 9	<i>Streptomyces avidinii</i> strain 173656	100	EU570450.1	
FS 12	<i>Mycobacterium</i> sp. MOLA 520	99	AM990744	
FS 13	<i>Arthrobacter</i> sp. HSL-2	96	AY714235	
FS 14	<i>Streptomyces</i> sp.10-3	99	EU054378	
FS 16	<i>Arthrobacter</i> sp. MH30	99	EU182858	
FS 19	<i>Mycobacterium</i> sp. D9-7	99	AM403216	
FS 24	<i>Arthrobacter</i> sp. Pi4	97	AM905949	
FS 25	<i>Streptomyces</i> sp. Lz531	99	EF125929	
FS 27	<i>Streptomyces ederensis</i> strain 174483	99	EU593692	
FS 28	<i>Streptomyces</i> sp. HBUM87110	99	EU119192	
FS 29	<i>Arthrobacter</i> sp. HX2	99	EF601814	
FS 30	Uncultured actinobacterium	99	AM114429	
FS 31	<i>Arthrobacter</i> sp. OS-13	98	EF612312	
FS 34	<i>Arthrobacter</i> sp. 16.43	98	DQ157988	
FS 36	<i>Streptomyces</i> sp. MJM8416	99	EU603366	
FS 37	<i>Streptomyces</i> sp. HBUM87110	98	EU119192	
FS 44	Uncultured actinobacterium	98	AM114429	
FS 45	<i>Arthrobacter</i> sp. OS-13	99	EF612312	
FS 51	Uncultured actinobacterium	99	AM114429	
FS 53	<i>Streptomyces</i> sp. MJM3179	99	AY371246	

FS 56	<i>Arthrobacter</i> sp. CL11	98	EF125929		
FS 57	<i>Streptomyces</i> sp. Lz531	96	EF125929		
FS 2	<i>Aminobacter aminovorans</i>	97	AF329835	D	Proteobacteria
FS 3	<i>Bradyrhizobium</i> sp. CCBAU 85057	99	EU256463		
FS 6	<i>Sinorhizobium</i> sp. CAF63	99	EU399910		
FS 7	<i>Aminobacter aminovorans</i> strain DSM7048T	99	AJ011759		
FS 15	Bradyrhizobiaceae bacterium HTCC407	98	AY429694.1		
FS 18	<i>Aminobacter</i> sp. MSH1	99	DQ401867		
FS 21	<i>Sinorhizobium</i> sp. CAF63	98	EU399910		
FS 23	<i>Ensifer adhaerens</i> strain S-30.7.5	99	DQ140416		
FS 26	<i>Aminobacter aminovorans</i>	100	AF329835		
FS 33	<i>Aminobacter aminovorans</i>	99	AF329835		
FS 38	<i>Ensifer adhaerens</i> strain REG34	99	EU647697		
FS 46	<i>Sinorhizobium meliloti</i> strain KYA71	98	EU603721		
FS 50	<i>Aminobacter</i> sp. C4	99	AJ622941.1		
FS 54	<i>Aminobacter</i> sp. C4	98	AJ622941.1		
FS 55	<i>Aminobacter</i> sp. C4	98	AJ622941.1		
FS 10	<i>Stenotrophomonas maltophilia</i> strain A1Y15	98	AY512626	B	
FS 17	<i>Alcaligenes</i> sp. HI-ABCE2	99	DQ205295		
FS 42	<i>Alcaligenes</i> sp. HI-ABCE2	99	DQ205295		
FS 35	<i>Lysobacter</i> sp. 13-1	99	DQ188260	Y	
FS 41	<i>Lysobacter antibioticus</i> strain Q-2	99	EF108304		
FS 48	<i>Escherichia coli</i> strain PM-11	100	HQ326791.1		
FS 49	<i>Lysobacter</i> sp. 13-1	99	DQ188260		

Table A.3. LS isolates' phylogenetic associations based on MerA amino acid sequences.

Isolate	Closest relative	% similarity	GenBank Accession number	Phylogenetic grouping
LS 1	<i>Streptomyces</i> sp. CHR28 pRJ28	72	AAF64138	Actinobacteria (High G+C)
LS 2	<i>Acidothermus cellulolyticus</i> 11B	56	YP_872449	
LS 3	<i>Arthrobacter chlorophenolicus</i> A6	100	ACL42462	
LS 4	<i>Streptomyces</i> sp. CHR28 pRJ28	71	AAF64138	
LS 7	<i>Pseudonocardia dioxanivorans</i> CB1190 pSED01	79	AEA28805.1	
LS 10	<i>Streptomyces</i> sp. CHR28 pRJ28	69	AAF64138	
LS 11	<i>Acidothermus cellulolyticus</i> 11B	68	YP_872449	
LS 13	<i>Streptomyces</i> sp. CHR28 pRJ28	69	AAF64138	
LS 14	<i>Streptomyces lividans</i>	72	CAA46460.1	
LS 16	<i>Streptomyces</i> sp. CHR28 pRJ28	80	AAF64138	
LS 17	<i>Streptomyces</i> sp. CHR28 pRJ28	71	AAF64138	
LS 18	<i>Streptomyces</i> sp. CHR28 pRJ28	68	AAF64138	
LS 24	<i>Nocardioides</i> sp. JS614	83	ABL79525	
LS 25	<i>Streptomyces</i> sp. CHR28 pRJ28	78	AAF64138	
LS 26	<i>Streptomyces</i> sp. CHR28 pRJ28	75	AAF64138	
LS 27	<i>Arthrobacter chlorophenolicus</i> A6	80	ACL42462	
LS 28	<i>Acidothermus cellulolyticus</i> 11B	65	YP_872449	
LS 31	<i>Streptomyces</i> sp. CHR28 pRJ28	77	AAF64138	
LS 32	<i>Arthrobacter phenanthrenivorans</i> Sphe3 plasmid pASPHE301	90	ADX75145.1	
LS 33	<i>Micrococcus luteus</i> NCTC 2665	77	ACS30152	
LS 34	<i>Arthrobacter phenanthrenivorans</i> Sphe3 plasmid pASPHE301	84	ADX75145.1	

LS 36	<i>Arthrobacter chlorophenolicus</i> A6	82	ZP_02836069		
LS 41	<i>Streptomyces</i> sp. Is-BDOE1	86	ABO45911.1		
LS 6	Rhizobiales bacterium Is-B040	79	ABO45919	D	Proteobacteria
LS 9	Rhizobiales bacterium Is-B040	99	ABO45919		
LS 15	Rhizobiales bacterium Is-B040	81	ABO45919		
LS 19	Rhizobiales bacterium Is-B040	87	ABO45919		
LS 40	<i>Xanthobacter autotrophicus</i> Py2	63	YP_001417797		
LS 21	<i>Ralstonia pickettii</i> 12J	85	ACD26925.1		
LS 8	Uncultured bacterium <i>merA</i>	73	FN678311.1	Unknown	

Table A.4. FS isolates' phylogenetic associations based on MerA amino acid sequence.

Isolate	Closest relative	% similarity	GenBank Accession number	Phylogenetic grouping	
FS 1	<i>Streptomyces</i> sp. CHR28 pRJ28	72	AAF64138	Actinobacteria (High G+C)	
FS 4	<i>Streptomyces</i> sp. CHR28 pRJ28	72	AAF64138		
FS 5	<i>Arthrobacter chlorophenolicus</i> A6	83	ZP_02836069		
FS 9	<i>Streptomyces</i> sp. CHR28 pRJ28	72	AAF64138		
FS 12	<i>Acidothermus cellulolyticus</i> 11B	67	YP_872449		
FS 13	<i>Arthrobacter chlorophenolicus</i> A6	86	ZP_02836069		
FS 14	<i>Acidothermus cellulolyticus</i> 11B	64	YP_872449		
FS 19	<i>Streptomyces</i> sp. CHR28 pRJ28	72	AAF64138		
FS 25	<i>Streptomyces</i> sp. CHR28 pRJ28	83	AAF64138		
FS 27	<i>Acidothermus cellulolyticus</i> 11B	64	YP_872449		
FS 28	<i>Acidothermus cellulolyticus</i> 11B	66	YP_872450		
FS 29	<i>Arthrobacter aurescens</i> TC1 pTC1	83	ABM10430		
FS 30	<i>Arthrobacter phenanthrenivorans</i> Sphe3 plasmid pASPHE301	72	ADX75145.1		
FS 36	<i>Streptomyces</i> sp. CHR28 pRJ28	70	AAF64138		
FS 37	<i>Streptomyces</i> sp. CHR28 pRJ29	68	AAF64138		
FS 44	<i>Arthrobacter</i> sp. FB24 plasmid 1	96	YP_829216		
FS 45	<i>Arthrobacter aurescens</i> TC1 pTC1	70	YP_950110		
FS 51	<i>Arthrobacter aurescens</i> TC1 pTC1	78	ABM10430		
FS 56	<i>Arthrobacter chlorophenolicus</i> A6	99	ZP_02836069		
FS 57	<i>Streptomyces</i> sp. CHR28 pRJ29	66	AAF64138		
FS 33	<i>Bacillus cereus</i> AH820	43	ZP_02262558	Firmicutes (Low G+C)	
FS 54	<i>Bacillus cereus</i> AH820	45	ZP_02262558		
FS 2	<i>Bradyrhizobium</i> sp. Is-D308	88	EF455065		□

FS 3	<i>Oligotropha carboxidovorans</i> OM5	78	EDT32092		
FS 6	<i>Bradyrhizobium</i> sp. Is-D308	95	EF455065		
FS 7	<i>Aurantimonas</i> sp. SI85-9A1	72	ZP_01227191.1		
FS 18	<i>Bradyrhizobium</i> sp. Is-D308	83	EF455065		
FS 21	<i>Bradyrhizobium</i> sp. Is-D302	97	ABO45915		
FS 23	<i>Aurantimonas</i> sp. SI85-9A1	72	ZP_01227191		
FS 38	<i>Rhizobium</i> sp. Is-B203a	100	ABO45917		
FS 50	<i>Bradyrhizobium</i> sp. Is-D254	87	ABO45913		
FS 55	<i>Bradyrhizobium</i> sp. Is-D271	83	ABO45914		
FS 17	<i>Ralstonia pickettii</i> 12J	89	YP_001899357	β	Proteobacteria
FS 41	<i>Polaromonas</i> sp. JS666	78	YP_549052		
FS 42	<i>Ralstonia pickettii</i> 12J	88	YP_001899357		
FS 49	<i>Stenotrophomonas maltophilia</i> K279a	92	YP_001972199		
FS 10	<i>Salmonella enterica</i> subsp. <i>enterica</i> serovar Kentucky	100	ABQ57371	γ	
FS 35	<i>Pseudomonas aeruginosa</i>	81	YP_001427358		
FS 46	<i>Pseudomonas aeruginosa</i> D2	100	GU595062		
FS 48	<i>Salmonella enterica</i> subsp. <i>enterica</i> serovar Kentucky	81	ABQ57371		

Bibliography

- Allison, S. D., Martiny, J. B. H. (2008).** Resistance, resilience, and redundancy in microbial communities. *Proceedings of the National Academy of Sciences* **105**, 11512-11519.
- Amann, R. I., Stromley, J., Devereux, R., Key, R. & Stahl, D. A. (1992).** Molecular and microscopic identification of sulfate-reducing bacteria in multispecies biofilms. *Appl Environ Microbiol* **58**, 614-623.
- Andersson, D. I., and Hughes, D. (2010).** Antibiotic Resistance and its Cost: is it Possible to Reverse Resistance? *Nature Reviews Microbiology* **8**, 260-271.
- Ashelford, K. E., J. C. Fry, M. J. Day, K. E. Hill, M. A. Learner, J. R. Marchesi, C. D. Perkins, A. J. Weightman. (1997).** Using microcosms to study gene transfer in aquatic habitats. *FEMS Microbiology Ecology* **23**, 81-94.
- Avaniss-Aghajani, E., K., Jones, D., Chapman, and C., Brunk. (1994).** A molecular technique for identification of bacteria using small sub-unitribosomal RNA sequences. *Biotechniques* **17**, 144-146.
- Baas Becking, L. G. M. (1934).** *Geobiologie of Inleiding Tot de Milieukunde. (Geobiology and Introduction to the Environmental Science)*. The Hague, the Netherlands: W.P. Van Stockum & Zoon.
- Bakir, F., Damluji, S. F., Amin-Zaki, L. & other authors (1973).** Methylmercury Poisoning in Iraq. *Science* **181**, 230-241.
- Baldi, F. (1997).** Microbial transformation of mercury species and their importance in the biogeochemical cycle of mercury. *Met Ions Biol Syst* **34**, 213-257.
- Barkay, T. (1987).** Adaptation of Aquatic Microbial Communities to Hg²⁺ Stress. *Appl Environ Microbiol* **53**, 2725-2732.
- Barkay, T., Miller, S. M. & Summers, A. O. (2003).** Bacterial mercury resistance from atoms to ecosystems. *FEMS Microbiol Rev* **27**, 355-384.
- Barkay, T. & Schaefer, J. (2001).** Metal and radionuclide bioremediation: issues, considerations and potentials. *Current Opinion in Microbiology* **4**, 318-323.
- Barkay, T. & Wagner-Dobler (2005).** Microbial Transformations of Mercury: Potentials, Challenges, and Achievements in Controlling Mercury Toxicity in the Environment. In *Advances in Applied Microbiology*, pp. 1-52: Academic Press.
- Barnett, M. O. & Turner, R. R. (2001).** Bioaccessibility of Mercury in Soils. *Soil & Sediment Contamination* **10**, 301.
- Beijerinck, M. W. (1913).** *De Infusies en de Ontdekking der Backteriën. (Infusions and the Discovery of Bacteria)*. Amsterdam, the Netherlands: Müller.
- Bogdonova, E., S., Bass, I., A., Minakhin, L., S., Petrova, M., A., Mindlin, S., Z., Volodin, A., A., Kalyaeva, E., S., Tiegje, J., M., Hobman, J., L., Brown, N.,**

- L., Nikiforov, V., G. (1998).** Horizontal Spread of mer Operons Among Gram-positive Bacteria in Natural Environments. *Microbiology* **144**, 609-620.
- Brooks, S. C. & Southworth, G. R. (2011).** History of mercury use and environmental contamination at the Oak Ridge Y-12 Plant. *Environmental Pollution* **159**, 219-228.
- Bruce, K. D. (1997).** Analysis of mer Gene Subclasses within Bacterial Communities in Soils and Sediments Resolved by Fluorescent-PCR-Restriction Fragment Length Polymorphism Profiling. *Applied and Environmental Microbiology* **63**, 4914-4919.
- Campbell, K. R., Ford, C. J. & Levine, D. A. (1998).** Mercury distribution in poplar creek, Oak Ridge, Tennessee, USA. *Environmental Toxicology and Chemistry* **17**, 1191-1198.
- Cao, Y., Cherr, G., Cvrdova-Kreylos, A. & other authors (2006).** Relationships between Sediment Microbial Communities and Pollutants in Two California Salt Marshes. *Microbial Ecology* **52**, 619-633.
- Carter, L. J. (1977).** Chemical Plants Leave Unexpected Legacy for Two Virginia Rivers. *Science* **198**, 1015-1020.
- Castresana, J. (2000).** Selection of Conserved Blocks from Multiple Alignments for Their Use in Phylogenetic Analysis. *Molecular Biology and Evolution* **17**, 540-552.
- Casucci, C., Okeke, B. & Frankenberger, W. (2003).** Effects of mercury on microbial biomass and enzyme activities in soil. *Biological Trace Element Research* **94**, 179-191.
- Chang, J.-S., Hong, J., Ogunseitan, O. A., Olson, B. H. (1993).** Interaction of Mercuric Ions with the Bacterial Growth Medium and Its Effects on Enzymatic Reduction of Mercury. *Biotechnology Progress* **9**, 526-532.
- Chao, A., Lee, S-M. (1992).** Estimating the Number of Classes via Sample Coverage. *Journal of the American Statistical Association* **87**, 210-217.
- Chatziefthimiou, A. D., Crespo-Medina, M., Wang, Y., Vetriani, C., Barkay, T. (2007).** The Isolation and Initial Characterization of Mercury Resistant Chemolithotrophic Thermophilic Bacteria from Mercury Rich Geothermal Springs. *Extremophiles* **11**, 469-479.
- Clarkson, T., W. (2002).** The Three Modern Faces of Mercury. *Environmental Health Perspectives* **110**, 11-23.
- Conn, V. M. & Franco, C. M. M. (2004).** Analysis of the Endophytic Actinobacterial Population in the Roots of Wheat (*Triticum aestivum* L.) by Terminal Restriction Fragment Length Polymorphism and Sequencing of 16S rRNA Clones. *Appl Environ Microbiol* **70**, 1787-1794.
- Coombs, J. M. & Barkay, T. (2004).** Molecular evidence for the evolution of metal homeostasis genes by lateral gene transfer in bacteria from the deep terrestrial subsurface. *Appl Environ Microbiol* **70**, 1698-1707.

- Craine, J. M., Morrow, C. & Fierer, N. (2007).** Microbial Nitrogen Limitation Increases Decomposition *Ecology* **88**, 2105-2113.
- Cristol, D. A., Brasso, R. L., Condon, A. M., Fovargue, R. E., Friedman, S. L., Hallinger, K. K., Monroe, A. P. & White, A. E. (2008).** The Movement of Aquatic Mercury Through Terrestrial Food Webs. *Science* **320**, 335.
- Cronquist, A. (1988).** *The Evolution and Classification of Flowering Plants*. Bronx: New York Botanical Garden.
- Davison, J. (1999).** Genetic exchange between bacteria in the environment. *Plasmid* **42**, 73-91.
- De Gelder, L., Williams, J. J., Ponciano, J. M., Sota, M. & Top, E. M. (2008).** Adaptive Plasmid Evolution Results in Host-Range Expansion of a Broad-Host-Range Plasmid. *Genetics* **178**, 2179-2190.
- De Leij, F. A. A. M., Whipps, J. M. & Lynch, J. M. (1994).** The use of colony development for the characterization of bacterial communities in soil and on roots. *Microbial Ecology* **27**, 81-97.
- de Liphay, J. R., L. D. Rasmussen, G. Oregard, K. Simonsen, Martin I. Bahl, N. Kroer, S. J. Sørensen, (2008).** Acclimation of subsurface microbial communities to mercury. *FEMS Microbiology Ecology* **65**, 145-155.
- De Wit, R. & Bouvier, T. (2006).** 'Everything is everywhere, but, the environment selects'; what did Baas Becking and Beijerinck really say? *Environmental Microbiology* **8**, 755-758.
- Dean, W. E. (1974).** Determination of carbonate and organic matter in calcareous sediments and sedimentary rocks by loss on ignition; comparison with other methods. *Journal of Sedimentary Research* **44**, 242-248.
- DeLong, E. F., Preston, C. M., Mincer, T. & other authors (2006).** Community Genomics Among Stratified Microbial Assemblages in the Ocean's Interior. *Science* **311**, 496-503.
- Dixon, R. O. D., Wheeler, C. T. (1986).** *Nitrogen Fixation in Plants*. Glaskow, UK: Blackie and Son.
- Dobzhansky, T. (1950).** Evolution in the Tropics. *American Scientist* **38**, 209-221.
- Drexel, R. D., Haitzer, M., Ryan, J. N., Aiken, G. R., and Nagy, K. L. (2002).** Mercury(II) Sorption to Two Florida Everglades Peats: Evidence for Strong and Weak Binding and Competition by Dissolved Organic Matter Released from the Peat. *ES&T* **36**, 4058-4064.
- Dunbar, J., Ticknor, L. O. & Kuske, C. R. (2001).** Phylogenetic Specificity and Reproducibility and New Method for Analysis of Terminal Restriction Fragment Profiles of 16S rRNA Genes from Bacterial Communities. *Appl Environ Microbiol* **67**, 190-197.
- Dworkin, M., Falkow, S., Rosenberg, E., Schleifer, K-H., Stackenrandt, E.**

(2006). *The Prokaryotes*, 3rd ed. edn. New York: Springer Science+Business Media, LLC.

Elton, C. S. (1958). *The Ecology of Invasions by Animals and Plants*. London: Chapman & Hall.

EPA (2010). Fate and Transport and Ecological Effects of Mercury.
<http://epagov/hg/indexhtml>.

Escobar-Paramo, P., Ghosh, S. & DiRuggiero, J. (2005). Evidence for Genetic Drift in the Diversification of a Geographically Isolated Population of the Hyperthermophilic Archaeon *Pyrococcus*. *Molecular Biology and Evolution* **22**, 2297-2303.

Ettema, C. H. & Wardle, D. A. (2002). Spatial soil ecology. *Trends in Ecology & Evolution* **17**, 177-183.

Falkowski, P. G., Fenchel, T. & DeLong, E. F. (2008). The Microbial Engines That Drive Earth's Biogeochemical Cycles. *Science* **320**, 1034-1039.

FDA. (2000). Guidance for Industry: Action Levels for Poisonous or Deleterious Substances in Human Food and Animal Feed.
<http://www.fda.gov/Food/GuidanceComplianceRegulatoryInformation/GuidanceDocuments/ChemicalContaminantsandPesticides/ucm077969htm#merc>.

Fenchel, T., Esteban, G. F., Finlay, B. J. (1997). Local Versus Global Diversity of Microorganisms: Cryptic Diversity of Ciliated Protozoa. *Oikos* **80**, 220-225.

Fierer, N. & Jackson, R. B. (2006). The diversity and biogeography of soil bacterial communities. *Proceedings of the National Academy of Sciences of the United States of America* **103**, 626-631.

Finkel, S. E. & Kolter, R. (1999). Evolution of microbial diversity during prolonged starvation. *Proceedings of the National Academy of Sciences* **96**, 4023-4027.

Flanders, J. R. (2009). Personal Communication.

Flanders, J. R., Turner, R. R., Morrison, T., Jensen, R., Pizzuto, J., Skalak, K. & Stahl, R. (2010). Distribution, behavior, and transport of inorganic and methylmercury in a high gradient stream. *Applied Geochemistry* **25**, 1756-1769.

Galtier, N., Gouy, M. & Gautier, C. (1996). SEAVIEW and PHYLO_WIN: two graphic tools for sequence alignment and molecular phylogeny
10.1093/bioinformatics/12.6.543. *Comput Appl Biosci* **12**, 543-548.

Gao, B., Paramanathan, R., Gupta, R. S. (2006). Signature Proteins that are Distinctive Characteristics of Actinobacteria and their Subgroups. *Antonie van Leeuwenhoek* **90**, 69-91.

Giller, K. E., Witter, E. & McGrath, S. P. (2009). Heavy metals and soil microbes. *Soil Biology and Biochemistry* **41**, 2031-2037.

Girvan, M. S., Bullimore, J., Pretty, J. N., Osborn, A. M. & Ball, A. S. (2003).

Soil Type Is the Primary Determinant of the Composition of the Total and Active Bacterial Communities in Arable Soils. *Appl Environ Microbiol* **69**, 1800-1809.

Gogarten, J. P. & Townsend, J. P. (2005). Horizontal gene transfer, genome innovation and evolution. **3**, 679-687.

Gonzalez, V., Bustos, P., Ramirez-Romero, M. & other authors (2003). The mosaic structure of the symbiotic plasmid of *Rhizobium etli* CFN42 and its relation to other symbiotic genome compartments. *Genome Biology* **4**, 1-13.

Gonzalez, V., Santamaria, R., I., Bustos, P. & other authors (2006). The partitioned *Rhizobium etli* genome: Genetic and metabolic redundancy in seven interacting replicons. *Proceedings of the National Academy of Sciences of the United States of America* **103**, 3834-3839.

Gottel, N. R., Castro, H. F., Kerley, M. & other authors (2011). Distinct Microbial Communities within the Endosphere and Rhizosphere of *Populus deltoides* Roots across Contrasting Soil Types. *Appl Environ Microbiol* **77**, 5934-5944.

Green, J. L., Bohannan, B. J. M., Whitaker, R. J. (2008). Microbial Biogeography: From Taxonomy to Traits. *Science* **320**, 1039-1042.

Grigal, D. F. (2003). Mercury Sequestration in Forests and Peatlands: A Review. *Journal of Environmental Quality* **32**, 393-405.

Grime, J. P. (1977). Evidence for the Existence of Three Primary Strategies in Plants and its Relevance to Ecological and Evolutionary Theory. *The American Naturalist* **111**, 1169-1194.

Group, S. E. (1971). Methylmercury in fish. A toxicological epidemiological evaluation of risks. *Nord Hyg Tidskr 4 (suppl)*, 19-364.

Gu, B., Bian, Y., Miller, C. L., Dong, W., Jiang, X. & Liang, L. (2011). Mercury reduction and complexation by natural organic matter in anoxic environments. *Proceedings of the National Academy of Sciences* **108**, 1479-1483.

Han, F., Shiyab, S., Chen, J., Su, Y., Monts, D., Waggoner, C. & Matta, F. (2008). Extractability and Bioavailability of Mercury from a Mercury Sulfide Contaminated Soil in Oak Ridge, Tennessee, USA. *Water, Air, & Soil Pollution* **194**, 67-75.

Han, F. X., Su, Y., Monts, D. L., Waggoner, C. A. & Plodinec, M. J. (2006). Binding, distribution, and plant uptake of mercury in a soil from Oak Ridge, Tennessee, USA. *Science of The Total Environment* **368**, 753-768.

Hartman, W. H., Richardson, C. J., Vilgalys, R. & Bruland, G. L. (2008). Environmental and anthropogenic controls over bacterial communities in wetland soils. *Proc Natl Acad Sci U S A* **105**, 17842-17847.

Hashimoto, T., Whang, K.-S. & Nagaoka, K. (2006). A quantitative evaluation and phylogenetic characterization of oligotrophic denitrifying bacteria harbored in subsurface upland soil using improved culturability. *Biology and Fertility of Soils* **42**, 179-185.

Hewson, I. & Fuhrman, J. A. (2004). Richness and Diversity of Bacterioplankton Species along an Estuarine Gradient in Moreton Bay, Australia. *Appl Environ Microbiol* **70**, 3425-3433.

Hill, K. E., E. M. Top. (1998). Gene transfer in soil systems using microcosms. *FEMS Microbiol Ecol* **25**, 319-329.

Hoffmann, T., Horz, H.-P., Kemnitz, D. & Conrad, R. (2002). Diversity of the Particulate Methane Monooxygenase Gene in Methanotrophic Samples from Different Rice Field Soils in China and the Philippines. *Systematic and Applied Microbiology* **25**, 267-274.

Holt J. G., B., D. J., Krieg, N. R., Staley, J. T., Garrity, G. M. (2005). *Bergey's Manual of Determinative Bacteriology*, 2 edn. New York: Springer.

Horner-Devine, M. C., Carney, K. M. & Bohannon, B. J. M. (2004). An ecological perspective on bacterial biodiversity. *Proceedings of the Royal Society of London Series B: Biological Sciences* **271**, 113-122.

Hughes, J. B., Hellmann, J. J., Ricketts, T. H. & Bohannon, B. J. M. (2001). Counting the Uncountable: Statistical Approaches to Estimating Microbial Diversity. *Appl Environ Microbiol* **67**, 4399-4406.

Ikeda, S., Omura, T., Ytow, N., Komaki, H., Minamisawa, K., Ezura, H., Fujimura, T. (2006). Microbial Community Analysis in the Rhizosphere of a Transgenic Tomato that Overexpresses 3-Hydroxy-3-methylglutaryl Coenzyme A Reductase. *Microbes and Environments* **4**, 261-271.

Jain, R., Rivera, M. C., Moore, J. E. & Lake, J. A. (2003). Horizontal Gene Transfer Accelerates Genome Innovation and Evolution. *Molecular Biology and Evolution* **20**, 1598-1602.

Janssen, P. H. (2006). Identifying the Dominant Soil Bacterial Taxa in Libraries of 16S rRNA and 16S rRNA Genes. *Appl Environ Microbiol* **72**, 1719-1728.

Jordan, W. C., Morrison, T. W., Green, J. W., Berti, W. R. (2008). An Investigation of Mercury Concentrations in the South River, Virginia Floodplain. In *SETAC Tampa*. Tampa, Florida.

Kemper, W. D., Rosenau, R. C. (1986). Size Distribution of Aggregates. In *Methods of Soil Analysis Part 1 - Physical and Mineralogical Methods*. Edited by A. Klute. Madison: American Society of Agronomy, Inc., Soil Science Society of America, Inc.

Kerkhof, L., Marc Santoro, M., Garland, J. (2000). Response of soybean rhizosphere communities to human hygiene water addition as determined by community level physiological profiling (CLPP) and terminal restriction fragment length polymorphism (TRFLP) analysis. *FEMS Microbiology Letters* **184**, 95-101.

Kibbe, W. A. (2007). OligoCalc: an online oligonucleotide properties calculator. *Nucleic Acids Research* **35**, W43-W46.

Kim, H. J., Boedicker, J. Q., Choi, J. W. & Ismagilov, R. F. (2008). Defined spatial structure stabilizes a synthetic multispecies bacterial community. *Proceedings*

of the National Academy of Sciences **105**, 18188-18193.

Kis-Papo, T., Kirzhner, V., Wasser, S. P. & Nevo, E. (2003). Evolution of genomic diversity and sex at extreme environments: Fungal life under hypersaline Dead Sea stress. *Proceedings of the National Academy of Sciences* **100**, 14970-14975.

Kitts, C. L. (2001). Terminal Restriction Fragment Patterns: A Tool for Comparing Microbial Communities and Assessing Community Dynamics. *Current Issues in Intestinal Microbiology* **2.1**, 17-25.

Koch, A. L. (2001). Oligotrophs versus copiotrophs. *BioEssays* **23**, 657-661.

Komura, I., Izaki, K. (1971). Mechanism of Mercuric Chloride Resistance in Microorganisms: I. Vaporization of a Mercury Compound from Mercuric Chloride by Multiple Drug Resistant Strains of Escherichia coli. *Journal of Biochemistry* **70**, 885-893.

Konstantinidis, K. T. & Tiedje, J. M. (2004). Trends between gene content and genome size in prokaryotic species with larger genomes. *Proceedings of the National Academy of Sciences of the United States of America* **101**, 3160-3165.

Lal, D., Lal, R. (2010). Evolution of Mercuric Reductase (merA) Gene: A Case of Horizontal Gene Transfer. *Microbiology* **79**, 500-508.

Lawrence, J. G. & Ochman, H. (2002). Reconciling the many faces of lateral gene transfer. *Trends in Microbiology* **10**, 1-4.

Levin, B. R. a. C. T. B. (2000). Bacteria are different: observations, interpretations, speculations, and opinions about the mechanisms of adaptive evolution in prokaryotes. *PNAS* **97**, 6981-6985.

Lilley, A., Young, P., Bailey, M. (2000). Bacterial population genetics: do plasmids maintain bacterial diversity and adaptation? In *The horizontal gene pool*, pp. 287-300. Edited by C. M. Thomas: harvard Academic Publisher.

Liu, W., Marsh, T., Cheng, H. & Forney, L. (1997). Characterization of microbial diversity by determining terminal restriction fragment length polymorphisms of genes encoding 16S rRNA. *Appl Environ Microbiol* **63**, 4516-4522.

MacArthur, R. H., Wilson, E. O (1967). *The Theory of Island Biogeography*. Princeton: Princeton University Press.

Mannisto, M., Tiirola, M. & Haggblom, M. (2009). Effect of Freeze-Thaw Cycles on Bacterial Communities of Arctic Tundra Soil. *Microbial Ecology* **58**, 621-631.

Martiny, J. B. H., Bohannan, B. J. M., Brown, J. H. & other authors (2006). Microbial biogeography: putting microorganisms on the map. *Nat Rev Micro* **4**, 102-112.

Maynard Smith, J. (1974). The Theory of Games and the Evolution of Animal Conflicts. *Journal of Theoretical Biology* **47**, 209-221.

- Mayr, E. (1942).** *Systematics and the Origin of Species*. New York Columbia University Press.
- McCaig, A. E., Glover, L. A. & Prosser, J. I. (2001).** Numerical Analysis of Grassland Bacterial Community Structure under Different Land Management Regimens by Using 16S Ribosomal DNA Sequence Data and Denaturing Gradient Gel Electrophoresis Banding Patterns. *Appl Environ Microbiol* **67**, 4554-4559.
- McCune, B., Mefford, M. J. (1999).** *PC-ORD: Multivariate Analysis of Ecological Data*: MjM Software Design.
- McGarigal, K., Cushman, S., Stafford, S. (2000).** *Multivariate Statistics for Wildlife and Ecology Research*. New York: Springer Science+Business Media, Inc.
- McGrady-Steed, J. & Morin, P. J. (2000).** Biodiversity, Density Compensation, and the Dynamics of Populations and Functional Groups. *Ecology* **81**, 361-373.
- McGrath, S. P., Chaudri, A. M. & Giller, K. E. (1995).** Long-term effects of metals in sewage sludge on soils, microorganisms and plants. *Journal of Industrial Microbiology & Biotechnology* **14**, 94-104.
- McGuinness, L. M., Salganik, M., Vega, L., Pickering, K. D. & Kerkhof, L. J. (2005).** Replicability of Bacterial Communities in Denitrifying Bioreactors as Measured by PCR/T-RFLP Analysis. *Environmental Science & Technology* **40**, 509-515.
- Moore, B. (1960).** A new screen test and selective medium for the rapid detection of epidemic strains of *Staph. aureus*. *Lancet* **27**, 453-458.
- Muller, A. K., Westergaard, K., Christensen, S. & Sorensen, S. J. (2001).** The effect of long-term mercury pollution on the soil microbial community. *FEMS Microbiol Ecol* **36**, 11-19.
- Nakamura, K., S. Silver (1994).** Molecular analysis of mercury-resistant *Bacillus* isolates from sediment of Minamata Bay, Japan. *Appl Environ Microbiol* **60**, 4596-4599.
- Nemergut, D. R., Townsend, A. R., Sattin, S. R., Freeman, K. R., Fierer, N., Neff, J. C., Bowman, W. D., Schadt, C. W., Weintraub, M. N., Schmidt, S. K. (2008).** The effects of chronic nitrogen fertilization on alpine tundra soil microbial communities: implications for carbon and nitrogen cycling. *Environmental Microbiology* **10**, 3093-3150.
- Novick, R. P. & Roth, C. (1968).** Plasmid-linked Resistance to Inorganic Salts in *Staphylococcus aureus*. *J Bacteriol* **95**, 1335-1342.
- Nunan, N., Wu, K., Young, I. M., Crawford, J. W. & Ritz, K. (2003).** Spatial distribution of bacterial communities and their relationships with the micro-architecture of soil. *FEMS Microbiology Ecology* **44**, 203-215.
- Olson, B. H., Thornton, I. (1982).** The Resistance Patterns to Metals of Bacterial Populations. *Journal of Soil Science* **33**, 271-277.

- Oregaard, G. & Sorensen, S. J. (2007).** High diversity of bacterial mercuric reductase genes from surface and sub-surface floodplain soil (Oak Ridge, USA). *1*, 453-467.
- Osborn, A., M. Bruce, K. D. Strike, P. Ritchie, D. A. (1997).** Distribution, Diversity and Evolution of the Bacterial Mercury Resistance (mer) Operon. *FEMS Microbiology Reviews* **19**, 239-262.
- Pace, N. R. (1997).** A Molecular View of Microbial Diversity and the Biosphere. *Science* **276**, 734-740.
- Palijan, G., Bogut, I., Vidakovic, J. (2008).** The Impact of Inundation-Isolation Cycles on the Culturable Bacterioplankton in the Danube River Floodplain. *Polish Journal of Ecology* **56**, 391-403.
- Pant, P., Allen, M. & Tansel, B. (2007).** Mercury contamination in the riparian zones along the East Fork Poplar Creek at Oak Ridge. *Ecotoxicology and Environmental Safety* **74**, 467-472.
- Patriarca, E. J., Tate, R. & Iaccarino, M. (2002).** Key Role of Bacterial NH₄⁺ Metabolism in Rhizobium-Plant Symbiosis. *Microbiol Mol Biol Rev* **66**, 203-222.
- Perret, X., Freiberg, C., Rosenthal, A., Broughton, W. J. & Fellay, R. (1999).** High-resolution transcriptional analysis of the symbiotic plasmid of Rhizobium sp. NGR234. *Molecular Microbiology* **32**, 415-425.
- Philippot, L., Andersson, S. G. E., Battin, T. J., Prosser, J. I., Schimel, J. P., Whitman, W. B. & Hallin, S. (2010).** The ecological coherence of high bacterial taxonomic ranks. *Nat Rev Micro* **8**, 523-529.
- Pianka, E. R. (1970).** On r- and K-Selection. *American Naturalist* **104**, 592-597.
- Pointdexter, J. (1981).** Oligotrophy. Fast and Famine Existence. *Advances in Microbial Ecology* **5**, 63-89.
- R. Todd Drexel, M. H., Joseph N. Ryan, George R. Aiken, and Kathryn L. Nagy (2002).** Mercury(II) Sorption to Two Florida Everglades Peats: Evidence for Strong and Weak Binding and Competition by Dissolved Organic Matter Released from the Peat. *ES&T* **36**, 4058-4064.
- Ramamoorthy, S. & Kushner, D. J. (1975).** Binding of mercuric and other heavy metal ions by microbial growth media. *Microbial Ecology* **2**, 162-176.
- Ranjard L., A. R., L. Jocteur-Monrozier, S. Nazaret. (1997).** Response of soil bacteria to Hg(II) in relation to soil characteristics and cell location. *FEMS Microbiology Ecology* **24**, 321-331.
- Rasmussen, L. D. & Sorensen, S. J. (2001).** Effects of mercury contamination on the culturable heterotrophic, functional and genetic diversity of the bacterial community in soil. *FEMS Microbiol Ecol* **36**, 1-9.
- Rasmussen, L. D., Zawadsky, C., Binnerup, S. J., Oregaard, G., Sorensen, S. J. & Kroer, N. (2008).** Cultivation of Hard-To-Culture Subsurface Mercury-Resistant

Bacteria and Discovery of New merA Gene Sequences. *Appl Environ Microbiol* **74**, 3795-3803.

Reche, I., Pulido-Villena, E., Morales-Baquero, R. & Casamayor, E. O. (2005). Does Ecosystem Size Determine Aquatic Bacterial Richness? . *Ecology* **86**, 1715-1722.

Richmond, M. H. & John, M. (1964). Co-transduction by a Staphylococcal Phage of the Genes Responsible for Penicillinase Synthesis and Resistance to Mercury Salts. *Nature* **202**, 1360-1361.

Riemann, L. a. M., M. (2002). Stability of Bacterial and Viral Community Compositions in Danish Coastal Waters as Depicted by DNA Fingerprinting Techniques. *Aquatic Microbial Ecology* **27**, 219-232.

Ruby, M. V., Davis, A., Schoof, R., Eberle, S. & Sellstone, C. M. (1996). Estimation of Lead and Arsenic Bioavailability Using a Physiologically Based Extraction Test. *Environmental Science & Technology* **30**, 422-430.

Rumbo, C., Fernandez-Moreira, E., Merino, M., Poza, M., Mendez, J. A., Soares, N. C., Mosquera, A., Chaves, F. & Bou, G. (2011). Horizontal Transfer of the OXA-24 Carbapenemase Gene via Outer Membrane Vesicles: a New Mechanism of Dissemination of Carbapenem Resistance Genes in *Acinetobacter baumannii*. *Antimicrob Agents Chemother* **55**, 3084-3090.

Sandaa, R.-A., Torsvik, V., Enger, Ø., Daae, F. L., Castberg, T. & Hahn, D. (1999). Analysis of bacterial communities in heavy metal-contaminated soils at different levels of resolution. *FEMS Microbiology Ecology* **30**, 237-251.

Santisteban, J. I., Mediavilla, R., LÃ°pez-Pamo, E., Dabrio, C. J., Zapata, M. B. R., GarcÃ±a, M. J. G., CastaÃ±o, S. & MartÃ±ez-Alfaro, P. E. (2004). Loss on ignition: a qualitative or quantitative method for organic matter and carbonate mineral content in sediments? *Journal of Paleolimnology* **32**, 287-299.

Scala, D. J. & Kerkhof, L. J. (2000). Horizontal Heterogeneity of Denitrifying Bacterial Communities in Marine Sediments by Terminal Restriction Fragment Length Polymorphism Analysis. *Appl Environ Microbiol* **66**, 1980-1986.

Schloss, P. D. & Handelsman, J. (2004). Status of the Microbial Census. *Microbiol Mol Biol Rev* **68**, 686-691.

Schloss, P. D., Westcott, S. L., Ryabin, T. & other authors (2009). Introducing mothur: Open-Source, Platform-Independent, Community-Supported Software for Describing and Comparing Microbial Communities. *Appl Environ Microbiol* **75**, 7537-7541.

Schutte, U., Abdo, Z., Bent, S., Shyu, C., Williams, C., Pierson, J. & Forney, L. (2008). Advances in the use of terminal restriction fragment length polymorphism (T-RFLP) analysis of 16S rRNA genes to characterize microbial communities. *Applied Microbiology and Biotechnology* **80**, 365-380.

Semenov, A. (1991). Physiological bases of oligotrophy of microorganisms and the concept of microbial community. *Microbial Ecology* **22**, 239-247.

- Shannon, C. E. (1948).** A Mathematical Theory of Communication. *The Bell System Technical of Communication* **27**, 379-423.
- Siripong, S. & Rittmann, B. E. (2007).** Diversity study of nitrifying bacteria in full-scale municipal wastewater treatment plants. *Water Research* **41**, 1110-1120.
- Slater, F., Bruce, K., Ellis, R., Lilley, A. & Turner, S. (2010).** Determining the Effects of a Spatially Heterogeneous Selection Pressure on Bacterial Population Structure at the Sub-millimetre Scale. *Microbial Ecology* **60**, 873-884.
- Slater, F. R., Mark J. Bailey, Adrian J. Tett, Sarah L. Turner, (2008).** Progress towards understanding the fate of plasmids in bacterial communities. *FEMS Microbiology Ecology* **66**, 3-13.
- Spain, A. M., Krumholz, L. R. & Elshahed, M. S. (2009).** Abundance, composition, diversity and novelty of soil Proteobacteria. *ISME J* **3**, 992-1000.
- Stenström, J., Svensson, K. & Johansson, M. (2001).** Reversible transition between active and dormant microbial states in soil. *FEMS Microbiology Ecology* **36**, 93-104.
- Summers, A. O. (1986).** Organization, Expression, and Evolution of Genes for Mercury Resistance. *Annual Reviews in Microbiology* **40**, 607-634.
- Summers, A. O. (1992).** Untwist and Shout: A heavy Metal-responsive Transcriptional Regulator. *Journal of Bacteriology* **174**, 3097-3101.
- Takacs, L. (2000).** Quicksilver from cinnabar: The first documented mechanochemical reaction? *JOM Journal of the Minerals, Metals and Materials Society* **52**, 12-13.
- Talavera, G. & Castresana, J. (2007).** Improvement of Phylogenies after Removing Divergent and Ambiguously Aligned Blocks from Protein Sequence Alignments. *Systematic Biology* **56**, 564-577.
- ter Braak, C. J. F. (1986).** Canonical Correspondence Analysis: A New Eigenvector Technique for Multivariate Direct Gradient Analysis. *Ecology* **67**, 1167-1179.
- Theophrastus (1956).** *On Stones*. Columbus, Ohio: Ohio State University, Columbus.
- Thompson, J., Gibson, T., Plewniak, F., Jeanmougin, F. & Higgins, D. (1997).** The CLUSTAL_X windows interface: flexible strategies for multiple sequence alignment aided by quality analysis tools. *Nucl Acids Res* **25**, 4876-4882.
- Tilman, D. (1996).** Biodiversity: Population Versus Ecosystem Stability. *Ecology* **77**, 350-363.
- Tilman, D. & Downing, J. A. (1994).** Biodiversity and stability in grasslands. *Nature* **367**, 363-365.
- Top, E. M. & Springael, D. (2003).** The role of mobile genetic elements in bacterial

adaptation to xenobiotic organic compounds. *Current Opinion in Biotechnology* **14**, 262-269.

Torsvik, V., Goksoyr, J. & Daae, F. L. (1990). High diversity in DNA of soil bacteria. *Appl Environ Microbiol* **56**, 782-787.

Torsvik, V., Ovreas, L. & Thingstad, T. F. (2002). Prokaryotic diversity--magnitude, dynamics, and controlling factors. *Science* **296**, 1064-1066.

Trevors, J. T., van Elsas, J. D., van Overbeek, L. S. & Starodub, M. E. (1990). Transport of a genetically engineered *Pseudomonas fluorescens* strain through a soil microcosm. *Appl Environ Microbiol* **56**, 401-408.

Tyson, G. W., Chapman, J., Hugenholtz, P. & other authors (2004). Community structure and metabolism through reconstruction of microbial genomes from the environment. *Nature* **428**, 37-43.

van Elsas, J. D., Bailey, M. J. (2002). The ecology of mobile genetic elements. *FEMS Microbiology Ecology* **42**, 187-197.

van Elsas, J. D., L. Tam, R. D. Finlay, K. Killham, J. T. Trevors. (2007). Microbial interactions in soil. In *Modern soil microbiology*, pp. 177-210. Edited by J. D. van Elsas, J.K. Jansson, J. T. Trevors. New York: CRC Press, Taylor & Francis Group.

Van Valen, L. (1976). Ecological Species, Multispecies and Oaks. *Taxon* **25**, 233-239.

Ventura, M., Canchaya, C., Tauch, A., Chandra, G., Fitzgerald, G. F., Chater, K. F. & van Sinderen, D. (2007). Genomics of Actinobacteria: Tracing the Evolutionary History of an Ancient Phylum. *Microbiol Mol Biol Rev* **71**, 495-548.

Vishnivetskaya, T. A., Mosher, J. J., Palumbo, A. V. & other authors (2011). Mercury and Other Heavy Metals Influence Bacterial Community Structure in Contaminated Tennessee Streams. *Appl Environ Microbiol* **77**, 302-311.

Wang, Y., Boyd, E., Crane, S., Lu-Irving, P., Krabbenhoft, D., King, S., Dighton, J., Geesey, G. & Barkay, T. (2011). Environmental Conditions Constrain the Distribution and Diversity of Archaeal *merA* in Yellowstone National Park, Wyoming, U.S.A. *Microbial Ecology*, 1-14.

Weiher, E., Keddy, P. A. (1995). Assembly Rules, Null Models, and Trait Dispersion: New Questions for Old Patterns. *Oikos* **74**, 159-164.

Wessels Perelo, L. (2010). Review: In situ and bioremediation of organic pollutants in aquatic sediments. *Journal of Hazardous Materials* **177**, 81-89.

Whang, K. & Hattori, T. (1988). Oligotrophic bacteria from rendzina forest soil. *Antonie van Leeuwenhoek* **54**, 19-36.

Whicker, F. W., Hinton, T. G., MacDonell, M. M., Pinder, J. E. & Habegger, L. J. (2004). Avoiding Destructive Remediation at DOE Sites. *Science* **303**, 1615-1616.

- Whitaker, R. J., Grogan, D. W. & Taylor, J. W. (2003).** Geographic Barriers Isolate Endemic Populations of Hyperthermophilic Archaea. *Science* **301**, 976-978.
- White, D. C., Flemming, C. A., Leung, K. T. & Macnaughton, S. J. (1998).** In situ microbial ecology for quantitative appraisal, monitoring, and risk assessment of pollution remediation in soils, the subsurface, the rhizosphere and in biofilms. *Journal of Microbiological Methods* **32**, 93-105.
- Wilke, B.-M. (2005).** Determination of chemical and physical soil properties. In *Manual for soil analysis: monitoring and assessing soil bioremediation*, pp. 47-95. Edited by R. Mergesin, Schinner, F. Berlin: Springer.
- Wittebolle, L., Marzorati, M., Clement, L., Balloi, A., Daffonchio, D., Heylen, K., De Vos, P., Verstraete, W. & Boon, N. (2009).** Initial community evenness favours functionality under selective stress. *Nature* **458**, 623-626.
- Yu, R., Flanders, J. R., Mack, E. E., Turner, R., Mirza M. B., Barkay, T. (2011).** Coexisting Sulfate and Iron Reducing Bacteria Contribute to Methylmercury Production in Freshwater River Sediments. *Environmental Science & Technology Submitted*.
- Yurieva, O., Kholodii, G., Minakhin, L., Gorlenko, Z., Kalyaeva, E., Mindlin, S., Nikiforov, V. (1997).** Intercontinental Spread of Promiscuous Mercury-Resistant Transposons in Environmental Bacteria. *Molecular Microbiology* **23**, 321-329.

Curriculum Vita

Aspassia D. Chatziefthimiou

Education

- 2005-2012 Ph.D. Candidate, Graduate Program in Ecology and Evolution and Natural Resources, Department of Biochemistry and Microbiology Rutgers, The State University of New Jersey, New Brunswick, NJ.
- 2001-2006 M.S. in Microbiology and Molecular Genetics Rutgers, The State University of New Jersey, Piscataway, NJ.
- 1996-2000 B.S. Biology Montclair State University, Montclair, NJ.

Publications

Crespo-Medina, M., **Chatziefthimiou, A. D.**, Cruz-Matos, R., Perez-Rodriguez, I., Barkay, T., Lutz, R., Starovoytov, V., Vetriani, C. 2009. *Salinisphaera hydrothermalis* sp. nov, a Mesophilic, Halotolerant, Facultative Autotrophic, Thiosulfate Oxidizing "*gammaproteobacterium*" from Deep-sea Hydrothermal Vents, and Emended Description of the Genus *Salinisphaera*. *Intl. J. Syst. Evol. Microbiol.* 59: 1497-1503.

Crespo-Medina, M., **Chatziefthimiou, A. D.**, Bloom, N. S., Luther, G. W., Wright, D. D., Reinfelder, J. R., Vetriani, C., Barkay, T. 2009. Adaptation of Chemosynthetic Microorganisms to Elevated Mercury Concentrations in Deep-Sea Hydrothermal Vents. *Limnology and Oceanography.* 54 (1). 41-49.

Lutz, R., Shank, T., Luther, G., Vetriani, C., Tolstoy, M., Nuzzio, D., Moore, T., Waldhauser, F., Crespo-Medina, M., **Chatziefthimiou, A. D.**, Annis, E., Reed, A.. 2008. Interrelationships between Vent Fluid Chemistry, Temperature, Seismic Activity and Biological Community Structure at a Deep-Sea Hydrothermal Vent along the East Pacific Rise. *Journal of Selfish Research.* Vol. 27, No. 1, 177-190.

Chatziefthimiou, A. D., Crespo-Medina, M., Wang, Y., Vetriani, C., Barkay, T. 2007. The Isolation and Initial Characterization of Mercury Resistant Chemolithotrophic Thermophilic Bacteria from Mercury Rich Geothermal Springs. *Extremophiles.* 11: 469-479.

Chatziefthimiou, A. D., Coombs, J. M., Barkay, T. 2007. The Design, Optimization, and Testing of a Hybridization Array for the Characterization of Broad Host Range Metal Resistance Plasmids. Meeting Abstracts: Proceedings of the International Symposium on Plasmid Biology. *Plasmid.* 57:182-243

Teaching Experience

- 2002-2011 Teaching Assistant in Applied and General Microbiology, and Microbial Ecology, Department of Biochemistry and Microbiology Rutgers, The State University of New Jersey, New Brunswick, NJ.